Characterizing and modeling wet stream length dynamics in Appalachian headwaters

Carrie Killeen Jensen

Dissertation submitted to the faculty of the Virginia Polytechnic Institute and State University in partial fulfillment of the requirements for the degree of

Doctor of Philosophy
In
Geospatial and Environmental Analysis

Kevin J. McGuire, Chair
C. Andrew Dolloff
Daniel L. McLaughlin
Durelle T. Scott
Yang Shao

March 22, 2018
Blacksburg, Virginia

Keywords: Appalachian Highlands, drainage density, headwaters, hysteresis, logistic regression, physiographic provinces, stream length, temporary streams

Characterizing and modeling wet stream length dynamics in Appalachian headwaters

Carrie Killeen Jensen

ABSTRACT

Headwater streams change in wet length in response to storm events and seasonal moisture conditions. These low-order channels with temporary flow are pervasive across arid and humid environments yet receive little attention in comparison to perennial waterways. This dissertation examines headwater stream length dynamics at multiple spatial and temporal scales across the Appalachians. I mapped wet stream length in four Appalachian physiographic provinces—the Appalachian Plateau, Blue Ridge, New England, and Valley and Ridge—to characterize seasonal expansion and contraction of the wet network at a broad, regional scale. Conversely, most existing field studies of stream length in headwaters are limited to a single study area or geographic setting. Field mappings showed that wet stream length varies widely within the Appalachians; network dynamics correlated with regional geology as well as local site lithology, geologic structure, and the depth, size, and spatial distribution of surficial sediment deposits. I used the field data to create logistic regression models of the wet network in each physiographic province at high and low runoffs. Topographic metrics derived from elevation data were able to explain the discontinuous pattern of headwater streams at different flow conditions with high classification accuracy. Finally, I used flow intermittency sensors in a single Valley and Ridge catchment to record channel wetting and drying at a high temporal resolution. The sensors indicated stream length hysteresis during storms with low antecedent moisture, with a higher wet network proportion on the rising limb than on the falling limb of events. As a result, maximum network extension can precede peak runoff by minutes to hours. Accurate maps of headwater streams and an understanding of wet network dynamics through time are invaluable for applications surrounding watershed management and environmental policy. These findings will contribute to the burgeoning research on temporary streams and are additionally relevant for studies of runoff generation, biogeochemical cycling, and mass fluxes of material from headwaters.

Characterizing and modeling wet stream length dynamics in Appalachian headwaters

Carrie Killeen Jensen

GENERAL AUDIENCE ABSTRACT

During a rain storm, we may think of streams increasing in depth, width, and velocity. However, we may not necessarily envision streams also getting longer. Headwaters, which form the upstream extremities of river systems, consist of many temporary streams that expand and contract in length due to storms and changes in seasonal moisture conditions. Headwaters are spatially expansive, comprising a majority of total river length, and serve as a primary control on downstream water quality. Therefore, understanding stream length dynamics can inform policy and land use decisions to effectively conserve and manage headwater regions and protect water sources for human use and consumption. This dissertation examines changes in stream length across four study areas of the Appalachian Mountains. I mapped the wet, or active, stream network multiple times at different flow conditions in each study area. Stream length dynamics varied considerably across the Appalachians and demonstrated the same range of network expansion and contraction as other studies observed in diverse settings around the world. Wet stream length greatly depended on regional and local geology. I then sought to predict the location of wet streams at high and low flows using metrics such as slope and drainage area that I calculated from digital elevation information. Comparisons with the field maps I made showed that simple terrain metrics explained the location, length, and disconnected nature of wet networks in each province with high accuracy. I also observed stream length dynamics during storm events in one watershed using sensors that recorded the presence or absence of water. These observations demonstrated that stream length was often higher for a given flow at the beginning of a storm on the rising limb than on the falling limb when flow was decreasing, particularly if conditions were dry before the storm. The findings of this dissertation contribute to existing knowledge of temporary streams and are relevant for future studies investigating the hydrology, biology, and ecology of headwaters.

Acknowledgements

There are many people to acknowledge for the completion of a dissertation, but I would first like to thank my advisor, Kevin McGuire. In particular, Kevin was extremely supportive when I changed my dissertation topic my first year, when he could have easily been exasperated or discouraged my choice. I never felt "alone" with the various unavoidable problems that arise with research, as Kevin was always accessible and eager to help. The rest of my committee—Andy Dolloff, Daniel McLaughlin, Durelle Scott, and Yang Shao—came to my aid with equipment, manuscript reviews, job and grant recommendations, as well as insights that encouraged me to think beyond my immediate research focus.

Funding for my dissertation research came from the National Science Foundation under grant LTER DEB 1114804, the Consortium of Universities for the Advancement of Hydrologic Science Pathfinder Fellowship, and the Cunningham Graduate Fellowship, Virginia Water Resources Research Center 2015 Competitive Grant, and Graduate Student Association Graduate Research Development Fund Award at Virginia Tech. I am grateful to the Fernow and Hubbard Brook Experimental Forests, Coweeta Hydrologic Laboratory, and George Washington and Jefferson National Forests for their cooperation and participation in the project. I would especially like to thank Pam Edwards, Freddie Wood, and Patsy Clinton for sending me data on numerous occasions, finding gear I needed, and even mapping out bike routes for me. Tal Roberts helped me assemble various field supplies and was the only reason I was able to build my flow intermittency sensors. I also thank Jake Diamond, Gracie Erwin, Dave Jensen, Joe Famularo, Philip Prince, Morgan Schulte, and Eryn Turney for help with field work as well as the anonymous reviewers of the manuscripts in Chapters 2 and 3 of this dissertation. I am especially indebted to Philip Prince for sharing my love of the Appalachian Mountains over the course of countless driving, hiking, and boating expeditions.

Finally, I have enormous gratitude that I cannot adequately express for my friends and family who have always supported me in both the academic realm and other extracurricular pursuits. My parents have never hesitated to say that they are proud of me.

Table of Contents

List of Figures

Chapter 2:

Chapter 3:

Chapter 4:

List of Tables

Chapter 2:

Chapter 3:

Chapter 4:

List of Abbreviations

AP	Appalachian Plateau (Chapter 3)
AP	Antecedent precipitation (Chapter 4)
API	Antecedent precipitation index
BMPs	Best management practices
BR	Blue Ridge
C-Q	Concentration-discharge
CWT	Coweeta Hydrologic Laboratory
DEM	Digital elevation model
GPS	Global Positioning System
HB	Hubbard Brook Experimental Forest
IDF	Intensity-duration-frequency
NE	New England
NHD	National Hydrography Dataset
PVY	Poverty Creek
SFP	South Fork of Potts Creek
TPI	Topographic position index
TWI	Topographic wetness index
UAA	Upslope accumulated area
USGS	U.S. Geological Survey
VR	Valley and Ridge

Attribution

Chapter 2

Chapter 2 was published in the journal Hydrological Processes in 2017.

Kevin J. McGuire, Ph.D., (Virginia Tech, Forest Resources and Environmental Conservation and Virginia Water Resources Research Center) helped with the selection and coordination of study sites, data analysis, and editing of the manuscript.

Philip S. Prince, Ph.D., (Virginia Tech, Geosciences) helped with the interpretation of site geology and editing of the manuscript.

Chapter 3

Chapter 3 is in revision with the journal Earth Surface Processes and Landforms in 2018.

Kevin J. McGuire, Ph.D., (Virginia Tech, Forest Resources and Environmental Conservation and Virginia Water Resources Research Center) helped with the selection and coordination of study sites and editing of the manuscript.

Yang Shao, Ph.D., (Virginia Tech, Geography) helped with model-building and editing of the manuscript.

C. Andrew Dolloff, Ph.D., (Virginia Tech, Fish and Wildlife Conservation and U.S. Forest Service Southern Research Station) helped with editing of the manuscript.

Chapter 4

Chapter 4 is in preparation for submission to Environmental Monitoring and Assessment in 2018.

Kevin J. McGuire, Ph.D., (Virginia Tech, Forest Resources and Environmental Conservation and Virginia Water Resources Research Center) helped with the study design, data analysis, and editing of the manuscript.

Daniel L. McLaughlin, Ph.D., (Virginia Tech, Forest Resources and Environmental Conservation and Virginia Water Resources Research Center) helped with the study design, interpretation of results, and editing of the manuscript.

Durelle T. Scott, Ph.D., (Virginia Tech, Biological Systems Engineering) helped with the study design, interpretation of results, and editing of the manuscript.

Chapter 1: Introduction

1.0 Objectives and Organization

Temporary ephemeral and intermittent streams that expand and contract in length comprise up to half of headwater networks (Buttle et al., 2012), which themselves account for more than 80% of total river length (Downing et al., 2012). In addition, temporary streams will likely become more vulnerable in the future as climate change and population growth strain the global supply of fresh water resources (Larned et al., 2010; Jaeger et al., 2014). Despite the enormous length and geographic extent of temporary headwaters and their critical role in maintaining downstream water quality (Alexander et al., 2007; Dodds & Oakes, 2008), most knowledge of stream network dynamics is qualitative, site-specific, and predominantly reflects research in arid and semi-arid environments (Day, 1978; Day, 1980; Stanley et al., 1997; Jaeger & Olden, 2012; Godsey & Kirchner, 2014; Whiting & Godsey, 2016). Maps of headwaters are highly inaccurate (Skoulikidis et al., 2017) and generally offer only categorical descriptions of flow duration that fail to fully characterize the complex and time-varying spatial extent of surface flow along temporary channels. Improved mapping of headwaters over broad geographic regions (Leibowitz et al., 2008) and quantitative metrics describing stream length dynamics (Larned et al., 2010) are essential for more representative delineations of temporary networks through time.

This dissertation examines headwater stream length dynamics at multiple spatial and temporal scales across four physiographic provinces of the Appalachian Highlands: the New England, Appalachian Plateau, Valley and Ridge, and Blue Ridge. Repeated stream mapping and high-frequency presence/absence data of flow in channels improve understanding of geologic and topographic controls on wet stream length and enable predictions of the variable location of temporary headwaters. This dissertation consists of five chapters, including this introduction (Chapter 1) that organizes the objectives of each chapter and provides justification for the current research. Chapters 2-4 provide three linked studies that collectively seek to characterize and model the expansion and

contraction of headwater networks. The conclusion integrates the findings of the three studies to summarize the contributions of the dissertation to temporary stream hydrology.

Chapter 2 compares wet stream length versus runoff across four Appalachian physiographic provinces. Multiple field mappings of the wet stream network in three catchments per province permit calculation of length and connectivity metrics for various flow conditions. Regional geologic attributes at the scale of physiographic provinces, such as the distinction between sedimentary and crystalline rock, correlate with the watershed position of flow origins, while the local lithology and geologic structure of individual catchments superimpose additional controls on network dynamics.

Chapter 3 utilizes the field data from Chapter 2 to create logistic regression models of the dynamic wet stream network in each province as a function of topographic metrics and runoff. The models have high classification accuracy and reproduce the spatially discontinuous pattern of wet reaches using primarily the topographic wetness index (TWI) and topographic position index (TPI) parameters. Adjustment of the probability threshold of the model output to lower or higher values results in realistic network delineations at high and low flows, respectively.

Chapter 4 describes the use of stream intermittency sensors to examine stream length dynamics during storms. The sensors provide point measurements of the presence or absence of flow along the network of a single Valley and Ridge headwater catchment at a high temporal resolution (every 15 minutes). The relationship between the wet network proportion and runoff matches field observations in the same catchment in Chapter 2, although the sensors show hysteresis on the rising and falling limbs of storm events. Stream length is higher on the rising limb for events with dry antecedent conditions. Upslope area and the degree of valley incision correlate with flow duration at the sensor locations.

1.1 Relevance and Justification

1.1.1 Ecological significance of temporary flow

Temporary headwater streams provide numerous ecosystem services including aquatic habitat, biogeochemical processing, and flood control (Larned et al., 2010) and are key sources of water, sediment, organic matter, and solutes for downstream water supplies. The importance of temporary streams for river systems not only corresponds to the intermittent periods when channels carry water but, additionally, to times when the wet stream is spatially discontinuous or even completely contracted. Disconnected stream networks with intervening dry reaches serve as "punctuated longitudinal biogeochemical reactors" (Larned et al., 2010) that transport, store, and transform nutrients and organic matter. Dry channel reaches accumulate solutes, sediment, and other material that perennial flow would normally carry continuously downstream. In this manner, temporary stream disconnections can delay the transport of contaminants, increasing the residence time for transformation in the hyporheic zone or binding to the channel substrate before re-mobilization during subsequent storm events (Cohen et al., 2016). When dry channels do activate with flow, the flushing of stored material may result in mass fluxes that differ from those of perennial networks (Zimmer & McGlynn, 2018).

Alternating wet and dry reaches create opportunities for aerobic as well as anaerobic biogeochemical reactions (Cohen et al., 2016). Aerobic conditions in dry reaches aid essential processes such as nitrification and photodegradation (Steward et al., 2012). Bärlocher et al. (1978) found that decaying organic matter in a dry channel actually had more protein and palatability for aquatic invertebrates than that remaining underwater. Conversely, anaerobic processes such as denitrification can occur in the substrate of wet channels (Welter & Fisher, 2016).

Discontinuous temporary streams possess a variety of channel environments in terms of the width, depth, temperature, and velocity of surface flow (Cohen et al., 2016) and, thus, offer habitat for lotic, lentic, and terrestrial species to increase overall biodiversity (Datry et al., 2014; Stubbington et al., 2017). Many aquatic plants and animals have adaptations to survive low flow or dry conditions, such as aestivation, high dispersal potential,

desiccation resistance, burrowing into sediment and leaf litter, and using pools or the hyporheic zone as refugia (Larned et al., 2010; Steward et al., 2012; Datry et al., 2014). The life history events of some organisms even depend on dry phases (Larned et al., 2010; Steward et al., 2012). Dry channel beds also serve as egg and seed banks for aquatic species and storage sites for food sources such as organic matter (Steward et al., 2012).

1.1.2 Temporary streams under the Clean Water Act

The simple question of "what is a stream?" should intuitively have a straightforward answer. In reality, an exact definition of what constitutes a stream is challenging and can vary dramatically among scientists, policymakers, and land managers. Consequently, temporary streams that vary in length seasonally or in response to storms are a major topic in discussions regarding "waters of the United States" (33 CFR § 328) under the Clean Water Act. Following the *Rapanos v. United States* decision in 2006, proof of a "significant nexus" (40 CFR § 110) in terms of a physical, chemical, or biological effect on downstream navigable waterways was necessary for the designation of a water body as "waters of the United States." In 2015, the most recent ruling determined that temporary ephemeral and intermittent streams, as well as features like Prairie potholes and Carolina bays, do demonstrate a "significant nexus" and, thus, fall under the jurisdiction of the Clean Water Act. However, the ruling also states that ephemeral channels must possess physical indicators of flow, including a high water mark and a defined bed and banks, for consideration as tributaries under the current definition. In 2017, the Environmental Protection Agency proposed a new rule to redefine "waters of the United States." Temporary hydrologic features presently remain under the protections of the Clean Water Act, but the exact definition of "waters of the United States" guides the implementation of best management practices (BMPs), pollution regulations, and urban and commercial development. Therefore, opposition to the current definition and proposed modifications to the ruling will certainly continue in the coming years.

1.1.3 Contributions of research on temporary stream length

Watershed conservation, policy, and research typically focus on perennial streams because of the perception that flow intermittency decreases the importance of temporary channels. However, temporary and spatially discontinuous flow actually increases the diversity of ecological functions. Metrics describing the length and connectivity of wet streams can provide more realistic estimates of aquatic habitat and indicate the relative contributions of aerobic and anaerobic biogeochemical processes along the channel through time. Predictions of the magnitude and frequency of network expansion and contraction in diverse settings can improve the accuracy of ecological models and calculations of watershed mass fluxes. Finally, inaccurate maps and limited access to headwater regions that contain an enormous length of ephemeral and intermittent channels (Buttle et al., 2012) contribute to the persistent underestimation of both the spatial expanse and ecological significance of temporary streams. Research that more accurately characterizes stream length and flow duration is critical for policymakers, landowners, and natural resource managers, but can also help increase awareness among the public of the importance and prevalence of temporary channels.

References

Alexander, R. B., Boyer, E. W., Smith, R. A., Schwarz, G. E., & Moore, R. B. (2007). The role of headwater streams in downstream water quality. *Journal of the American Water Resources Association*, *43*, 41-59.

Bärlocher, F., Mackay, R. J., & Wiggins, G. B. (1977). Detritus processing in a temporary vernal pool in southern Ontario. *Archiv fur Hydrobiologie*, *81*, 269-295.

Buttle, J. M., Boon, S., Peters, D. L., Spence, C., van Meerveld, H. J., & Whitfield, P. H. (2012). An overview of temporary stream hydrology in Canada. *Canadian Water Resources Journal*, *37*, 279-310.

Cohen, M. J., Creed, I. F., Alexander, L., Basu, N. B., Calhoun, A. J., Craft, C., ... & Jawitz, J. W. (2016). Do geographically isolated wetlands influence landscape functions? *Proceedings of the National Academy of Sciences*, *113*, 1978-1986.

Datry, T., Larned, S. T., & Tockner, K. (2014). Intermittent rivers: a challenge for freshwater ecology. *Bioscience*, *64*, 229-235.

Day, D. G. (1978). Drainage density changes during rainfall. *Earth Surface Processes*, *3*, 319-326.

Day, D. G. (1980). Lithologic controls of drainage density: A study of six small rural catchments in New England, NSW. *Catena*, *7*, 339-351.

Dodds, W. K., & Oakes, R. M. (2008). Headwater influences on downstream water quality. *Environmental Management*, *41*, 367-377.

Downing J. A., Cole J. J., Duarte C. M., Middelburg J. J., Melack J. M., Prairie Y. T., ... & Tranvik L. J. (2012). Global abundance and size distribution of streams and rivers. *Inland Waters*, *2*, 229-236.

Godsey, S. E., & Kirchner, J. W. (2014). Dynamic, discontinuous stream networks: Hydrologically driven variations in active drainage density, flowing channels and stream order. *Hydrological Processes*, *28*, 5791-5803.

Jaeger, K. L., & Olden, J. D. (2012). Electrical resistance sensor arrays as a means to quantify longitudinal connectivity of rivers. *River Research and Applications*, *28*, 1843-1852.

Jaeger, K. L., Olden, J. D., & Pelland, N. A. (2014). Climate change poised to threaten hydrologic connectivity and endemic fishes in dryland streams. *Proceedings of the National Academy of Sciences*, *111*, 13894-13899.

Larned, S. T., Datry, T., Arscott, D. B., & Tockner, K. (2010). Emerging concepts in temporary-river ecology. *Freshwater Biology*, *55*, 717-738.

Leibowitz, S. G., Wigington Jr, P. J., Rains, M. C., & Downing, D. M. (2008). Non-navigable streams and adjacent wetlands: addressing science needs following the Supreme Court's Rapanos decision. *Frontiers in Ecology and the Environment*, *6*, 364-371.

Skoulikidis, N. T., Sabater, S., Datry, T., Morais, M. M., Buffagni, A., Dörflinger, G., … & Rosado, J. (2017). Non-perennial Mediterranean rivers in Europe: status, pressures, and challenges for research and management. *Science of The Total Environment*, *577*, 1-18.

Stanley, E. H., Fisher, S. G., & Grimm, N. B. (1997). Ecosystem expansion and contraction in streams. *Bioscience*, *47*, 427-435.

Steward, A. L., von Schiller, D., Tockner, K., Marshall, J. C., & Bunn, S. E. (2012). When the river runs dry: Human and ecological values of dry riverbeds. *Frontiers in Ecology and the Environment*, *10*, 202-209.

Stubbington, R., England, J., Wood, P. J., & Sefton, C. E. (2017). Temporary streams in temperate zones: recognizing, monitoring and restoring transitional aquatic- terrestrial ecosystems. *Wiley Interdisciplinary Reviews: Water*, *4*, e1223.

Welter, J. R., & Fisher, S. G. (2016). The influence of storm characteristics on hydrological connectivity in intermittent channel networks: implications for nitrogen transport and denitrification. *Freshwater Biology*, *61*, 1214-1227.

Whiting, J. A., & Godsey, S. E. (2016). Discontinuous headwater stream networks with stable flowheads, Salmon River Basin, Idaho. *Hydrological Processes*, *30*, 2305-2316.

Zimmer, M. A., & McGlynn, B. L. (2018). Lateral, vertical, and longitudinal source area connectivity drive runoff and carbon export across watershed scales. *Water Resources Research*.

Chapter 2: Headwater stream length dynamics across four physiographic provinces of the Appalachian Highlands

Authors

Carrie K. Jensen

Kevin J. McGuire

Philip S. Prince

Abstract

Understanding patterns of expansion, contraction, and disconnection of headwater stream length in diverse settings is invaluable for the effective management of water resources as well as for informing research in the hydrology, ecology, and biogeochemistry of temporary streams. More accurate mapping of the stream network and quantitative measures of flow duration in the vast headwater regions facilitate implementation of water quality regulation and other policies to protect waterways. We determined the length and connectivity of the wet stream and geomorphic channel network in three forested catchments (< 75 ha) in each of four physiographic provinces of the Appalachian Highlands: the New England, Appalachian Plateau, Valley and Ridge, and Blue Ridge. We mapped wet stream length seven times at each catchment to characterize flow conditions between exceedance probabilities of < 5% and > 90% of the mean daily discharge. Stream network dynamics reflected geologic controls at both regional and local scales. Wet stream length was most variable at two Valley and Ridge catchments on a shale scarp slope and changed the least in the Blue Ridge. The density and source area of flow origins differed between the crystalline and sedimentary physiographic provinces, as the Appalachian Plateau and Valley and Ridge had fewer origins with much larger contributing areas than New England and the Blue Ridge. However, the length and surface connectivity of the wet stream depended on local lithology, geologic structure, and the distribution of surficial deposits such as boulders, glacially-derived material, and colluvial debris or sediment valley fills. Several proxies indicate the magnitude of stream length dynamics, including bankfull channel width, network connectivity, the base flow index, and the ratio of geomorphic channel to wet stream length. Consideration of

geologic characteristics at multiple spatial scales is imperative for future investigations of flow intermittency in headwaters.

2.0 Introduction

Nearly half of first- and second-order headwaters consist of temporary ephemeral and intermittent streams that expand and contract seasonally or in response to storm events (Nadeau & Rains, 2007; Buttle et al., 2012; Datry et al., 2014). Headwaters provide essential ecosystem services, including flood attenuation, biogeochemical cycling, and aquatic habitat (Larned et al., 2010) yet are challenging to characterize and study due to their dynamic nature, enormous extent, and remote or inaccessible locations. As a result, maps of the stream network are often inaccurate (Bishop et al., 2008; Skoulikidis et al., 2017). Common representations of river networks such as the National Hydrography Dataset (NHD) in the U.S. underestimate headwater length by up to 200% (Fritz et al., 2013) and fail to indicate the range of drainage density values that can easily span an order of magnitude (Gregory & Walling, 1968). The basic task of locating where and when streams are flowing has myriad implications for watershed policy and management activities like the delineation of riparian buffers and implementation of best management practices (BMPs). Quantitative data on the frequency and duration of flow in temporary streams across broad geographic regions would enable more targeted conservation efforts to ensure the ecological integrity of headwaters as well as downstream waterways.

Variability in headwater length produces a suite of landscape functions that shift through time. Channelized surface flow efficiently transports water, sediment, and solutes to water supplies destined for human consumption (Alexander et al., 2007) when stream length and connectivity are high. Accordingly, BMPs are more stringent for streams designated as perennial on maps (Blinn & Kilgore, 2001; National Research Council, 2002). Headwater networks often become discontinuous during low flows, with wet reaches separated by intervening dry channel segments (Stanley et al., 1997). Surface water-ground water exchange occurs between disconnected reaches via hyporheic flow paths that moderate water temperatures, provide habitat refugia, and facilitate biogeochemical reactions such as denitrification (Boulton et al., 1998). Alternating patches of flowing water, dry channel bed, and standing pools simultaneously transport, store, and process organic matter, nutrients, and toxins, creating opportunities for both aerobic and anaerobic transformations (Larned et al., 2010). In addition, Cohen et al.

(2016) emphasize the ecological benefits that result from a *lack* of surface or subsurface connection between water bodies. Dry channels serve as egg and seed banks for aquatic species and retention sites to slow the downstream movement of sediment, organic matter, and contaminants (Steward et al., 2012). Thus, metrics describing not only stream length but the connectivity and configuration of wet and dry reaches are necessary to accurately model available habitat and species distributions, pollutant transmission, and rates of biogeochemical processes.

Early hydrological investigations recognized that headwater stream length is not static (Hewlett & Hibbert, 1967; Gregory & Walling, 1968; Morgan, 1972; Roberts & Klingeman, 1972; Blyth & Rodda, 1973; Day, 1978; Day, 1980), but, as Godsey & Kirchner (2014) highlight, the topic was largely abandoned until the early 2000s, with some notable exceptions (Calver, 1990; De Vries, 1994). Following growing recognition of the legal considerations of headwaters and their significance for aquatic ecosystems (Doyle & Bernhardt, 2010; Acuña et al., 2014), interest in the expansion and contraction of temporary networks has renewed in recent years. However, measuring changes in stream length is challenging (Wharton, 1994). Several mapping studies involve walking the entire stream network of watersheds multiple times (Godsey & Kirchner, 2014; Shaw, 2016, Whiting & Godsey, 2016; Zimmer & McGlynn, 2017). Owing to the time and effort required to traverse rough terrain, field campaigns are usually limited to mapping a few catchments in the same region seasonally—e.g., 4 catchments over 3 or 4 mapping dates (Godsey & Kirchner, 2014; Whiting & Godsey, 2016)—or a single watershed more frequently—e.g., 12 (Shaw, 2016) or 77 mapping surveys (Zimmer & McGlynn, 2017). At a coarser scale, other studies locate intermittent and perennial flow origins during wet and dry seasons, respectively, without noting disconnections in the stream network or the position of origins during intermediate flows or after storms (Paybins, 2003; Jaeger et al., 2007; Russell et al., 2015; Brooks & Colburn, 2011). Electrical resistance sensors that detect the presence or absence of water are increasingly popular for monitoring channel wetting and drying at a fine temporal resolution (Jaeger & Olden, 2012; Goulsbra et al., 2014; Peirce & Lindsay, 2015). These sensors determine the timing of flow more accurately and require less data interpretation than temperature-based methods (Blasch et

al., 2002). Although electrical resistance sensors are one of the cheapest ways to automatically detect stream flow, the cost of $75-100 per sensor (Blasch et al., 2002; Chapin et al., 2014) renders dense instrumentation of large or multiple networks impractical. Aerial photographs (Wigington et al., 2005) and unmanned aerial vehicles can also aid temporary stream mapping, but image processing is labor-intensive, and clear views of the stream are not always possible in densely vegetated areas (Spence & Mengistu, 2016).

While temporary stream research continues to advance, headwater networks vary across the tremendous diversity of landscapes in the world, reflecting complex combinations of climatic, geologic, ecological, and land use factors (Costigan et al., 2016).). This inherent complexity precludes the generalization of a single, straightforward rule that encapsulates all headwater behavior (Bishop et al., 2008). Owing to the logistical difficulties of examining headwater processes over large areas, studies are almost always site-specific and conducted at the scale of small watersheds or even hillslopes. Although the detail possible at these finer scales is necessary to adequately characterize headwaters, we must extend our focus to understand regional trends that may be more applicable to managing water resources.

Costigan et al. (2016) recognize geology as one of the three major controls on flow permanence, in addition to climate and land cover. Studies demonstrate that the underlying geology correlates to the mobility of flow origins (Paybins, 2003; Jaeger et al., 2007; Winter, 2007) and variability of stream length (Day, 1980; Whiting & Godsey, 2016). Geology also impacts geomorphic channel development and the resulting drainage density (Hadley & Schumm, 1961; Abrahams, 1984). The purpose of this project is to further investigate the role of geology in headwater stream length dynamics along a physiographic gradient in the Appalachian Highlands. We mapped three catchments in each of four physiographic provinces seven times across multiple flow conditions. Research questions include: (1) How do stream length, network connectivity, and the number and upslope area of flow origins change with runoff and the associated exceedance probability? (2) At what flow does the wet stream approximate geomorphic

channel length? (3) Do stream length dynamics vary systematically by physiographic province?

2.1 Study Areas

We examined forested headwater catchments from study areas spanning four physiographic provinces of the Appalachian Highlands: the Hubbard Brook Experimental Forest (HB) of New Hampshire in New England, Fernow Experimental Forest (FNW) in the Appalachian Plateau of West Virginia, Jefferson National Forest at Poverty Creek (PVY) and the South Fork of Potts Creek (SFP) in the Valley and Ridge of Virginia, and the Coweeta Hydrologic Laboratory (CWT) in the Blue Ridge of North Carolina (Figure 1). HB, FNW, and CWT are experimental watersheds overseen by the U.S. Forest Service and, thus, have gauged catchments, long-term hydroclimatic datasets, and reference areas that do not undergo experimental manipulation. We chose PVY and SFP because of their location on National Forest, full coverage by mature forest, relatively easy access by road, and the availability of a 3 m Digital Elevation Model (DEM).

The study areas exhibit a range of climate (Table 1), geology (Table 2), topography (Table 2), and vegetation. HB is located in the central highlands of New England in the White Mountain National Forest. HB is the coldest site, and stream flow peaks in the late spring following snowmelt. Rounded, hummocky topography is typical of the glacial HB landscape. The study catchments are underlain by Lower Silurian pelitic schist and calc-silicate granulite of the Upper and Lower Rangeley Formation (Barton, 1997) and have a mantle of basal and ablation till and reworked glacial drift derived from Early Devonian granodiorite of the Kinsman Formation and other granitic, metasedimentary, and metavolcanic units (Bailey, S. et al., 2003).

FNW lies within the Allegheny Mountains of the Appalachian Plateau in the Monongahela National Forest. The greatest rainfall generally occurs from May to July in the form of high-intensity convective thunderstorms. The Alleghenies have a gently folded structure characterized by low-amplitude folds with strata displaying low (< 10°) and often nearly horizontal dip. Partial dissection of the landscape has produced steep

slopes leading to broad, flat uplands. Devonian shales and sandstones of the Hampshire Formation form the bedrock at FNW (Cardwell et al., 1968).

PVY and SFP are part of the Jefferson National Forest in Montgomery and Giles Counties, Virginia. The catchments lie in a rain shadow in the central Valley and Ridge, receiving the least precipitation of the study areas. Precipitation is usually highest from May to July, but stream flows peak during the winter and early spring. Erodibility contrasts within strongly folded and thrust faulted sedimentary rock in the Valley and Ridge create parallel ridges and distinct trellis drainage patterns. Bedrock at PVY is made up of Devonian shales, siltstones, and sandstones of the Brallier and Chemung Formations (Virginia Division of Mineral Resources, 1993). SFP is underlain by Devonian Oriskany sandstones at lower elevations and by Silurian Keefer and Rose Hill sandstones at higher elevations (Schultz et al., 1986).

CWT is located in the Nantahala National Forest in the Southern Blue Ridge Mountains. CWT is both the warmest and wettest of the study areas. Precipitation is greatest in the winter and early spring and increases with elevation (Laseter et al., 2012). Intensely deformed metamorphic rock is exposed in an extremely steep, rugged, and relatively high-elevation landscape. The substrate consists of Middle to Late Proterozoic biotite gneiss and amphibolite of the Coweeta Group and Tallulah Falls Formation (Hatcher, 1988) that has weathered into thick saprolite (on average 6 m; Price et al. 2005) due to the warm, humid climate.

Logging occurred at all sites through the early twentieth century. Second-growth forests range from primarily northern hardwoods at HB to oak-hickory associations at CWT. Unlike the other study areas, PVY and SFP are not part of an experimental forest and have been subject to more recent timber harvests. Forests at PVY and SFP are mature (~60 years old) but are estimated to be a few decades younger than at HB, FNW, and CWT.

2.2 Methods

2.2.1 Site selection

We selected three catchments smaller than 45 ha with no recent history of logging or experimental treatment in each study area (Table 2). SFP70 is the only exception at 70 ha. We determined during field work at HB and CWT that a 40-45 ha catchment requires a full day to map the stream network. Mapping larger watersheds over multiple days increases the risk of precipitation events in the humid Appalachians and widens the range of discharge pertaining to the mapped wet stream length. Perennial stream flow in the Appalachians frequently begins at smaller catchment source areas than in arid regions (Rivenbark & Jackson, 2004), so mapping downstream of persistent flow may not be necessary to address the question of stream length variability. However, many Valley and Ridge headwaters contract to a few isolated pools and flowing reaches during the late summer. We ultimately decided to include two Valley and Ridge catchments within the given size constraints (PVY25 & PVY35) and another larger site with a greater length of perennial flow (SFP70) to be consistent with the other study areas that all have perennial streams at the catchment outlets. For this study, we adhere to the definition of perennial channels by Hedman & Osterkamp (1982) as having flow present more than 80% of the year. Mapping of SFP70 was still possible within a day.

2.2.2 Field mapping of the stream network

We mapped the wet stream network of each catchment seven times at varying discharges. We follow the general terminology of Day (1980) and Goulsbra et al. (2014) by referring to the "wet" stream, but other studies use "flowing stream" (Calver, 1990; Godsey & Kirchner, 2014), "active channel network" (Shaw, 2016), "active drainage network" (Godsey & Kirchner, 2014; Peirce & Lindsay, 2015; Whiting & Godsey, 2016), and "active surface drainage length" (Zimmer & McGlynn, 2017). We did not want to use the term "flowing," as disconnected pools are not always visibly flowing downstream. Referring to surface water as "active" can imply that hyporheic exchange and ground water flow in the subsurface are inactive processes, unless specified as "active surface" water (Zimmer & McGlynn, 2017). We chose "wet stream" because the term is simple, encompasses both flowing reaches and standing pools, and avoids the term "channel,"

which corresponds to a geomorphic feature. However, we emphasize that "wet stream" only applies to surface water greater than 1 m in length and not to damp or saturated channel sediments.

We walked along the stream during each mapping from the outlet until we located the flow origin of every tributary. We continued walking upslope past the flow origins to make sure the origins were points of surface flow initiation rather than a network disconnection. Flow origins and disconnections were marked with a Bad Elf GNSS Surveyor Global Positioning System (GPS) unit. We also mapped the geomorphic channel at each site as reaches with defined banks (Dunne & Leopold, 1978) and sorted bed materials (Dietrich & Dunne, 1993) regardless of surface flow. The GPS unit has 1 m reported accuracy, but accuracy was normally between 3 and 10 m depending on vegetation cover and weather. Owing to the lower than reported accuracy, we used field notes and pin flags marking the wet stream in addition to the GPS points to compare stream length between mappings. The same individual performed all mappings with the same GPS unit to ensure the maximum consistency possible. We measured bankfull width and depth at 4 to 6 designated cross-sections distributed among the tributaries that had a simple channel pattern and were clear of woody debris. We recorded water width and depth at the cross-sections during each mapping as an indicator of the flow condition, since real-time stream discharge data were not always available. Field work was completed at HB in the summer of 2015, at FNW in the summer, fall, and winter of 2016, and at CWT and PVY/SFP in the fall of 2015 and winter, spring, and summer of 2016.

2.2.3 Stream discharge

Eight of the twelve study sites are gauged with weirs measuring stream flow at 5-minute intervals (sites that also have watershed numbers in Table 2). We developed flow duration curves for each of the gauged catchments using 10 years (2006-2015) of mean daily flow data. We determined discharge at the remaining catchments (HB25, PVY25, PVY35, & SFP70) during each field visit using salt dilution gauging (Calkins & Dunne, 1970). Pressure transducers installed at PVY25, PVY35, and SFP70 recorded stream stage every 30 minutes for six months to create a stage-discharge curve and provide a

continuous estimate of flow. We did not measure stage at HB25 because the site is adjacent to long-term gauged catchments (WS7 & WS8) of a similar size to permit an estimate of flow exceedance probabilities. We extended the six months of discharge data at PVY/SFP to 10 years (2006-2015) of mean daily flow values based on U.S. Geological Survey (USGS) gauges at John's Creek (02017500), Walker Creek (03173000), Wolf Creek (03175500), and the South Fork of the Roanoke (02053800) with the Streamflow Record Extension Facilitator (SREF version 1.0) software package from the USGS (Granato, 2009) to develop flow duration curves for the three Valley and Ridge catchments.

We strove to map the streams at flows between at least the 25 and 75% exceedance probabilities rather than major storms and droughts, as such extreme events are difficult to capture during a single field season. Hydrograph rises in response to storms occur rapidly in mountain streams and depend on antecedent moisture and the amount and duration of precipitation, which are hard to predict in advance. For this reason, we only mapped on the recession limb of events at least several hours after the hydrograph peak and compared discharge at the beginning and end of mapping to constrain the precision of our runoff (discharge normalized by catchment area) calculations. We consulted nearby USGS gauges for approximate flow conditions if real-time data for the study sites were not available.

2.2.4 Network delineation

We imported the GPS points into ArcGIS (ArcMap version 10.3.1, ESRI 2015, Redlands, CA) and digitized the stream network along lines of high flow accumulation according to the multiple triangular flow direction algorithm (Seibert & McGlynn, 2007) applied to 3 m DEMs for all sites. All DEM processing was completed in ArcGIS and the System for Automated Geoscientific Analyses software (SAGA version 2.3.1). The 1/9 arc-second DEMs for FNW, CWT, and SFP are from the West Virginia and North Carolina National Elevation Dataset of 2003. LiDAR data were collected during leaf-off and snow-free conditions at PVY in 2011 for the Virginia Geographic Information Network and at HB in 2012 by for the White Mountain National Forest. Bare earth DEMs classified from the

LiDAR datasets were re-sampled to 1 m and coarsened to 3 m via mean cell aggregation. We applied a low-pass (3 x 3) filter and sink-filling algorithm (Wang & Liu, 2006) to all DEMs for hydrological correction. We manually moved points located in low flow accumulation pixels due to GPS error to the nearest cell of high flow accumulation. We did not move points more than 3 pixels (9 m) based on the average GPS accuracy. Field notes aided this process to verify that point displacements were due to a change in stream length instead of positional error. Overall, we found the flow accumulation grid to be quite consistent with the GPS point locations.

We calculated several metrics from the digitized stream networks. We found wet drainage density by dividing the total length of wet reaches by the catchment area. Drainage density was similarly found for the geomorphic channel. Maximum network extent refers to the entire stream length from the outlet to flow origins, including intervening dry reaches. When considering subsurface flow between disconnected reaches, maximum network extent provides a more comprehensive stream length estimate. Network connectivity equals the total wet stream length divided by the maximum network (wet and dry) extent, and flow origin density is the number of origins normalized by catchment area. We also found the upslope area (Seibert & McGlynn, 2007) for each flow origin and geomorphic channel head. Following the method of Godsey & Kirchner (2014), we calculated the slope of the power-law relationship (β) between wet stream length and runoff for each site. We also determined Pearson product-moment correlation coefficients between β values and our wet stream and geomorphic channel metrics in addition to the base flow index (Lyne & Hollick, 1979) derived for each catchment.

2.3 Results

2.3.1 Wet stream pattern and metrics

We mapped the catchments across flows spanning exceedance probabilities of 3 and 90% at HB, 6 and 93% at FNW, 3 and 92% at PVY, 2 and 95% at SFP, and 0.1 and 99% at CWT (Figure 2). The pattern and flow duration of stream networks display contrasts between sites from both a planform (Figure 3) and longitudinal perspective (Figure 4).

The HB catchments produced numerous closely spaced tributaries in the plan view (Figure 3), whereas the network pattern was quite simple at FNW. Watersheds at CWT had one or two main channel stems but many bedrock springs that contributed short reaches along tributaries, which was most evident at CWT33. SFP70 developed short, isolated reaches at both high and low flows that did not form a surface connection with the rest of the network during any mappings. We observed that three of these high flow duration reaches were actually small wetlands at topographic lows with no inlet or outlet. The remaining reaches occurred on talus slopes or boulder-filled hollows. We heard water flowing under the boulders during the two wettest mappings; in these cases, water only emerged on top of the coarse deposits for short distances, possibly upon encountering a less conductive sediment lens. Coarse surficial material also coincided with the short, disconnected tributaries in the southeastern portion of HB42. Some of the larger stream disconnections at FNW37, CWT12, and CWT40 were associated with old landslide deposits where sediment depth locally increases. We observed that wetting and drying patterns at PVY and SFP frequently reflected the degree of valley confinement; reaches with steep valley side slopes and exposed bedrock had longer flow duration than unconfined sections with a wide, sediment-filled valley floor.

Stream longitudinal profiles suggest that higher-elevation tributaries that have not yet incised to the level of the main stem tended to dry up first, as was most evident for HB42, PVY25, PVY35, and CWT12 (Figure 4). In the case of HB42, the reaches with relatively low flow duration at shorter distances upstream were the southeastern disconnected tributaries in boulder deposits, which prevent channel downcutting (Figure 3). The streams at HB13 and HB25 all interestingly occurred at a similar elevation for a given distance upstream, perhaps corresponding to a water availability threshold or incision depth related to elevation.

Flow duration was greatest and most consistent at CWT and FNW14 and was lowest as well as more spatially variable at PVY (Figures 3 & 4). Wet drainage density (km/km^2) at each study area ranged across mapping periods from 1.8 to 11 at HB, 0.5 to 3.0 at FNW, 0.1 to 6.1 at PVY, 0.9 to 2.0 at SFP, and 3.2 to 6.1 at CWT. HB tended to have the

highest wet stream length for a given runoff (Figure 5) and associated exceedance probability (Figure 2). CWT sites maintained moderate-high stream lengths that changed little with discharge. FNW and PVY typically had shorter networks than HB and CWT for low flows with high exceedance probabilities, but more similar lengths at higher runoffs. Stream length at SFP did not decrease drastically at low runoffs like the other Valley and Ridge catchments at PVY, but rather followed a trajectory similar to FNW and HB.

The number and mean upslope area of flow origins differed markedly between physiographic provinces (Figure 5). FNW, PVY, and SFP in the Appalachian Plateau and Valley and Ridge had fewer flow origins with greater upslope areas than HB and CWT. Across all sites and mappings, HB in New England had the highest and most variable number of origins (Figure 6). Mean upslope area decreased slightly overall as runoff increased (Figure 5). Average upslope area was smallest at HB, but was also low for CWT. The number of flow origins remained practically the same for most mappings. One exception was SFP70, where the number of origins increased to reach a similar frequency as HB and CWT during high runoffs. However, SFP70 is almost twice the size of even the largest watersheds at the other study areas. Additionally, several of the new origins that developed at SFP70 belonged to short reaches in boulder deposits, which explains why wet stream length did not increase rapidly with runoff despite the proliferation of origins. A few origins activated or dried up at HB, PVY, and CWT watersheds, but only at the highest or lowest flows mapped.

Network connectivity varied widely at low flows, but generally increased with runoff (Figure 5). All CWT catchments remained highly connected, while the other study areas did not show consistent patterns. Connectivity did not always increase monotonically, as isolated reaches may activate at the extremities of dry tributaries during storms, decreasing the connected proportion of the now more extensive network. For SFP70, maximum connectivity actually occurred at a moderate runoff of 1 mm/day.

2.3.2 Geomorphic channel metrics

Geomorphic channel heads followed the same trends as flow origins, with fewer heads and larger mean upslope areas for FNW, PVY, and SFP (Table 3). Head density was highest at HB and lowest at SFP. We normalized bankfull width and depth measurements (m) by the logarithm of upslope area ($\log_{10}m^2$) at channel transects to calculate metrics of mean channel width and depth for each catchment (Table 3). Channels were wider at CWT and FNW and slightly deeper at HB. Similar to wet stream length, drainage density of the geomorphic channel was greatest at HB and shortest at FNW and SFP. However, PVY25 and PVY35 had fairly high geomorphic drainage density values despite producing low to moderate wet stream lengths on average. To compare the geomorphic and wet networks, we normalized the geomorphic drainage density by the estimated wet drainage density at exceedance probabilities of 25, 50, and 75% (Table 3). Because wet stream length hardly changed at CWT, all three geomorphic-wet drainage density ratios were near 1. For HB, FNW, and SFP, drainage density of the wet stream approached that of the geomorphic channel between exceedance probabilities of 25 and 50%, although the drainage density ratios remained slightly above 1 at HB25, FNW16, FNW37, and SFP70. Conversely, the ratios were all much greater than 1 at PVY, indicating that the eroded channel extended beyond the normal limits of the wet network. We should emphasize that the locations of the channel and wet stream did not always coincide. For example, we observed that reaches below small seeps at HB contained water at even the driest conditions mapped but did not necessarily have a defined channel bed owing to low flow rates. On the other hand, some reaches that possessed a geomorphic channel almost never carried flow.

2.3.3 Rates and correlates of network expansion

Slope values of the power-law function between wet stream length and runoff (β) were quite low for CWT and FNW14 (Table 4). At CWT, we performed one set of mappings at a particularly high flow that surpassed several of the peak floods on record and had an exceedance probability of less than 1% in terms of mean daily flow. Despite the sizeable storm, stream length barely grew (Figure 5). Aside from CWT, β values were highly variable among sites within the same physiographic province. The greatest β values

occurred at PVY35, HB25, and PVY25, indicating considerable network expansion and contraction (Table 4).

There was a significant negative correlation between bankfull width and β (Table 5). The narrowest channels in our study were at PVY25 and PVY35, which had two of the highest β values. A negative correlation also existed for bankfull depth but was not significant. The geomorphic-wet drainage density ratios were positively correlated to β, so streams that underwent greater changes in length commonly had a geomorphic channel that extended beyond the wet network. β was inversely related to the base flow index (Figure 7). The most significant relationships were for the mean and coefficient of variation of surface network connectivity across mappings. A negative correlation for the mean and positive correlation for the coefficient of variation suggests that networks with highly dynamic lengths had lower surface connectivity.

2.4 Discussion

2.4.1 Wet stream length dynamics

Basic rock type strongly correlates with the number and upslope contributing area of flow origins in the study catchments. Sites underlain by sedimentary rock at FNW, PVY, and SFP in the Appalachian Plateau and Valley and Ridge have fewer flow origins with greater upslope areas than catchments with crystalline substrate at HB and CWT (Figure 5). Jaeger et al. (2007) also attribute contrasts in upslope area in the Washington Coast Range to lithology, although, in this case, origins form at smaller source areas in sedimentary rock than in basalt watersheds. Paybins (2003) reports upslope areas of 3 to 18 ha for intermittent flow origins in the Appalachian Plateau, which are comparable but mostly larger than values for FNW. Streams at HB and CWT begin much higher in the watershed at contributing areas of less than 1 ha. Previous work at HB likewise discovered flow initiation at small upslope areas of 0.25 ha or less (Zimmer et al., 2013). However, the mean upslope area values at CWT are an order of magnitude lower than those found by Rivenbark & Jackson (2004) at nearby sites in the Blue Ridge. This study may not have included short reaches below bedrock springs that are common in the Blue Ridge, which could account for the discrepancy.

The number of flow origins changes little with runoff, with the exception of SFP70 (Figure 5). Whiting & Godsey (2016) also observed relatively stationary origins at their Idaho watersheds, although Godsey & Kirchner (2014) determined that the number of origins increases with runoff according to a power-law function for sites in California. In addition to the distinct regional setting of our study, this disagreement may be due to the exclusion of wet reaches shorter than 10 m by Godsey & Kirchner (2014) to match the available DEM resolution and GPS accuracy. Some of the tributaries at our sites contract to a single pool near the upstream end of the network during dry conditions, as is the case for the southwest branch of PVY35 (Figures 3 & 4), which would otherwise be omitted following the 10 m rule. While such small reaches are inconsequential for some purposes, these locations can serve as habitat refugia (Jaeger & Olden, 2012) and often maintain subsurface connection to downstream waters (Boulton et al., 1998). A small decrease in mean upslope area with increasing runoff accompanies the fairly consistent number of flow origins (Figure 5), signaling that network expansion and contraction mostly proceed by coalescence and disintegration of wet reaches (Bhamjee & Lindsay, 2011; Peirce & Lindsay, 2015) and, to a lesser extent, the migration of origins. Activation and deactivation of entire tributaries typically only occur at short reaches amid boulder fields at SFP70 or during quite wet or dry conditions (exceedance probabilities less than 25% or greater than 75%) at HB, PVY, and CWT (Figure 2).

Wet drainage density varies from 0.1 to 11 km/km^2 at our sites, which corresponds with values found in the western U.S. (Roberts & Klingeman, 1972; Wigington et al., 2005; Godsey & Kirchner, 2014; Whiting & Godsey, 2016), England (Gregory & Walling, 1968; Blyth & Rodda, 1973), and Australia (Day, 1978; Day, 1980). However, Goulsbra et al. (2014) measured a maximum wet drainage density of 30 km/km^2 in a peatland catchment in England. Stream length has a minor tendency to be highest at HB and CWT (Figure 5), but β slope values reveal more pronounced distinctions between sites (Table 4). The β values for our catchments range from 0.04 to 0.71, which is nearly identical to the range of 0.02 to 0.69 that Godsey & Kirchner (2014) report from the literature. Our project does not characterize the wet network across all seasons, antecedent conditions, or extreme events, so the actual variability is undoubtedly greater. Stream length at CWT

remains stable and highly connected for all mappings (Figure 5). Studies show that streams underlain by sedimentary rock generally have shorter flow durations, a wider range of lengths, and more network disconnections than in granite basins (Day, 1980; Whiting & Godsey, 2016). Likewise, streams lengths are less consistent at FNW, PVY, and SFP (Table 4), which lie in sandstones and shales (Table 2), than at CWT. However, the β value at FNW14 is practically the same as those at CWT. Furthermore, the glaciated HB catchments have β values similar to sites in the sedimentary Valley and Ridge and Appalachian Plateau. Thus, factors such as geologic structure and the depth, grain size distribution, and resulting water storage and permeability of surficial material must also influence stream length dynamics. In the case of CWT, the warm, humid climate has weathered deep, permeable soils that are able to transport and store huge volumes of subsurface flow between storms (Hewlett & Hibbert, 1963; Hatcher, 1988) to supply streams with perennial, connected flow.

2.4.2 Relationship between the geomorphic and wet stream networks

The geomorphic channel matches the wet stream almost exactly at CWT, but geomorphic and wet drainage density values converge at different flows for the remaining study areas (Table 3). At HB, FNW, and SFP, the geomorphic and wet drainage densities are nearly equal at moderate-high runoffs between exceedance probabilities of 25 and 50%. The geomorphic channel extends past the mapped wet network at PVY, even for an exceedance probability of 25%, instead representing events with longer recurrence intervals. Adams & Spotila (2005) found that channel-forming flows for steep headwater streams without floodplains in the Valley and Ridge have recurrence intervals on the order of decades. Despite residing in the Valley and Ridge, the geomorphic network at SFP70 reflects smaller, more frequent events like at HB and FNW. Both Day (1980) and Jaeger et al. (2007) note that the eroded channel is longer than the wet stream in sedimentary basins, which holds true for FNW, PVY, and SFP for exceedance probabilities greater than 50%. However, drainage density ratios at HB indicate that the geomorphic network is more extensive than the wet stream at these sites as well, even though the substrate is not sedimentary rock.

We should be careful to distinguish geomorphic channels and wet streams in research as well as policy, as the relationship between these features is not the same everywhere. Currently, decisions regarding stream networks often depend on the expression of the geomorphic channel. The final ruling of the U.S. Clean Water Act (33 CFR § 328) in 2015 mandates that ephemeral streams lacking physical indicators of flow, including a defined channel bed and banks, are not considered tributaries that fall under federal jurisdiction. While several of the catchments in our study have longer geomorphic networks than the wet stream at most flows, the actual locations of the channel and stream do not always coincide. Channel scouring is more likely where the landscape is locally steep or confined and can concentrate sufficient stream power to erode a bed at high runoffs (Bull, 1979; Taylor & Kite, 2006). On the other hand, we observed some perennial reaches that always carry water but do not have a defined channel. The recurrence interval of channel-forming flows also varies from less than 1 (Powell et al., 2006) to 10s of years (Adams & Spotila, 2005), so geomorphic channels represent floods of different magnitudes. Therefore, we risk misunderstanding the actual range of stream lengths and their associated flow duration by only considering geomorphic channel dimensions.

2.4.3 Regional versus local geology

Physiographic provinces, which define regions of similar rock type and structure, distinguish sites by the number and source area of flow origins and indicate approximate stream lengths (Figure 5). HB in New England exhibits high wet stream lengths, the greatest density of flow origins, and the smallest upslope areas. Stream length and origin density are moderately high and upslope areas are low at CWT in the Blue Ridge, but network dynamics are minimal. FNW in the Appalachian Plateau and PVY/SFP in the Valley and Ridge produce a small number of flow origins with source areas that are nearly an order of magnitude larger than those at HB and CWT. Despite these trends, the geomorphic networks and wetting and drying patterns of catchments within a single physiographic province reflect local geologic features.

PVY and SFP in the Valley and Ridge exemplify the impacts of site-specific geology on channel development. Bedrock consists of nonresistant shales at PVY and highly resistant sandstones at SFP (Table 2). Streams incise extensive networks of deep, V-shaped gullies into the erodible shales underlying PVY (Mills, 1981; Mills et al., 1987); the resulting geomorphic channel is much longer than the wet stream most of the time (Table 3). Geomorphic channel head and drainage density are lower at SFP and are closer to values for FNW in the Appalachian Plateau. A caprock of resistant Keefer and Rose Hill sandstones at SFP weathers into large boulders that fill stream hollows and prevent the downcutting of ravines with steep side slopes that is evident at PVY (Mills, 1981). Such coarse boulder deposits transport water without a need for lengthening surface flow and forming a geomorphic channel. Incidentally, although the geomorphic network is several times longer at PVY than SFP, the channels are narrower in width (Table 3). This observation suggests that PVY and SFP develop unique channel geometries to efficiently remove runoff and sediment according to the underlying rock type.

Local lithology additionally correlates to the variability of wet stream length at PVY and SFP. Shales have lower permeability and produce less base flow (Carlston, 1963) than more permeable sandstones. Smaller proportions of base flow in impermeable geology increase the likelihood that streams will contract or dry up (Winter, 2007) and create a higher eroded drainage density, owing to the predominance of quick runoff (Carlston, 1963). Our results similarly show that wet stream length has greater and more consistent flow duration with lower β values at SFP than at PVY (Figures 3 & 4; Table 4) and that the geomorphic channel is shorter. Kowall (1976) and Paybins (2003) also report greater, less variable summer low flows and a greater chance of perennial flow in basins underlain by sandstone rather than siltstone and shale. The significant inverse relationship between the base flow index and β (Figure 7) further indicates that flashier streams with a lower proportion of base flow experience more network dynamics.

Geologic structure provides another potential control on stream length dynamics. PVY is located on the scarp slope of a homoclinal ridge and cross-cuts various bedding planes, creating secondary permeability in an otherwise relatively impermeable shale. The

alternation of strata along a scarp slope produces opportunities for water to discharge from or infiltrate into the rock, depending on the porosity and permeability of the geologic layer. We observed that the sequence of high and low flow duration reaches along the PVY25 and PVY35 tributaries (Figure 3) largely follows local valley width, which can vary as a function of lithofacies resistance (Taylor & Kite, 2006). Valley confinement also explains patterns of network contraction in desert streams examined by Stanley et al. (1997), with wide, unconstrained reaches drying first. The bands of low flow duration in PVY25 occur at the same relative watershed position in all three tributaries, possibly corresponding to distinct stratigraphic layers within the shale and sandstone units exposed on the scarp slope. SFP and FNW, on the other hand, are on the dip slopes of folds. These catchments remain more connected and have greater flow durations than PVY conceivably because, in part, the streams flow along the top of the strata rather than across multiple layers. Further research at additional sites is necessary to better quantify the impacts of lithology versus structure on wet stream length.

Subwatershed-scale geology may explain discrepancies in β values that are also notable between catchments in other study areas. For example, the β value at HB25 is two to three times that of the other HB sites (Table 4). The till deposits overlying the bedrock at HB are heterogeneous in terms of depth (reaching 5-8 m in HB42; Benettin et al., 2015), grain size, and sorting. Boulder deposits are a common feature of poorly-sorted glacial material and are present in much of HB25 as well as the southeastern section of HB42, where streams are short and disconnected (Figure 3). Deep or coarse surficial material transmits water easily in the subsurface and may reduce the need for surface flow at low runoffs, which would account for the higher β value. Nonetheless, the inherent spatial heterogeneity of glacial till decreases the predictability of stream length dynamics, as is also evident from the large variation in flow origin density at HB in comparison to the other study areas (Figure 6).

As Costigan et al. (2016) describe, flow permanence is a function of geologic attributes operating at spatial scales ranging from sediment particles to watersheds. Consideration of geology at all scales is essential to comprehensively characterize stream intermittency.

Because of the time and expense associated with data collection, understanding the information available at each scale can help focus efforts for a particular research question or management goal. Our work suggests that larger physiographic regions or basic rock type (e.g., sedimentary or crystalline) may be sufficient to estimate the relative frequency and mean upslope area of flow origins. To approximate the degree of network expansion and contraction in a catchment, knowledge of the lithology and structure may be necessary. More detailed mapping of lithofacies and surficial material can locate specific stream disconnections. The appropriate scale of analysis ultimately depends on the informational needs of a particular project.

2.4.4 Predictors of stream length variability

Repeated stream mappings and thorough geologic characterization are essential to accurately represent the length and flow duration of headwaters. However, field mapping is time-intensive, and high resolution geologic maps are not always available. Forgoing these data, we found that fairly simple measurements can serve as useful proxies of network dynamics. The negative correlation between bankfull width and β (Table 5) demonstrates that wide channels are able to accommodate a huge range of flows without needing to lengthen. CWT and FNW have the widest channels in our study, although Day (1980) observed that channels are usually wider in crystalline granite than in sedimentary basins. Bankfull width is easy to measure and compare between catchments as a first approximation of stream length variability.

Streams with less base flow and a geomorphic channel that extends past the wet network most of the time undergo greater changes in length. Calculation of the base flow index from discharge data is simple, objective, and can be performed remotely. Base flow proportions do vary with watershed size, but a regional base flow index can be estimated from USGS gauges. Finally, surface connectivity of the wet stream is the most significant indicator of network expansion and contraction. Streams with low mean connectivity also tend to have the most variable connectivity and extreme length dynamics. Thus, although these streams are more disconnected on average, the flow becomes nearly continuous during wet conditions. Such catchments have the potential to provide a greater diversity

of landscape functions than networks that remain mostly connected at all times, like CWT. Stream mapping is the most reliable, albeit time-consuming, method to determine network connectivity, although unmanned aerial vehicles and other technologies may ease this burden in the future (Spence & Mengistu, 2016).

2.5 Conclusion

Our results demonstrate that wet stream length in headwaters varies regionally by physiographic province. New England and the Blue Ridge have high stream length and flow origin density, although the Blue Ridge streams remain mostly connected and undergo far less expansion and contraction than the remaining study areas. In comparison, catchments in the Appalachian Plateau and Valley and Ridge have fewer flow origins with much larger drainage areas than in the other two provinces. Site lithology, geologic structure, and surficial materials superimpose additional controls on headwater behavior. For example, shale bedrock on a scarp slope corresponds to lower flow duration, a more extensively eroded geomorphic channel network, and higher coefficients describing the degree of network expansion with increasing runoff (β) than for sandstone catchments in the same Valley and Ridge province. Transmissive surficial deposits of coarse boulders or deep sediment valley fills reduce the need for surface flow and coincide with stream disconnections. Simple measurements permit an approximation of β values, as streams with wide channels, more base flow, high surface connectivity, and little difference between the geomorphic and wet stream networks change less in length with runoff.

Stream mapping is labor-intensive and usually limited to small areas. Forgoing field surveys of all headwaters, some level of generalization by geographic region, climate zone, geologic unit, or land cover class is necessary to inform watershed management. However, traditional divisions may not suffice for the optimum classification of headwaters. For example, the Appalachian Mountains are often considered a single entity, but β values from our study span the entire range of those reported in the literature from catchments around the world. More data on wet stream length in distinct locations will help inform the appropriate criteria and scale by which to categorize headwaters for

various policy initiatives. Our study only examines forested watersheds, so other factors likely influence stream wetting and drying in agricultural and urban environments. In addition to obvious relevance for surface water policy, this and similar work has implications for mass fluxes of sediment and solutes from headwaters, organism dispersal and refugia, biogeochemical transformations, and furthering our understanding of the processes that generate surface flow in watersheds.

Figures and Tables

Table 1. Average climatic attributes of the four study areas.

Study area	Mean January/July temperature (°C)	Mean annual precipitation (cm)	Snowfall (% of precipitation)	Reference
HB	-9/18	140	33	Bailey, A. et al. (2003)
FNW	-3/20	146	15	Adams et al. (1994); Adams et al. (2012)
PVY/SFP	-1/22	100	5	SERCC (2012) (Blacksburg, Radford, and Staffordsville)
CWT	3/21	179	2	Laseter et al. (2012)

Table 2. Characteristics of the study catchments.

Physiographic province	Study area	Site name[a] (watershed number[b])	Latitude (°N), Longitude (°W)	Drainage area[c] (ha)	Aspect	Mean elevation[c] (m)	Mean slope[c] (%)	Geology
New England	HB	HB13 (WS 6)	43.95, 71.74	13.4	SE	690	28	schist, granulite
		HB25	43.93, 71.77	25.1	NW	740	28	schist, granulite
		HB42 (WS 3)	43.96, 71.72	42.4	S	632	28	schist, granulite
Appalachian Plateau	FNW	FNW14 (WS 13)	39.06, 79.70	13.9	NE	773	32	shale, sandstone
		FNW16 (WS 10)	39.05, 79.68	15.7	SW	767	31	shale, sandstone
		FNW37 (WS 4)	39.05, 79.69	36.6	SE	822	22	shale, sandstone
Valley and Ridge	PVY	PVY25	37.28, 80.46	25	NW	750	32	shale, sandstone
		PVY35	37.26, 80.48	34.8	N	729	35	shale, sandstone
	SFP	SFP70	37.45, 80.49	69.9	S	1029	27	sandstone
Blue Ridge	CWT	CWT12 (WS 18)	35.05, 83.44	12.4	NW	823	53	gneiss, amphibolite
		CWT33 (WS 34)	35.06, 83.45	32.7	SE	1019	51	gneiss, amphibolite
		CWT40 (WS 32)	35.05, 83.46	39.6	E	1052	44	gneiss

[a]Numbers in site name correspond to the drainage area in hectares
[b]If applicable, for gauged catchments at the experimental forests with a designated watershed number
[c]As determined from 3 m DEMs

Table 3. Geomorphic channel attributes and geomorphic-wet drainage density ratios.

Site	Mean UA[a] (ha)	Channel head density (heads/km^2)	Mean bankfull width/UA (m/log$_{10}$m^2)	Mean bankfull depth/UA (m/log$_{10}$m^2)	DD[b] (km/km^2)	DD[b]/75[c]	DD[b]/50[c]	DD[b]/25[c]
HB13	0.25	67.11	0.31	0.08	8.65	1.21	1.04	0.90
HB25	0.37	39.81	0.32	0.05	6.65	2.85	1.73	1.05
HB42	0.51	40.12	0.31	0.05	6.68	1.44	1.12	0.92
FNW14	1.14	14.43	0.54	0.06	2.74	1.14	1.05	0.97
FNW16	3.93	6.37	0.42	0.04	2.29	1.96	1.38	1.06
FNW37	2.57	8.19	0.38	0.05	2.43	1.81	1.39	1.13
PVY25	0.82	15.97	0.27	0.05	6.79	6.82	3.65	1.95
PVY35	2.13	11.49	0.24	0.03	4.91	41.49	11.89	3.41
SFP70	3.90	5.72	0.33	0.04	1.67	1.56	1.28	1.05
CWT12	0.91	32.35	0.42	0.04	5.10	1.06	0.98	0.92
CWT33	0.47	15.30	0.33	0.05	3.06	0.99	0.96	0.93
CWT40	0.37	27.76	0.47	0.04	4.72	1.03	1.00	0.98

[a]Upslope area (Seibert & McGlynn, 2007) of the geomorphic channel heads

[b]Drainage density of the geomorphic network

[c]Wet drainage density associated with the 25, 50, and 75% exceedance probabilities (km/km^2)

Table 4. β (± standard error) and the associated R^2 values of the power-law function between wet stream length and runoff for each site.

Site	β	R^2
HB13	0.15 (±0.020)	0.92
HB25	0.59 (±0.033)	0.98
HB42	0.24 (±0.023)	0.95
FNW14	0.06 (±0.004)	0.97
FNW16	0.26 (±0.043)	0.88
FNW37	0.18 (±0.017)	0.96
PVY25	0.43 (±0.020)	0.99
PVY35	0.71 (±0.065)	0.96
SFP70	0.14 (±0.006)	0.99
CWT12	0.08 (±0.016)	0.84
CWT33	0.04 (±0.006)	0.91
CWT40	0.04 (±0.008)	0.82

Table 5. Pearson correlations (r) between variables and β. Bold indicates significance at p = 0.05. See Table 3 for abbreviations.

Variable	r
Mean UA (ha)	0.35
Channel head density (heads/km^2)	-0.05
Mean bankfull width/UA (m/m^2)	**-0.65**
Mean bankfull depth/UA (m/m^2)	-0.19
DD (km/km^2)	0.33
DD/75	**0.73**
DD/50	**0.76**
DD/25	**0.76**
Base flow index (Lyne and Hollick, 1979)	**-0.69**
Network connectivity—mean	**-0.88**
Network connectivity—coefficient of variation	**0.92**

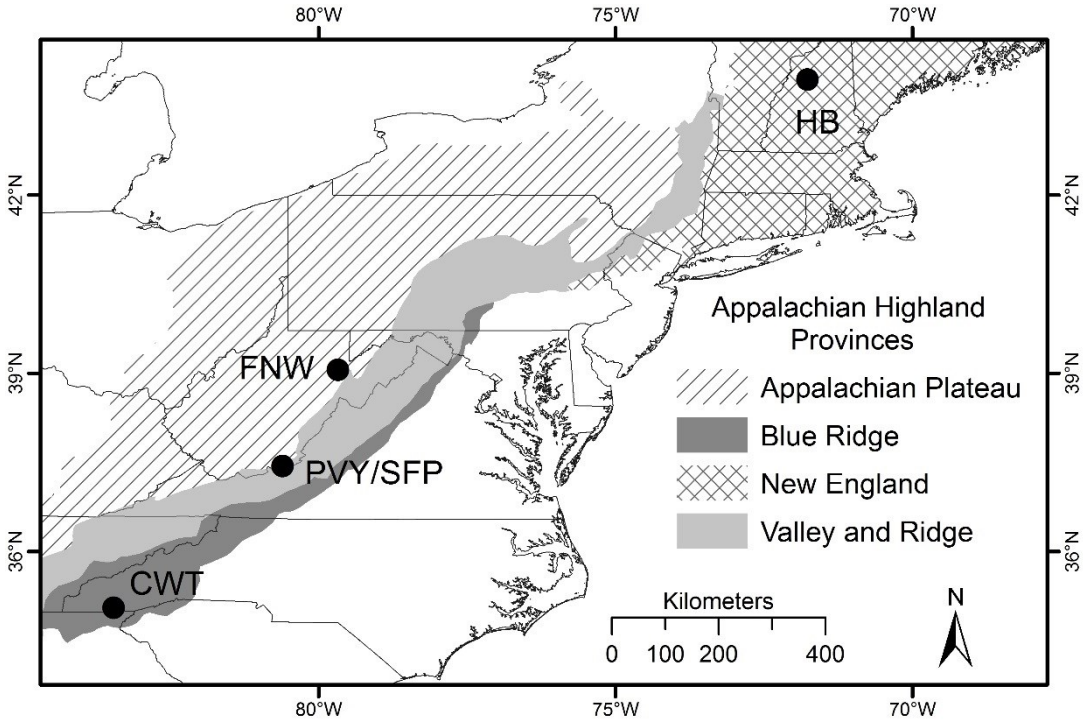

Figure 1. Study areas.

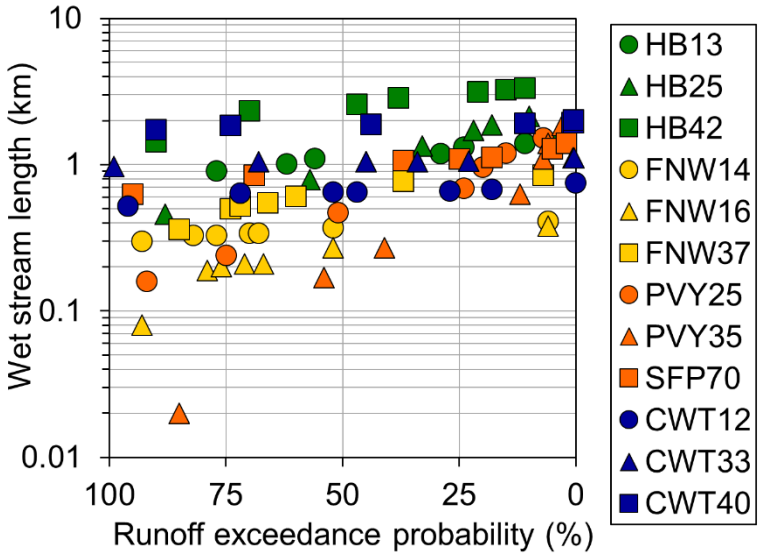

Figure 2. Wet stream length versus the exceedance probability of the runoff for each mapping, as determined from flow duration curves of mean daily flow from 2006-2015. Colors correspond to physiographic province: green for New England, yellow for Appalachian Plateau, orange for Valley and Ridge, blue for Blue Ridge.

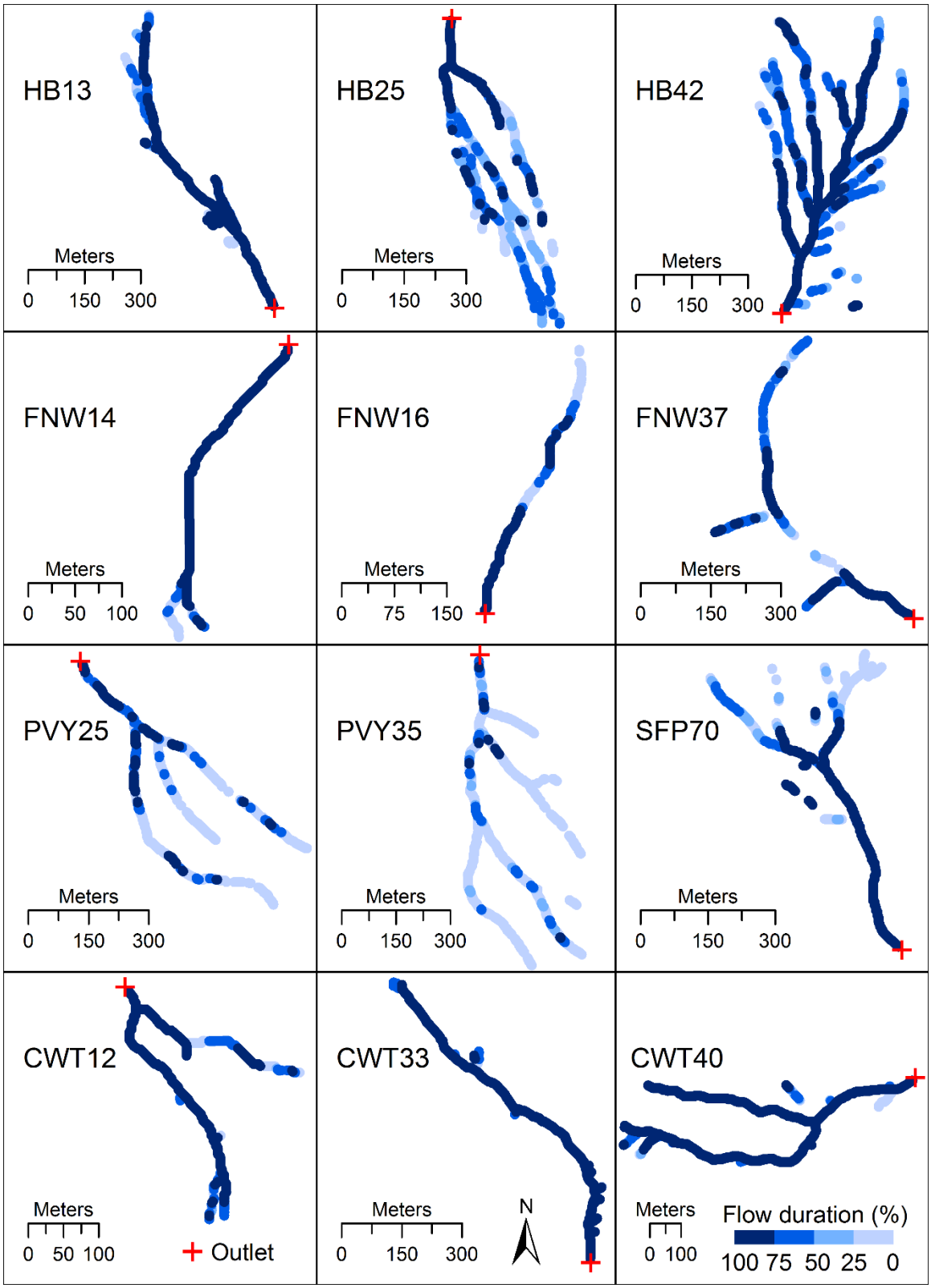

Figure 3. Planform view of the wet stream network.

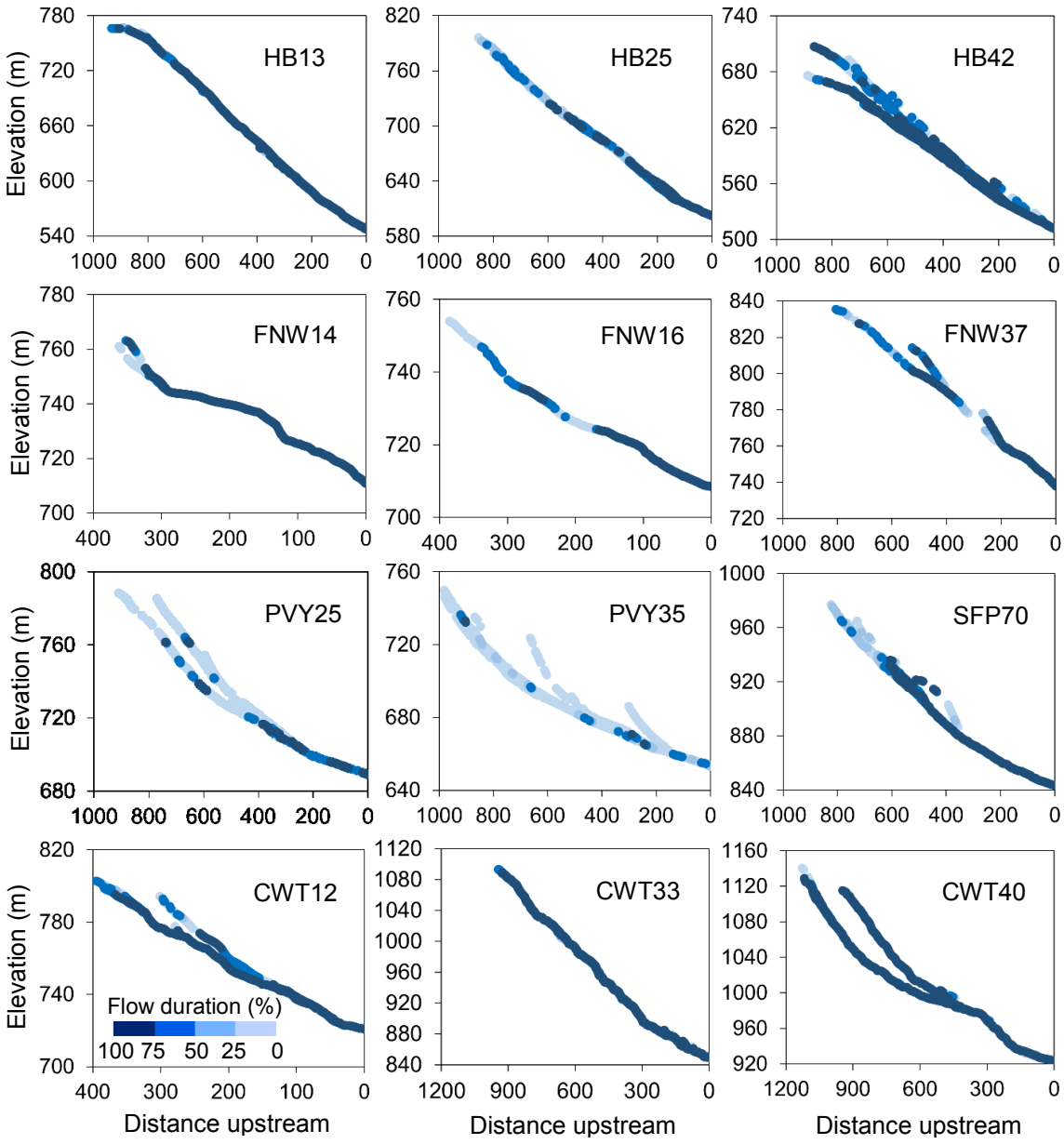

Figure 4. Longitudinal profiles of the wet stream network.

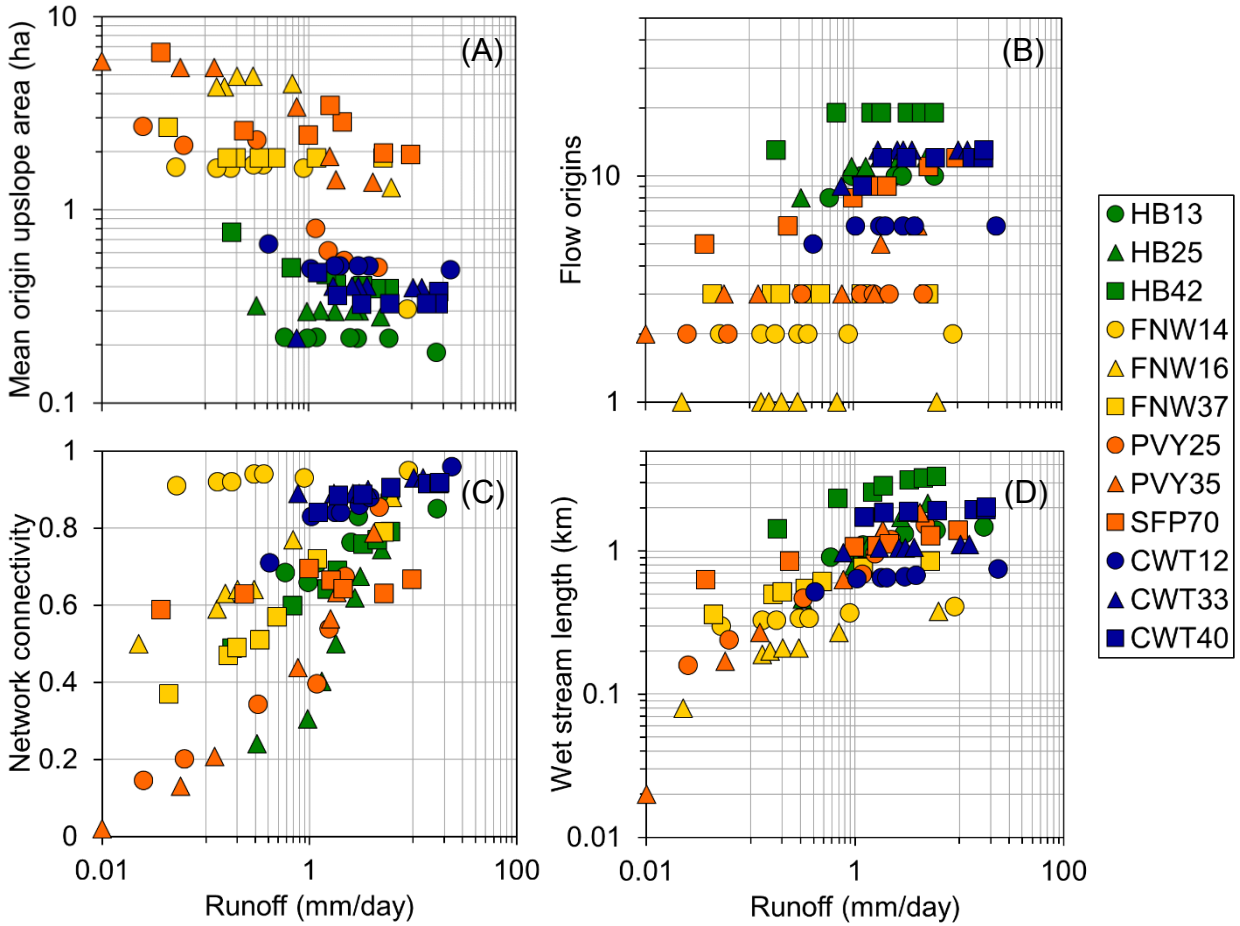

Figure 5. Mean upslope area of flow origins (A), number of flow origins (B), network surface connectivity (C), and wet stream length (D) versus runoff for each mapping. Color scheme same as Figure 2.

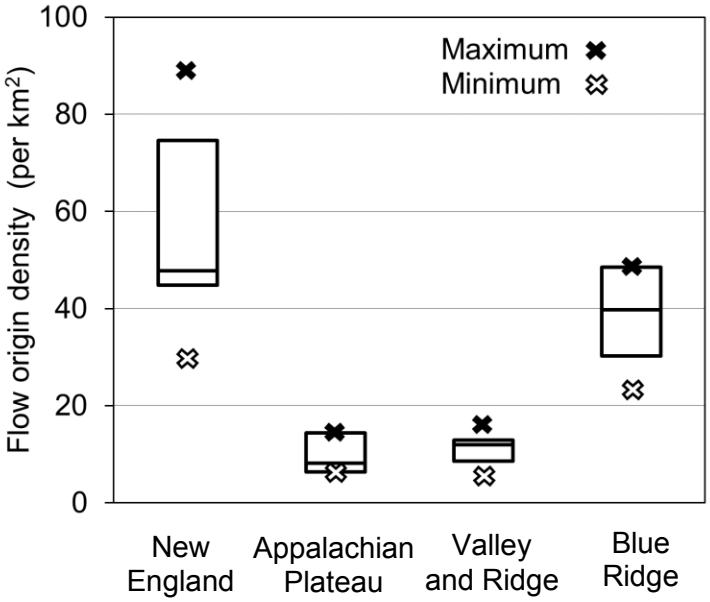

Figure 6. Flow origin density by physiographic province. Each box plot represents data from 21 mappings (3 catchments in each province; 7 mappings per catchment).

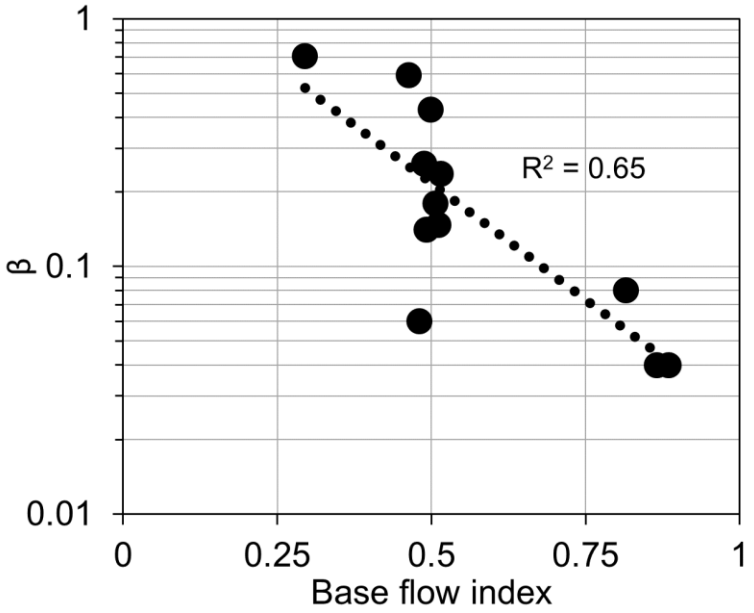

Figure 7. Base flow index (Lyne and Hollick, 1979) versus β. Trendline shows an exponential function.

References

Abrahams, A. D. (1984). Channel networks: a geomorphological perspective. *Water Resources Research*, *20*, 161-188.

Acuña, V., Datry, T., Marshall, J., Barceló, D., Dahm, C. N., Ginebreda, A., … & Palmer, M. A. (2014). Why should we care about temporary waterways?. *Science*, *343*, 1080-1081.

Adams, M. B., Kochenderfer, J. N., Wood, F., Angradi, T. R., & Edwards, P. (1994). Forty years of hydrometeorological data from the Fernow Experimental Forest, West Virginia. U.S. Department of Agriculture, Forest Service, Northeastern Forest Experiment Station.

Adams, R. K., & Spotila, J. A. (2005). The form and function of headwater streams based on field and modeling investigations in the Southern Appalachian Mountains. *Earth Surface Processes and Landforms*, *30*, 1521-1546.

Adams, M. B., Edwards, P. J., Ford, W. M., Schuler, T. M., Thomas-Van Gundy, M., & Wood, F. (2012). Fernow Experimental Forest: research history and opportunities. U.S. Department of Agriculture, Forest Service, Experimental Forests and Ranges.

Alexander, R. B., Boyer, E. W., Smith, R. A., Schwarz, G. E., & Moore, R. B. (2007). The role of headwater streams in downstream water quality. *Journal of the American Water Resources Association*, *43*, 41-59.

Bailey, S. W., Buso, D. C., & Likens, G. E. (2003). Implications of sodium mass balance for interpreting the calcium cycle of a forested ecosystem. *Ecology*, *84*, 471-484.

Bailey, A. S., Hornbeck, J. W., Campbell, J. L., & Eagar, C. (2003).Hydrometeorological database for Hubbard Brook Experimental Forest: 1955-2000, 305. U.S. Department of Agriculture, Forest Service, Northeastern Research Station.

Barton, C.C. (1997). Bedrock geologic map of Hubbard Brook Experimental Forest and maps of fractures and geology in roadcuts along Interstate 93, Grafton County, New Hampshire, Scale 1:2000. U.S. Geological Survey Miscellaneous Investigation Series I-2562.

Benettin, P., Bailey, S. W., Campbell, J. L., Green, M. B., Rinaldo, A., Likens, G. E., McGuire, K. J., & Botter, G. (2015). Linking water age and solute dynamics in streamflow at the Hubbard Brook Experimental Forest, NH, USA. *Water Resources Research*, *51*, 9256–9272.

Bhamjee, R., & Lindsay, J. B. (2011). Ephemeral stream sensor design using state loggers. *Hydrology and Earth System Sciences*, *15*, 1009-1021.

Bishop, K., Buffam, I., Erlandsson, M., Fölster, J., Laudon, H., Seibert, J., & Temnerud, J. (2008). Aqua Incognita: The unknown headwaters. *Hydrological Processes*, *22*, 1239-

1242.

Blasch, K. W., Ferré, T., Christensen, A. H., & Hoffmann, J. P. (2002). New field method to determine streamflow timing using electrical resistance sensors. *Vadose Zone Journal*, *1*, 289-299.

Blyth, K., & Rodda, J. C. (1973). A stream length study. *Water Resources Research*, *9*, 1454-1461.

Boulton, A. J., Findlay, S., Marmonier, P., Stanley, E. H., & Valett, H. M. (1998). The functional significance of the hyporheic zone in streams and rivers. *Annual Review of Ecology and Systematics*, *29*, 59-81.

Brooks, R. T., & Colburn, E. A. (2011). Extent and channel morphology of unmapped headwater stream segments of the Quabbin watershed, Massachusetts. *Journal of the American Water Resources Association*, *47*, 158-168.

Bull, W. B. (1979). Threshold of critical power in streams. *Geological Society of American Bulletin*, *90*, 453-464.

Buttle, J. M., Boon, S., Peters, D. L., Spence, C., van Meerveld, H. J., & Whitfield, P. H. (2012). An overview of temporary stream hydrology in Canada. *Canadian Water Resources Journal*, *37*, 279-310.

Calkins, D., & Dunne, T. (1970). A salt tracing method for measuring channel velocities in small mountain streams. *Journal of Hydrology*, *11*, 379-392.

Calver, A. (1990). Stream head migration: an indicator of runoff processes on chalklands. *Catena*, *17*, 399-408.

Cardwell, D.H., Erwin, R.B., & Woodward, H.P. (1968) Geologic map of West Virginia, 2 sheets, Scale 1:250,000. West Virginia Geological and Economic Survey.

Carlston, C. W. (1963). Drainage density and streamflow. U.S. Geological Survey Professional Paper 422-C.

Chapin, T. P., Todd, A. S., & Zeigler, M. P. (2014). Robust, low-cost data loggers for stream temperature, flow intermittency, and relative conductivity monitoring. *Water Resources Research*, *50*, 6542-6548.

Cohen, M. J., Creed, I. F., Alexander, L., Basu, N. B., Calhoun, A. J., Craft, C., ... & Jawitz, J. W. (2016). Do geographically isolated wetlands influence landscape functions? *Proceedings of the National Academy of Sciences*, *113*, 1978-1986.

Costigan, K. H., Jaeger, K. L., Goss, C. W., Fritz, K. M., & Goebel, P. C. (2016). Understanding controls on flow permanence in intermittent rivers to aid ecological research: integrating meteorology, geology and land cover. *Ecohydrology*, *9*, 1141-1153.

Datry, T., Larned, S. T., & Tockner, K. (2014). Intermittent rivers: a challenge for freshwater ecology. *Bioscience*, *64*, 229-235.

Day, D. G. (1978). Drainage density changes during rainfall. *Earth Surface Processes*, *3*, 319-326.

Day, D. G. (1980). Lithologic controls of drainage density: A study of six small rural catchments in New England, NSW. *Catena*, *7*, 339-351.

De Vries, J. J. (1994). Dynamics of the interface between streams and groundwater systems in lowland areas, with reference to stream net evolution. *Journal of Hydrology*, *155*, 39-56.

Dietrich, W. E., & Dunne, T. (1993). The channel head. In K. J. Beven, & M. J. Kirkby (Eds.), *Channel Network Hydrology* (pp. 175-219). Chichester, UK: John Wiley & Sons.

Doyle, M. W., & Bernhardt, E. S. (2010). What is a stream?. *Environmental Science & Technology*, *45*, 354-359.

Dunne, T., & Leopold, L. B. (1978). *Water in Environmental Planning*. San Francisco, CA: W. H. Freeman and Company.

Fritz, K. M., Hagenbuch, E., D'Amico, E., Reif, M., Wigington, P. J., Leibowitz, S. G., … & Nadeau, T. L. (2013). Comparing the extent and permanence of headwater streams from two field surveys to values from hydrographic databases and maps. *Journal of the American Water Resources Association*, *49*, 867-882.

Godsey, S. E., & Kirchner, J. W. (2014). Dynamic, discontinuous stream networks: Hydrologically driven variations in active drainage density, flowing channels and stream order. *Hydrological Processes*, *28*, 5791-5803.

Goulsbra, C., Evans, M., & Lindsay, J. (2014). Temporary streams in a peatland catchment: pattern, timing, and controls on stream network expansion and contraction. *Earth Surface Processes and Landforms*, *39*, 790-803.

Granato, G. E. (2009). Computer programs for obtaining and analyzing daily mean stream flow data from the U.S. Geological Survey National Water Information System Web Site. U.S. Geological Survey Open-File Report 2008-1362.

Gregory, K. J., & Walling, D. E. (1968). The variation of drainage density within a catchment. *Hydrological Sciences Journal*, *13*, 61-68.

Hadley, R. F., & Schumm, S. A. (1961). Sediment sources and drainage basin characteristics in upper Cheyenne River basin. U.S. Geological Survey Water-Supply Paper 1531-B, 137-198.

Hatcher Jr., R. D. (1988). Bedrock geology and regional geologic setting of Coweeta Hydrologic Laboratory in the eastern Blue Ridge. In W. T. Swank, & D. A. Crossley Jr. (Eds.), *Ecological Studies: Forest Hydrology and Ecology at Coweeta* (Vol. 66, pp. 81-92). New York, NY: Springer-Verlag.

Hedman, E. R., & Osterkamp, W. R. (1982). Streamflow characteristics related to channel geometry of streams in western United States. U.S. Geological Survey Water Supply Paper 2193.

Hewlett, J. D., & Hibbert, A. R. (1963). Moisture and energy conditions within a sloping soil mass during drainage. *Journal of Geophysical Research*, *68*, 1081-1087.

Hewlett, J. D., & Hibbert, A. R. (1967). Factors affecting the response of small watersheds to precipitation in humid areas. *Forest Hydrology*, *1*, 275-290.

Jaeger, K. L., Montgomery, D. R., & Bolton, S. M. (2007). Channel and perennial flow initiation in headwater streams: management implications of variability in source-area size. *Environmental Management*, *40*, 775-786.

Jaeger, K. L., & Olden, J. D. (2012). Electrical resistance sensor arrays as a means to quantify longitudinal connectivity of rivers. *River Research and Applications*, *28*, 1843-1852.

Kowall, S. J. (1976). The hypsometric integral and low streamflow in two Pennsylvania provinces. *Water Resources Research*, *12*, 497-502.

Larned, S. T., Datry, T., Arscott, D. B., & Tockner, K. (2010). Emerging concepts in temporary-river ecology. *Freshwater Biology*, *55*, 717-738.

Laseter, S. H., Ford, C. R., Vose, J. M., & Swift, L. W. (2012). Long-term temperature and precipitation trends at the Coweeta Hydrologic Laboratory, Otto, North Carolina, USA. *Hydrology Research*, *43*, 890-901.

Lyne, V., & Hollick, M. (1979). Stochastic time-variable rainfall-runoff modelling. In *Proceedings of the Hydrology and Water Resources Symposium* (Vol. 79/10, pp. 89-93). Institute of Engineers Australia National Conference.

Mills, H. H. (1981). Boulder deposits and the retreat of mountain slopes, or," gully gravure" revisited. *The Journal of Geology*, *89*, 649-660.

Mills, H. H., Brakenridge, G. R., Jacobson, R. B., Newell, W. L., Pavich, M. J., & Pomeroy, J. S. (1987). Appalachian mountains and plateaus. In W. L. Graf (Ed.), *Geomorphic Systems of North America* (Centennial Special, Vol. 2, pp. 5-50). Boulder, CO: Geological Society of America.

Morgan, R. P. C. (1972). Observations on factors affecting the behaviour of a first-order stream. *Transactions of the Institute of British Geographers*, *56*, 171-185.

Nadeau, T. L., and Rains, M. C. (2007). Hydrological connectivity between headwater streams and downstream waters: how science can inform policy. *Journal of the American Water Resources Associations*, *43*, 118-133.

Paybins, K. S. (2003). Flow origin, drainage area, and hydrologic characteristics for headwater streams in the mountaintop coal-mining region of southern West Virginia, 2000-01. U.S. Geological Survey.

Peirce, S. E., & Lindsay, J. B. (2015). Characterizing ephemeral streams in a southern Ontario watershed using electrical resistance sensors. *Hydrological Processes*, *29*, 103-111.

Powell, G. E., Mecklenburg, D., & Ward, A. (2006). Evaluating channel-forming discharges: a study of large rivers in Ohio. *Transactions of the ASABE*, *49*, 35-46.

Price, J. R., Velbel, M. A., & Patino, L. C. (2005). Rates and time scales of clay-mineral formation by weathering in saprolitic regoliths of the southern Appalachians from geochemical mass balance. *Geological Society of America Bulletin*, *117*, 783-794.

Rivenbark, B. L., & Jackson, C. R. (2004). Average discharge, perennial flow initiation, and channel initiation-small Southern Appalachian basins. *Journal of the American Water Resources Association*, *40*, 639-646.

Roberts, M. C., & Klingeman, P. C. (1972). The relationship of drainage net fluctuation and discharge. Proceedings of the 22nd International Geographical Congress, Canada, 181-91.

Russell, P. P., Gale, S. M., Muñoz, B., Dorney, J. R., & Rubino, M. J. (2015). A spatially explicit model for mapping headwater streams. *Journal of the American Water Resources Association*, *51*, 226-239.

Schultz, A. P., Stanley, C. B., Gathright II, T. M., Rader, E. K., Bartholomew, M. J., Lewis, S. E., & Evans, N. H. (1986). Geologic map of Giles County, Virginia, Scale 1:50,000. Virginia Division of Mineral Resources.

Seibert, J., & McGlynn, B. L. (2007). A new triangular multiple flow direction algorithm for computing upslope areas from gridded digital elevation models. *Water Resources Research*, *43*(4).

Shaw, S. B. (2016). Investigating the linkage between streamflow recession rates and channel network contraction in a mesoscale catchment in New York State. *Hydrological Processes*, *30*, 479-492.

Skoulikidis, N. T., Sabater, S., Datry, T., Morais, M. M., Buffagni, A., Dörflinger, G., … & Rosado, J. (2017). Non-perennial Mediterranean rivers in Europe: status, pressures, and challenges for research and management. *Science of The Total Environment*, *577*, 1-18.

The Southeast Regional Climate Center (SERCC) (2012). Historical Climate Summaries for Virginia. http://www.sercc.com/climateinfo/historical/historical_va.html.

Spence, C., & Mengistu, S. (2016). Deployment of an unmanned aerial system to assist in mapping an intermittent stream. *Hydrological Processes*, *30*, 493-500.

Stanley, E. H., Fisher, S. G., & Grimm, N. B. (1997). Ecosystem expansion and contraction in streams. *Bioscience*, *47*, 427-435.

Steward, A. L., von Schiller, D., Tockner, K., Marshall, J. C., & Bunn, S. E. (2012). When the river runs dry: Human and ecological values of dry riverbeds. *Frontiers in Ecology and the Environment*, *10*, 202-209.

Taylor, S. B., & Kite, J. S. (2006). Comparative geomorphic analysis of surficial deposits at three central Appalachian watersheds: Implications for controls on sediment-transport efficiency. *Geomorphology*, *78*, 22-43.

Virginia Division of Mineral Resources. (1993). Geologic Map of Virginia, Scale 1:500,000. Virginia Division of Mineral Resources.

Wang, L., & Liu, H. (2006). An efficient method for identifying and filling surface depressions in digital elevation models for hydrologic analysis and modelling. *International Journal of Geographical Information Science*, *20*, 193-213.

Wharton, G. (1994). Progress in the use of drainage network indices for rainfall-runoff modelling and runoff prediction. *Progress in Physical Geography*, *18*, 539-557.

Whiting, J. A., & Godsey, S. E. (2016). Discontinuous headwater stream networks with stable flowheads, Salmon River Basin, Idaho. *Hydrological Processes*, *30*, 2305-2316.

Wigington, P. J., Moser, T. J., & Lindeman, D. R. (2005). Stream network expansion: a riparian water quality factor. *Hydrological Processes*, *19*, 1715-1721.

Winter, T. C. (2007). The role of ground water in generating streamflow in headwater areas and in maintaining base flow. *Journal of the American Water Resources Association*, *43*, 15-25.

Zimmer, M. A., Bailey, S. W., McGuire, K. J., & Bullen, T. D. (2013). Fine scale variations of surface water chemistry in an ephemeral to perennial drainage network. *Hydrological Processes*, *27*, 3438-3451.

Zimmer, M. A., & McGlynn, B. L. (2017). Ephemeral and intermittent runoff generation processes in a low relief, highly weathered catchment. *Water Resources Research*, *53*, 7055-7077.

Chapter 3: Modeling headwater stream networks across multiple flow conditions in the Appalachian Highlands

Authors

Carrie K. Jensen

Kevin J. McGuire

Yang Shao

C. Andrew Dolloff

Abstract

Despite the advancement of remote sensing and geospatial technology in recent decades, maps of headwater streams continue to have high uncertainty and fail to adequately characterize temporary streams that expand and contract in length. However, watershed management and policy increasingly require information regarding the spatial and temporal variability of flow along streams. We used extensive field data on wet stream length at different flows to create logistic regression models of stream network dynamics for four physiographic provinces of the Appalachian Highlands: New England, Appalachian Plateau, Valley and Ridge, and Blue Ridge. The topographic wetness index (TWI) was the most important parameter in all four models, and the topographic position index (TPI) further improved model performance in the Appalachian Plateau, Valley and Ridge, and Blue Ridge. We included stream runoff as a continuous model predictor to represent the wetness state of the catchment, but adjustment of the probability threshold defining stream presence/absence to high values for low flows was the primary mechanism for approximating network extent at multiple flow conditions. Classification accuracy was high overall (> 0.90), and McFadden's pseudo R^2 values ranged from 0.69 for the New England model to 0.79 in the Appalachian Plateau. More notable errors included an overestimation of wet stream length in wide valleys and inaccurate reach locations amid boulder deposits and along headwardly eroding tributaries. Logistic regression was generally successful for modeling headwater streams at high and low flows with only a few simple terrain metrics. Modification and application of this modeling approach to other regions or larger areas would be relatively easy and provide a more accurate portrayal of temporary headwaters than existing datasets.

3.0 Introduction

First- and second-order headwater streams account for 70-80% of river network length (Downing et al., 2012) and transport water, sediment, nutrients, organic matter, and contaminants to downstream water bodies (Wohl, 2017). As a result, water quality largely reflects the state of contributing headwaters (Alexander et al., 2007; Dodds & Oakes, 2008). Approximately half of headwaters are temporary ephemeral or intermittent streams that vary in length seasonally or between storms (Nadeau & Rains, 2007; Buttle et al., 2012; Datry et al., 2014). Changes in the active or "wet" stream length can exceed 300% in humid (Jensen et al., 2017) as well as more arid environments (Godsey & Kirchner, 2014). The spatial variability of flow duration along streams impacts solute and sediment loads from catchments, rates and types of biogeochemical reactions, availability of aquatic habitat, and movement of organisms (Larned et al., 2010). However, maps that accurately portray temporary streams across wetness conditions are uncommon or nonexistent. Various logistical and technological challenges continue to impede a comprehensive inventory of headwaters and, instead, compel the use of modeling approaches to best represent these low-order stream systems.

The location and length of headwater streams are highly inaccurate on most existing maps (Skoulikidis et al., 2017). The National Hydrography Dataset (NHD), which serves as the standard representation of river networks for many environmental models and watershed management programs in the U.S., can underestimate headwater length by 200% or more (Elmore et al., 2013; Fritz et al., 2013). Inconsistencies during map production contribute to uncertainty, as source data are not the same for all NHD, topographic, or Natural Resources Conservation Service (NRCS) maps (Colson et al., 2008; Hughes et al., 2011). Aerial photograph interpretation is the most common method for delineating streams, but numerous individuals analyzed photographs over decades using distinct techniques, cartographic standards, and levels of precision (Colson et al., 2008; Hughes et al., 2011). Field surveys provide the source data for some maps, although there is usually no indication of whether the surveyor mapped the actively flowing stream or geomorphic channel as the network, which can result in quite different representations (Adams & Spotila, 2005; Jensen et al., 2017).

Maps rarely show the vast number of temporary headwater channels where networks expand and contract in length (Hansen, 2001). The temporary streams that do appear on maps receive categorical flow duration classifications as either intermittent or ephemeral. However, definitions of perennial, intermittent, and ephemeral streams are not standardized; classifications may reflect the frequency of flow (Hedman & Osterkamp, 1982; Hewlett, 1982), water table position (Hansen, 2001; Larned et al., 2007), seasonal position of flow origins at base flow (Paybins, 2003), or geomorphological and biological characteristics (Feminella, 1996; Hansen, 2001; Johnson et al., 2009). Researchers now highlight the need for objective, continuous measures of the frequency and duration of flow that provide more ecologically relevant information than categorical divisions (Leibowitz et al., 2008; Larned et al., 2010; Larned et al., 2011).

Flow duration is difficult to determine from aerial photographs, which capture the stream network at a single moment in time, or with limited field survey data. Perennial-intermittent and intermittent-ephemeral boundaries move between months or years (Fritz et al., 2008). Furthermore, streams networks are often discontinuous, with perennial reaches separated by dry channel segments that may rarely flow (Datry et al., 2014; Godsey & Kirchner, 2014). As a result, flow duration classifications for the NHD and NRCS maps generally have low accuracy, according to the given classification criteria (Svec et al., 2005; Colson et al., 2008, Fritz et al., 2013). Map errors also vary regionally; the NHD tends to overestimate flow duration in arid environments and underestimate flow duration in humid areas (Fritz et al., 2013).

Field surveying continues to be the most accurate and reliable mapping method for streams (Płaczkowska et al. 2015) yet is not feasible over large or remote areas. The increasing availability and advancement of geospatial data and analysis techniques in recent decades offers opportunities as well as unique challenges for characterizing headwaters. High-resolution aerial photographs only permit the identification of streams in areas without heavy vegetative cover (Heine et al., 2004). Satellite imagery and associated wetness or moisture indices can effectively classify larger water bodies and wetlands, but the spatial resolution is usually too coarse to detect headwater streams. One exception is high-resolution near-infrared LiDAR, which Hooshyar et al. (2015) employed to extract the wet stream network in a region with exposed channels. Even at sites without dense canopy cover, multiple collections of aerial photographs or LiDAR is

necessary during both wet and dry conditions to accurately describe stream length variability. Such efforts are expensive and impractical in many cases, although unmanned aerial vehicles may help to alleviate this burden in the future (Spence & Mengistu, 2016).

Automated stream extraction methods utilize Digital Elevation Models (DEMs), which are often freely available at resolutions finer than 10 m for the continental U.S. Channel initiation thresholds based on flow accumulation, upslope area, slope, or stream power are adequate for fourth-order and larger channels (James & Hunt, 2010) but do not consistently locate smaller headwaters (Heine et al., 2004). Alternatively, modeling the stream network with logistic regression outperforms channel initiation thresholds and other extraction techniques (Heine et al., 2004; Sun et al., 2011). Using variables like upslope area, slope, and curvature, logistic regression determines the probability of the presence of a stream at each catchment pixel. Despite the success of logistic regression for delineating headwaters, model accuracy remains lower for the temporary channel network (Russell et al., 2015). Alternatively, because flow duration varies widely both along and among non-perennial streams, we believe modeling efforts should shift to continuous predictions of the wet, active network through time rather than a single, stable configuration of perennial or temporary channel length.

The objective of this study is to utilize field data on the variability of wet stream length in forested catchments spanning four Appalachian physiographic provinces to create explanatory logistic regression models of the wet stream network as a function of topographic metrics and runoff. Jensen et al. (2017) found that expansion and contraction of headwater length with stream flow occurs but also differs considerably in magnitude across the Appalachian region. Flow permanence and, thus, wet stream length largely align with geologic controls such as lithology and the depth and heterogeneity of sediment (Winter, 2007; Jensen et al., 2017), which are not always evident from geologic maps. The current study investigates the efficacy of using topography, which reflects the underlying geology, to predict the distinct observed stream length dynamics of the Appalachians. This project is one of the first known attempts to model headwaters as dynamic networks by including a continuous wetness state variable (stream runoff) as a model parameter (but see the use of accumulated precipitation by Sun et al., 2011), whereas most published studies focus on reproducing the locations of geomorphic channel heads

or static representations of channel length. We developed explanatory rather than predictive models, as our goal was to understand how terrain attributes correspond to flow permanence in each province rather than to maximize predictive accuracy (MacNally, 2000; Sainani, 2014). Detailed field data on the location and length of wet stream reaches across flow conditions enabled us to identify additional site characteristics aside from catchment topography that contribute to model inaccuracy and can, therefore, inform future stream delineation efforts.

3.1 Study Area

We collected field data from headwater catchments in four physiographic provinces of the Appalachian Highlands: the New England (NE), Appalachian Plateau (AP), Valley and Ridge (VR), and Blue Ridge (BR). We selected three forested catchments smaller than 75 ha from each province (Table 1), as we discovered that larger watersheds in these regions require more than one day for an individual to map the stream network. The study sites are in the Hubbard Brook Experimental Forest in New Hampshire for NE, Fernow Experimental Forest in West Virginia for AP, Jefferson National Forest at Poverty Creek and the South Fork of Potts Creek in Virginia for VR, and Coweeta Hydrologic Laboratory in North Carolina for BR (Figure 1). We conducted field mapping at Hubbard Brook, Fernow, and Coweeta because these experimental watersheds have weirs recording stream flow and reference areas that are not subject to timber harvests or other experimental manipulation. We chose the VR sites at tributaries to Poverty Creek and the South Fork of Potts Creek based on the availability of 3 m DEM data, mature forest coverage, road access, and the location of the catchments on National Forest.

The climate, geology, topography, and vegetation vary across the four Appalachian provinces (Table 1; see Jensen et al. (2017) for further details). NE is the coldest study area and receives the most snow, so peak stream flow usually occurs after snowmelt in the late spring. The VR catchments are in a rain shadow and have the lowest precipitation totals, while the BR sites are the wettest. Snow is rare in BR due to warm winters. Substrate at the NE sites consists of glacial till and drift deposits that vary in thickness up to 8 m (Benettin et al., 2015) and are underlain by Lower Silurian pelitic schist and granulite of the Upper and Lower Rangeley Formation (Barton, 1997). The glacial landscape is rounded and hummocky with little channel incision (Figure 1). Soils are well-drained sandy loam Spodosols (Likens, 2013). The AP catchments are located in

the gently folded Allegheny Mountains, which are characterized by steep slopes and broad, flat uplands (Morisawa, 1962). Devonian shales and sandstones of the Hampshire Formation form the underlying bedrock (Cardwell et al., 1968), and soils are shallow (< 1 m) silt and sandy loam Inceptisols (Losche & Beverage, 1967). Folded and thrust faulted sedimentary rock with differing erodibilities creates the parallel ridges and associated trellis drainage pattern of the VR. The VR sites at Poverty Creek are underlain by Devonian shales, sandstones, and siltstones of the Brallier and Chemung Formations (Virginia Division of Mineral Resources, 1993), and bedrock at the South Fork of Potts Creek catchment includes Devonian Oriskany and Silurian Keefer and Rose Hill sandstones (Schultz et al., 1986). Soils consist of shallow, well-drained stony and clay loam Inceptisols (Adams & Stephenson, 1983). Middle to Late Proterozoic biotite gneiss and amphibolite of the Coweeta Group and Tallulah Falls Formation underlie thick saprolite at the BR catchments (Hatcher, 1988). Dominant soils include sandy and gravelly loam Inceptisols and Ultisols (Velbel, 1988). All of the study areas have second-growth forests that range from northern hardwoods in NE to oak-hickory associations in BR.

3.2 Methods

3.2.1 Field data collection

We mapped the wet stream network of each study catchment 7 times throughout 2015 and 2016 with a Bad Elf GNSS Surveyor Global Positioning System (GPS) unit, as detailed in Jensen et al. (2017). During each mapping, we walked along the stream from the catchment outlet until we found the flow origin of every tributary, marking disconnections in the wet network between flowing reaches or non-flowing pools. We included all surface water greater than 1 m in length as part of the wet network. The reported accuracy of the GPS unit is 1 m, but measured accuracy varied from 3 to 10 m depending on weather conditions and tree cover. To compensate for the lower accuracy, we used pin flags and field notes in addition to the GPS points to compare the location of the wet stream across mapping dates. The same individual also completed all mapping with the same GPS unit.

Eight of the twelve study catchments have weirs that gauge stream discharge at 5-minute intervals. We performed salt dilution gauging (Calkins & Dunne, 1970) to measure stream flow at the remaining sites (NE25, VR25, VR35, & VR70) during each mapping. Our goal was to map

the wet network seasonally across a range of flows between at least the 25 and 75% exceedance probabilities of mean daily discharge, rather than major storms or droughts. We only mapped during non-storm conditions or on the recession limb of storm events at least several hours after the hydrograph peak to minimize changes in discharge during an individual survey. Precipitation data were available for all sites, but some of the gauges were not in or immediately adjacent to the study catchments, which is especially problematic for isolated summer thunderstorms. Antecedent precipitation indices showed lower correlations with stream length than runoff (discharge normalized by catchment area), so we limited our wetness state variable to runoff as the more representative measurement of moisture conditions.

3.2.2 Terrain analysis

Following the procedure in Jensen et al. (2017), we brought the GPS points into ArcGIS (ArcMap version 10.3.1, ESRI 2015, Redlands, CA) to digitize the wet stream network along lines of high flow accumulation according to the multiple triangular flow direction algorithm (Seibert & McGlynn, 2007) applied to 3 m DEMs. DEMs with resolutions between 1 and 5 m tend to create more accurate stream networks (Li & Wong, 2010) and better predict channel head locations (Tarolli & Dalla Fontana, 2009) than coarser resolutions. Similarly, Gillin et al. (2015a) found that terrain metrics calculated from 3 and 5 m DEMs are most comparable to field-derived values for one of the NE catchments used in this study. We completed all DEM processing and terrain analysis in ArcGIS and the System for Automated Geoscientific Analyses software (SAGA version 2.3.1). The 1/9 arc-second DEM for AP, BR, and VR70 are from the 2003 West Virginia and North Carolina National Elevation Datasets. LiDAR data collections occurred during leaf-off and snow-free conditions at NE in 2012 for the White Mountain National Forest and at VR25 and VR35 in 2011 for the Virginia Geographic Information Network. We re-sampled the bare earth DEMs classified from the LiDAR data to 1 m and then coarsened the DEMs to 3 m by mean cell aggregation. We used a low-pass (3 x 3) filter and sink-filling algorithm (Wang & Liu, 2006) for hydrological correction of all DEMs.

We moved GPS points located in low flow accumulation pixels due to positional error to the nearest cell of comparatively high flow accumulation, although the maximum displacement we allowed was 3 pixels (9 m) in accordance with the average GPS accuracy. Because we mapped

each catchment 7 times, we were able to compare GPS points from all of the mappings to delineate the most accurate network possible. We assigned points from each mapping date to the flow lines of this "master" network to ensure consistency as we determined changes in wet stream length. We consulted field notes during this process to verify that point displacements between mappings were the result of variability in the wet network rather than GPS error.

We derived terrain metrics from the hydrologically-corrected 3 m DEMs. Metrics included: upslope accumulated area, calculated from the multiple triangular flow direction algorithm (Seibert & McGlynn, 2007); maximum slope (Travis et al., 1975); topographic wetness index (Beven & Kirkby, 1979), based on the multiple triangular flow direction and maximum slope algorithms; downslope index (Hjerdt et al., 2004); stream power index (Moore et al., 1991); profile, planform, tangential, longitudinal, and cross-sectional curvature (Evans, 1979; Wood, 1996; Wilson & Gallant, 2000); topographic position index (Guisan et al., 1999); and local lateral contributing area, calculated as the sum of the left- and right-side contributions (Grabs et al., 2010). We used the DEM Surface Tools for ArcGIS (version 2.1.375) (Jenness, 2013) to produce the curvature metrics. We created an additional raster grid for each metric by calculating the mean of all pixel values in the upslope accumulated area contributing to a given cell. Thus, we developed "local" as well as "mean upslope" rasters for all metrics except for upslope accumulated area and local lateral contributing area.

3.2.3 Logistic regression modeling

We used logistic regression to model the probability of each catchment pixel being a "wet" stream as a function of terrain metrics and runoff. In logistic regression, the relationship between the probability (p) of a binary response variable (in this case, the presence or absence of a wet stream at a pixel) and model predictors (x_i) can be expressed as

$$\hat{p} = exp(b_0 + b_1x_1 + b_2x_2 + \ldots b_nx_n)/(1 + exp(b_0 + b_1x_1 + b_2x_2 + \ldots b_nx_n)), \quad (1)$$

where $\hat{p}$ is the regression estimate of logit(p), which is

$$\text{logit}(p) = log(p/(1 - p)), \quad (2)$$

and b_0 is the model intercept, b_i (i = 1, 2, ... , n) are the regression coefficients, and x_i (i = 1, 2, ..., n) are the independent variables.

We transformed the delineated stream network from each mapping into a raster denoting the presence (1) or absence (0) of a wet stream. We utilized 100% of the wet stream cells with a value of 1 and randomly sampled 10% of the non-stream pixels with a value of 0 from across the entire catchment for modeling. Preliminary models using varying proportions of non-stream pixels showed a decrease in classification accuracy with more sample points but no apparent impact on the selection of model explanatory variables. We limited the sample of non-stream pixels to 10% owing to the comparatively low number of wet stream points and, additionally, because predictive accuracy was not the primary goal. We split the sampled stream and non-stream pixels into training (70%) and testing (30%) data for model building and validation, respectively.

Wet stream length dynamics and the mobility of flow origins reflect geologic attributes including lithology, structure, and depth to bedrock that vary at both local and regional scales (Winter, 2007; Whiting & Godsey, 2016; Jensen et al., 2017). We created a separate model for each physiographic province in our study to examine how regional, rather than site-specific, topography can help explain flow permanence in headwaters. We extracted terrain metric values from the raster grids at the sample points and assigned the same runoff value as a constant to all points from a single mapping. We log-transformed variables with non-normal distributions, performing all statistical analysis and modeling in R 3.2.1 (R Core Team, 2015). Variable selection for each of the four final models was based on p-values and step-wise improvements in McFadden's pseudo R^2 values, although we also sought to eliminate collinear predictors with a Pearson's correlation greater than 0.70 (Kuhn, 2008). We evaluated model performance with McFadden's pseudo R^2 values, classification accuracy, and errors of omission and commission of stream pixels. We repeated this process for each physiographic province to produce four models.

Selection of any probability threshold is possible with logistic regression to signify the presence of the response variable. We created an accuracy optimization procedure to choose threshold

values for each catchment that produced the maximum classification accuracy for the highest and lowest stream flows of the testing dataset. We applied the models to the three study catchments in each of the four provinces to examine the spatial distribution of omission and commission errors for the selected probability thresholds.

3.3 Results

3.3.1 Model parameters

The natural logarithm of the topographic wetness index (TWI) was the most important parameter in all of the final models (Table 2). We tested single-variable models using TWI to predict wet stream presence/absence, which resulted in McFadden's pseudo R^2 values of 0.67-0.68. TWI reflects both the upslope accumulated area and local slope at a pixel (Seibert & McGlynn, 2007). High TWI values indicating large contributing areas or low slopes increased the likelihood of stream presence. The AP, VR, and BR models all included either the local or mean upslope topographic position index (TPI), which increased McFadden's pseudo R^2 values by an additional 0.06-0.09 after the inclusion of TWI. TPI compares the elevation of a cell to the mean elevation in a neighborhood defined by a 100 m radius around the pixel: positive values correspond to ridges, and negative values indicate valleys (Guisan et al., 1999). TPI model coefficients were all negative. We also selected curvature metrics for the AP, VR, and BR models, but these parameters only increased McFadden's pseudo R^2 values by 0.02-0.03. The AP model included cross-sectional curvature, which is the same as "planform curvature" in the ArcGIS Spatial Analyst Toolbox (Zevenbergen & Thorne, 1987). Positive values of cross-sectional curvature correspond to convexities where water diverges, and negative values show concavities where flow converges (Jenness, 2013). Longitudinal curvature appeared in the VR model and is the same as "profile curvature" in ArcGIS (Zevenbergen & Thorne, 1987). The BR model incorporated mean upslope profile curvature. Both longitudinal and profile curvature indicate whether water accelerates or decelerates when flowing over a point, with positive values showing deceleration at concavities and negative values suggesting acceleration at convex parts of the landscape (Jenness, 2013). Runoff also appeared in all four models yet increased McFadden's pseudo R^2 values only slightly (< 0.02). Owing to the large number of sample points, all of the final model predictors were highly significant ($p << 0.001$) in the models.

3.3.2 Model performance

McFadden's pseudo R^2 values were highest for AP (0.79) but were similar for VR (0.77) and BR (0.76) (Table 2). NE had the lowest McFadden's pseudo R^2 value of 0.69. Classification accuracy was high overall, ranging from 0.90-0.99 across the study catchments (Table 3). The optimum probability threshold to maximize classification accuracy for each catchment varied from 0.50-0.94, with higher threshold values corresponding to low flows. Omission and commission errors did not display systematic trends but were greatest for NE25, VR35, and BR12 at low flows.

The NE model was able to reproduce the complex pattern of tributaries in the three Hubbard Brook catchments (Figure 2). One of the more prominent errors was the presence of high probability values for a wet stream along the western border of NE25. We did not map a stream in the field at the western edge of NE25, but we believe the catchment boundary delineated from the DEM is slightly inaccurate, as the stream appears to flow into the neighboring catchment. Thus, a wet stream may have actually been present at this location on some of the mapping dates. Although we optimized the probability threshold for each site, we found a slightly higher threshold value of approximately 0.75 yielded more visually accurate stream networks at high and low flows (Figure 3), particularly for NE13 and NE42.

The AP model effectively portrayed the simple network pattern of the Fernow catchments yet tended to overestimate the presence of wet streams at higher elevations (Figure 4 & 5). For AP16, the modeled network precisely matched the field map for the high flow but did not reflect the top-down contraction in stream length that occurred during the low flow, even at probability thresholds greater than 0.90. Similarly, we never observed surface water in the southwest tributary of AP37 as far upslope as the model indicated, and flow duration along the upper reaches of the main stem was much lower than the model predicted.

Model performance for the VR was distinct VR70 at the South Fork of Potts Creek and the two catchments draining to Poverty Creek, VR25 and VR35. The VR model produced realistic stream networks in VR25 and VR35 at high flows but greatly overestimated wet stream length for the low flows (Figure 6 & 7). Stream length changed considerably between high and low

flow conditions at these catchments, and we found that threshold values of 0.95-0.99 were necessary for a closer visual match between the model and field map at low flows. Nevertheless, the modeled network contraction patterns with decreasing runoff and increasing threshold values were consistent with field observations, with many of the same reaches drying first. Overestimation of stream length at low flows was less of an issue for VR70, which displayed much less network expansion and contraction. However, the modeled network continued too far upslope for both flow conditions, so increasing the probability thresholds to 0.80-0.90 visually improved the delineation. The model also omitted a number of short, disconnected reaches that activated during high flows at VR70, although the total missing stream length was relatively minor.

The BR model accurately delineated wet stream length along the main channel stems in each Coweeta catchment but overestimated the length of several small tributaries in BR33 and BR40 (Figures 8 & 9), which often corresponded to bedrock springs. As a result, probability thresholds of 0.75-0.90 yielded the most realistic stream networks. As was the case for the other study areas, these threshold values were higher than the threshold optimization procedure suggested (Table 3). The BR field maps showed almost negligible network expansion and contraction between high and low flows, but the model was not able to reproduce the more notable changes in stream length that did occur. In BR12, the model did not show contraction of the wet stream along the eastern tributary that we observed in the field and, instead, erroneously indicated drying further downstream.

3.4 Discussion

3.4.1 Terrain metrics

TWI is the most critical topographic metric for modeling wet stream length in our Appalachian catchments (Table 2). The TWI calculation incorporates the upslope area and slope at a pixel, which are generally among the best predictors of channel head locations (James & Hunt, 2010; Julian et al., 2012; Avcioglu et al., 2017) and most significant variables in stream network models (Sun et al., 2011; Elmore et al., 2013; Russell et al., 2015; González-Ferreras & Barquín, 2017). Substituting the upslope accumulated area (UAA) for TWI lowers model accuracy only slightly. We believe the most critical contribution of either TWI or UAA to the models is from

the calculation of area according to the multiple triangular flow direction algorithm (Seibert & McGlynn, 2007) using 3 m DEMs. This algorithm produces lines of high flow accumulation and TWI values that align almost precisely with our GPS tracks in the study catchments. Therefore, we recommend application of the multiple triangular flow direction algorithms to DEMs with a similar resolution for modeling Appalachian stream networks.

The effect of TWI on the probability of stream presence differs most notably between NE and the other three study areas (Table 2). For a given TWI value, the log odds of a wet stream in NE are 50-100% greater than for AP, VR, and BR. In other words, a stream is more likely to be wet in NE for a given TWI value. Likewise, a higher TWI owing to a larger area or lower slope would be necessary in the other provinces to have the same probability of stream presence as NE. TWI is the only terrain metric in the NE model yet is able to predict the complex arrangement of tributaries at the Hubbard Brook catchments surprisingly well. A lack of stream incision into the glacial till results in planar hillslopes and few defined valleys (Figure 1), which complicate channel delineation both from DEMs and aerial photographs as well as in the field. The success of the model suggests wet stream length at NE is mostly a function of upslope area and, to a lesser extent, slope in the unincised catchments.

TPI considerably improves model performance for AP, VR, and BR. As a measure of the relative elevation of a pixel, TPI distinguishes ridges and valleys and, accordingly, the degree of stream incision. More deeply incised valleys have a shorter depth to bedrock, increasing the likelihood that channels lie below the seasonally shifting saturated zone to provide stream flow (Whiting & Godsey, 2016). Likewise, we observed in the field that highly confined stream valleys tend to have a higher flow duration than wide, aggraded valleys, which studies have also noted elsewhere (Stanley et al., 1997). The lack of defined stream valleys at Hubbard Brook (Figure 1) may explain why neither the local nor mean upslope TPI appears in the final NE model.

We are not certain why the AP and VR models incorporate the mean upslope TPI parameter while the BR model includes the local TPI metric. Elmore et al. (2013) determined that slope and curvature variables averaged over the upslope contributing area were always more significant than local values in models of the geomorphic channel network for the Eastern U.S. Flow origins

in the AP and VR provinces tend to occur at upslope areas that are approximately an order of magnitude larger than those in NE and BR (Jensen et al., 2017). The appearance of flow origins lower in the catchment may reflect larger contributing areas produce a wet stream in AP and VR but may also reflect a need for the upstream concentration of subsurface flow in valleys. However, substitution of the local and mean TPI variables in each model reduces performance only marginally. Thus, we do not believe the specification of a mean or local value is integral to achieve reasonable representations of headwaters. We are not aware of any studies that examine TPI for stream network modeling, but Gillin et al. (2015b) did select TPI for a logistic regression model of hydropedologic units in NE42. Our results suggest this metric may be useful for future headwater modeling studies.

Curvature metrics improve model performance only slightly for AP, VR, and BR after the addition of TWI and TPI (Table 2). We tested a global model for all of the catchments using a factor variable to differentiate the physiographic provinces; TWI and TPI are the only two terrain metrics in the final model, reinforcing the comparatively minor role of curvature. In addition, the different types of curvature are highly correlated with each other and all generally indicate the degree of land surface convergence or divergence, so the selection of cross-sectional or profile versus longitudinal curvature in our models is not extremely meaningful. Even though curvature does not greatly increase model accuracy, Russell et al. (2015) found that curvature variables can help differentiate perennial and intermittent streams. Longitudinal and cross-sectional curvature (often known as "profile" and "planform" curvature, respectively, in ArcGIS) commonly correlate with the location of channel heads (Tarolli & Dalla Fontana, 2009; Julian et al., 2012) and flow origins (Whiting & Godsey, 2016) and are often of secondary importance in stream network models following upslope area and slope (Sun et al., 2011; Elmore et al., 2013; Russell et al., 2015). However, TWI and TPI seem to largely capture the topographic information that curvature metrics provide while producing higher model accuracy.

3.4.2 Characterizing network dynamics

Stream runoff is significant in all four models but provides only small improvements in model accuracy. As a constant value for each mapping rather than a metric that differs for every pixel, the purpose of runoff in the models is to increase the probability of stream presence for higher

flow conditions. For this reason, runoff has a greater model coefficient and t-statistic in the provinces where stream length changes more with flow (Table 2 & Figure 10). Jensen et al. (2017) explain stream length dynamics in the study catchments in terms of the permeability and water storage capacity of the underlying sediment and bedrock. Network expansion and contraction is minimal at BR (Figure 10), which is likely due to deep, permeable soils that can store and transport perennial flow to streams (Hewlett & Hibbert, 1963; Hatcher, 1988). Conversely, VR25 and VR35 at Poverty Creek display extreme wet network variability, as the underlying shale has lower permeability and, thus, produces less base flow (Carlston, 1963) than sandstones and other more permeable geology. At a finer spatial scale, wet stream length and flow duration tend to be lower amid transmissive boulder deposits and in wide, sediment-filled valleys, highlighting the additional need for valley incision to the saturated zone for greater flow permanence (Whiting & Godsey, 2016).

The minor contributions of runoff to the models suggest this variable may not be useful for predicting network dynamics. Because stream length is quite stable at Coweeta, we can easily remove runoff from the BR model. For the other three provinces, we created a separate model of the wet stream network at high and low flows, excluding runoff as a potential explanatory variable, to determine if distinct topographic metrics correlate with stream length during wet and dry conditions. The final parameters for the high and low flow models (Table 4) are nearly the same as those in the original models (Table 3). For NE, UAA is the single best metric at low flow instead of TWI (Table 4), although TWI and UAA are highly correlated and result in similar McFadden's pseudo R^2 values. The mean upslope downslope index (Hjerdt et al., 2004) replaces cross-sectional curvature for the low flow AP model, but each of these variables increases McFadden's pseudo R^2 values by just 0.03 after TWI and TPI. Longitudinal curvature is absent from the low flow VR model but provides only a small contribution to the high flow and original models. Overall, TWI and TPI remain the most important parameters at both flows. The primary difference between the high and low flow models is the model intercepts and coefficients, which serve to modify the probability of wet stream presence. We can produce a similar result with fewer models by simply varying the probability threshold value of the original model outputs. For this reason, we prefer the original modeling approach for the catchments in our study.

The optimum probability threshold values we calculate for each catchment are greater for low flows than high flows, since increasing the threshold excludes more pixels from classification as a wet stream. Catchments with highly dynamic networks, such as VR35, require a substantial change in threshold values between high and low flows (Table 3). Nearly identical probability thresholds are suitable for both flow conditions at sites with more constant stream length, like AP14. We tried incorporating interaction effects between runoff and the topographic metrics as well as the individual slopes of the log-log power relationship between stream length and runoff (Figure 10) as model parameters to help account for the inconsistency in threshold values. None of these attempts corrected the issue. In addition, further adjustment of the threshold is still necessary for most of the catchments to create a modeled network that is visually consistent with field observations. The optimized threshold values are almost always too low. We attempted to remedy this issue by doubling the number of non-stream pixels for model-building and validation to 20%. However, increasing the proportion of non-stream pixels heightens the imbalance with the number of wet stream sample points and results in optimized threshold values that are even further from the visually-selected thresholds than when we only use 10%.

We initially intended to use stream runoff as a continuous variable to delineate the wet network for a specific flow condition. While the models do not successfully predict wet stream length for a precise runoff value, characterizing the wet and dry extremes of network extent is possible by choosing the appropriate lower (0.50-0.75) or higher (0.75-1.0) threshold value, respectively, even if runoff data are not available. Any prior knowledge of the magnitude of stream length dynamics, which we can estimate from geologic characteristics or measurements like the base flow index (Jensen et al., 2017), can further inform the appropriate threshold for more realistic model outputs.

3.4.3 Model strengths and shortcomings for stream network delineation

The models are able to locate several disconnected wet reaches that often either escape detection or appear as continuous tributaries on maps. Coarse surficial deposits cover the southeastern portion of NE42 and coincide with short, disconnected tributaries, which is distinct from the network pattern in the remainder of the catchment. Terrain metrics do not necessarily reflect the surficial geology, so overestimation of wet stream length is common in this area. However, the

NE model accurately predicts a lower probability of wet stream pixels in the vicinity of the boulder deposits (Figures 2 & 3). The BR model also indicates a disconnected reach in the northern part of BR40 (Figures 8 & 9). This wet reach occurs in a valley with sediment fill from an old landslide deposit. The modeled location and length of the high probability pixels are quite similar to field observations of the disconnected tributary. The VR model does not identify all of the disconnected reaches in VR70 but, surprisingly, is able to find two isolated wetlands without a tributary inlet or outlet that persist during both high and low flows (Figures 6 & 7): one wetland lies west of the main stem, and the other is just above the junction of the two primary tributaries.

The modeled network contraction patterns evident by increasing the probability threshold values also show the formation of discontinuous reaches in addition to more sequential top-down drying (Figures 2-9). Disconnection of streams into separate wet reaches is common during dry periods (Godsey & Kirchner, 2014), but most maps and stream network models cannot recreate the fine-scale spatial variability in flow duration that actually exists in headwaters. Researchers increasingly recognize the significance of isolated wetlands (Cohen et al., 2016) and temporary or discontinuous stream reaches (Stanley et al., 1997; Larned et al., 2010; Datry et al., 2014) for ecological services including biodiversity, nutrient cycling, and downstream water quality. Disconnected water bodies frequently maintain a subsurface connection to perennial streams through hyporheic exchange (Boulton et al., 1998) and also serve as habitat refugia and storage sites for sediment, organic matter, and contaminants moving through the catchment (Larned et al., 2010). As a result, locating isolated wetlands and disconnected wet reaches is a high priority yet also frequently a challenge for scientists and policy-makers.

The models fail to adequately represent other aspects of the stream network that correspond to discontinuities in the surficial geology or watershed evolution processes. The main eastern tributary in BR12 has a major disconnection at a valley fill from a landslide deposit (Figures 8 & 9). A wide, sediment-filled valley floor also aligns with the disconnection along the main stem of AP37 (Figures 4 & 5). In both cases, the models overestimate stream length in wider valley sections where flow duration is lower. In VR70, channels with perennial flow originate at the base of boulder-filled hollows. Upslope of the origins, water emerges on top of the boulders for

only short distances at high flows before again infiltrating into the subsurface. The VR model does not identify most of these short reaches and, additionally, extends the streams too far up the catchment, as the model cannot account for the transmissive boulder deposits with the available terrain metrics (Figures 6 & 7). Finally, the AP model dramatically overestimates stream length and flow duration at higher elevations, especially for the southwest tributary of AP37 (Figures 4 & 5). Field observations suggest that the tributaries in this catchment are headwardly eroding into a relict upland in the same manner as a hanging valley. Thus, there will likely be streams at the predicted locations higher in the catchment in the future, but, meanwhile, the model does not accurately portray current conditions. In all cases, the overprediction of stream length occurs in areas where the channel has not incised into a valley fill, coarse boulder deposits, or a relict upland. This finding again emphasizes the importance of valley incision to the zone of saturation for flow permanence but also indicates a need for better metrics of relative incision and aggradation to improve future models.

3.4.4 Model application

Our study constitutes an exploratory analysis of the terrain variables that correlate with the location of the wet stream network in four Appalachian physiographic provinces. The overall agreement between the modeled probability of wet stream pixels and field maps indicates logistic regression is an effective way to characterize headwaters across flow conditions. Similar studies successfully apply logistic regression to delineate headwater channels (Elmore et al., 2013; Russell et al., 2015), and our results demonstrate that this fairly simple approach is also suitable for modeling network expansion, contraction, and disconnection at a finer reach scale by varying the probability threshold values of model outputs. Traditionally, physically mapping wet stream length multiple times is the only method for measuring wet network variability. A key improvement in our models is the prediction of disconnected reaches along streams for both wet and dry conditions, which provides a more realistic map of flow permanence than assigning a single flow duration classification to an entire tributary (Russell et al., 2015; Williamson et al., 2015).

Our models rely on terrain metrics, which are easy to derive from DEMs with programs like ArcGIS and SAGA. We can estimate the high and low extremes of wet stream length by simply

altering the probability threshold of the logistic regression model output. We also include stream runoff as a wetness state variable in the models because of visual and statistical improvements in the predicted probability of stream pixels, particularly for NE, AP, and VR. More training data of stream networks at different runoff conditions would undoubtedly increase the contribution of this variable to the models. Other wetness state variables such as an antecedent precipitation index would be an appropriate substitute if stream discharge measurements are not possible. However, neither runoff nor precipitation is essential to approximate the magnitude of stream length dynamics.

The twelve catchments in this study represent a limited sample of headwaters, despite the extensive time and effort associated with field data collection. The climate, geology, vegetation, and land use are consistent across the selected catchments in each province. Thus, our models may not be applicable to all headwaters in a given physiographic region. Incorporation of additional variables such as annual precipitation, evapotranspiration, lithology, and land cover would likely be necessary for a comprehensive stream extraction over larger areas.

3.5 Conclusion

Logistic regression is a suitable and straightforward method for modeling wet stream length dynamics in Appalachian headwaters. The most significant terrain metrics correlating with the probability of stream presence at a pixel include the topographic wetness index (TWI) followed by the topographic position index (TPI). In effect, catchment locations with larger upslope areas, lower slopes, and more valley incision have a higher flow duration. TPI is not a common parameter for stream network modeling, but our results show that this variable can greatly improve channel delineations. The contributions of curvature and runoff to the models are comparatively minor for the selected study areas.

The four models have high overall accuracy and predict high and low probability values of wet stream pixels that match the network patterns we observed in the field. In general, greater threshold values (> 0.75) correspond to dry conditions, and lower values (0.50-0.75) represent high flows. Catchments with highly variable lengths require more adjustment of the probability threshold. The models are able to distinguish several disconnected stream reaches and wetlands

but do not always portray the correct stream location and length in areas with less channel incision amid boulder deposits, wide valley segments, or along headwardly eroding tributaries. Future modeling efforts should further investigate these sources of error to improve the reliability of network predictions.

Accurate maps of headwaters are rare yet increasingly essential for ecological modeling and the enforcement of water policy for effective watershed conservation. Because many headwater streams have temporary flow, data describing not only the length but the associated flow duration of tributaries, disconnected reaches, and wetlands are critical for informing the research and management of river systems. Our logistic regression models approximate the wet stream network of catchments at high and low flows rather than provide a single prediction of static channel length. The modeling methodology is relatively simple, employing basic terrain metrics, which permits the application of this approach in other regions to improve the characterization of temporary headwaters.

Figures and Tables

Table 1. Study area attributes. Modified from Jensen et al. (2017).

Physiographic province	Site name[a] (watershed number[b])	Latitude (°N), Longitude (°W)	Drainage area (ha)	Aspect	Mean elevation (m)	Geology	Vegetation
New England	NE13 (WS6)	43.95, 71.74	13.4	SE	690	schist, granulite	northern
	NE25	43.93, 71.77	25.1	NW	740	schist, granulite	hardwoods
	NE42 (WS3)	43.96, 71.72	42.4	S	632	schist, granulite	
Appalachian	AP14 (WS13)	39.06, 79.70	13.9	NE	773	shale, sandstone	mixed
Plateau	AP16 (WS10)	39.05, 79.68	15.7	SW	767	shale, sandstone	hardwoods
	AP37 (WS4)	39.05, 79.69	36.6	SE	822	shale, sandstone	
Valley and	VR25	37.28, 80.46	25.0	NW	750	shale, sandstone	mixed
Ridge	VR35	37.26, 80.48	34.8	N	729	shale, sandstone	hardwoods
	VR70	37.45, 80.49	69.9	S	1029	sandstone	
Blue Ridge	BR12 (WS18)	35.05, 83.44	12.4	NW	823	gneiss, amphibolite	oak-hickory
	BR33 (WS34)	35.06, 83.45	32.7	SE	1019	gneiss, amphibolite	and cove
	BR40 (WS40)	35.05, 83.46	39.6	E	1052	gneiss	hardwoods

[a]Numbers in site name indicate the drainage area in hectares

[b]If applicable, designated watershed number at the experimental forests

Table 2. Model parameters. The p-value of all model parameters is << 0.001.

Model	McFadden's pseudo R^2	Parameters	Coefficient	Standard error	t-statistic
NE	0.69	TWI (ln)	15.57	0.16	94.50
		Flow	0.12	0.007	18.57
AP	0.79	TWI (ln)	8.11	0.22	37.61
		TPI (mean[a])	-4.75	0.15	-31.91
		Cross-sectional Curv.	-0.28	0.01	-19.39
		Flow	0.13	0.02	7.13
VR	0.77	TWI (ln)	9.56	0.12	80.12
		TPI (mean[a])	-3.26	0.08	-42.18
		Longitudinal Curv.	0.17	0.006	30.93
		Flow	0.18	0.009	18.59
BR	0.76	TWI (ln)	7.69	0.10	73.95
		TPI	-1.75	0.04	-40.23
		Profile (mean[a]) Curv.	2.14	0.08	26.89
		Flow	0.02	0.004	4.21

[a] Variable denoted as "mean" refers to the mean value of upslope pixels as opposed to the local value

Table 3. Probability threshold values selected by the optimization procedure and associated accuracy statistics for high and low flows. Omission and commission errors ≥ 0.20 in bold.

Site	Flow	Probability threshold	Classification accuracy	Balanced accuracy	Omission error	Commission error
NE13	High	0.50	0.94	0.94	0.06	0.11
	Low	0.63	0.95	0.90	0.17	0.09
NE25	High	0.50	0.90	0.85	**0.24**	**0.20**
	Low	0.80	0.96	0.86	**0.27**	**0.21**
NE42	High	0.50	0.95	0.92	0.11	0.12
	Low	0.57	0.98	0.96	0.06	0.12
AP14	High	0.53	0.97	0.88	**0.22**	0.09
	Low	0.56	0.98	0.91	0.18	0.05
AP16	High	0.53	0.99	0.95	0.11	0.00
	Low	0.65	0.99	0.96	0.08	**0.21**
AP37	High	0.50	0.98	0.95	0.10	0.09
	Low	0.57	0.99	0.91	0.17	0.15
VR25	High	0.50	0.96	0.92	0.16	0.03
	Low	0.80	0.99	0.96	0.07	0.14
VR35	High	0.56	0.96	0.90	0.19	0.04
	Low	0.94	0.99	0.83	**0.33**	**0.43**
VR70	High	0.58	0.98	0.90	0.18	0.10
	Low	0.62	0.99	0.90	**0.20**	0.09
BR12	High	0.50	0.95	0.89	**0.20**	0.10
	Low	0.56	0.96	0.88	**0.24**	0.04
BR33	High	0.54	0.97	0.93	0.13	0.14
	Low	0.70	0.97	0.91	0.16	0.16
BR40	High	0.50	0.97	0.93	0.12	0.09
	Low	0.52	0.97	0.93	0.13	0.09

Table 4. High and low flow model parameters for NE, AP, and VR. The p-value of all model parameters is << 0.001.

Province	Model	McFadden's pseudo R^2	Parameters	Coefficient	t-statistic
NE	High	0.68	Intercept	-34.97	-39.08
			TWI(ln)	15.74	38.89
	Low	0.71	Intercept	-35.57	-30.32
			UAA (ln)	1.71	31.25
AP	High	0.81	Intercept	-19.68	-17.41
			TWI(ln)	7.97	14.90
			TPI (mean[a])	-4.80	-13.47
			Cross-sectional Curv.	-0.37	-9.67
	Low	0.79	Intercept	-33.12	-15.69
			TWI(ln)	12.11	16.77
			TPI (mean[a])	-4.05	-7.72
			Downslope index (mean[a])	16.90	7.04
VR	High	0.79	Intercept	-24.79	-33.62
			TWI(ln)	10.97	31.99
			TPI (mean[a])	-2.71	-15.65
			Longitudinal Curv.	0.24	18.46
	Low	0.71	Intercept	-22.39	-24.89
			TWI(ln)	9.12	24.00
			TPI (mean[a])	-3.47	-12.88

[a] Variable denoted as "mean" refers to the mean value of upslope pixels as opposed to the local value

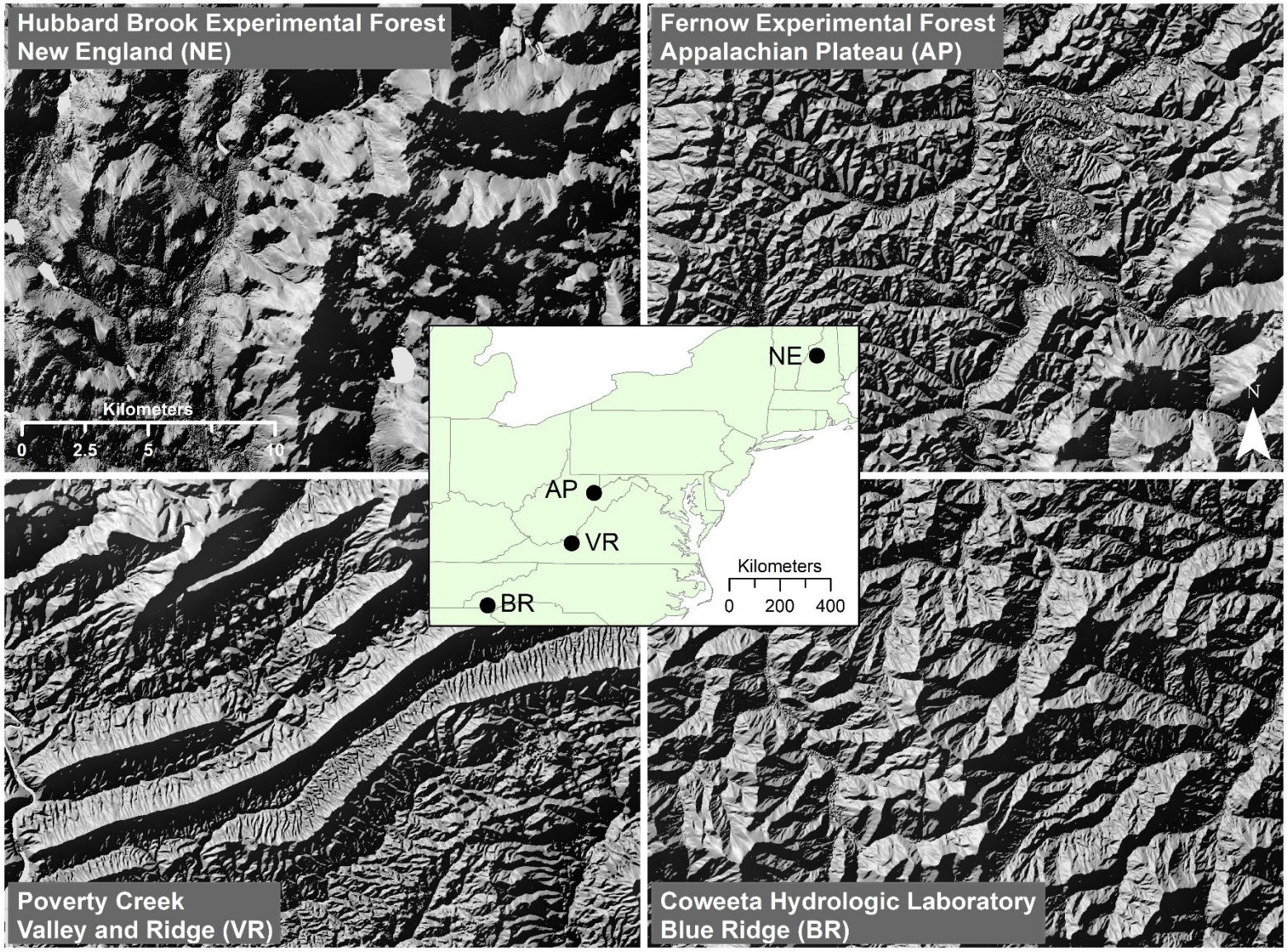

Figure 1. Hillshade views of regional topography in the four study areas.

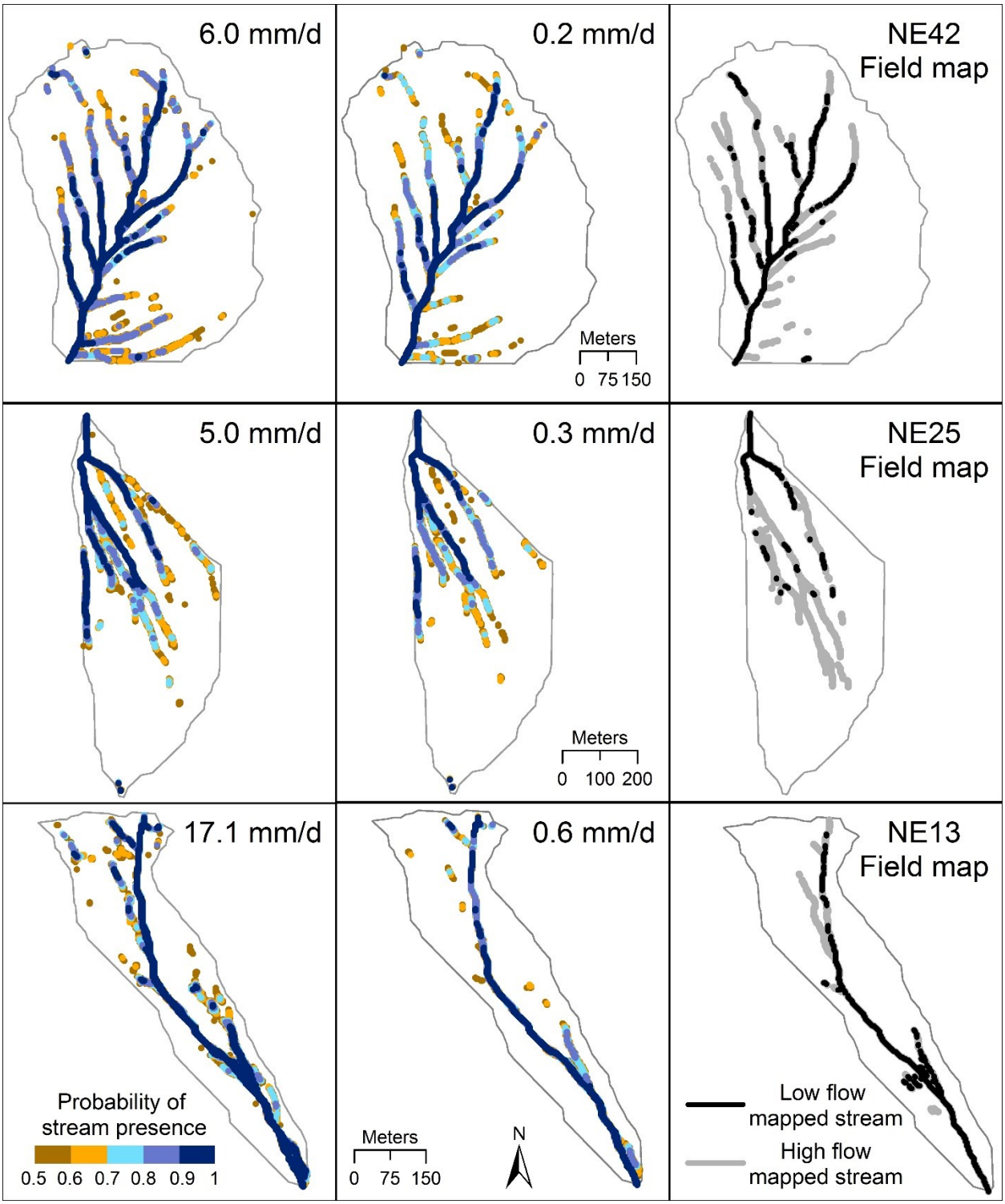

Figure 2. Modeled stream networks for high (left) and low (center) flows in NE. Right columns shows field-surveyed streams for the modeled flows. Only probability values > 0.50 are shown.

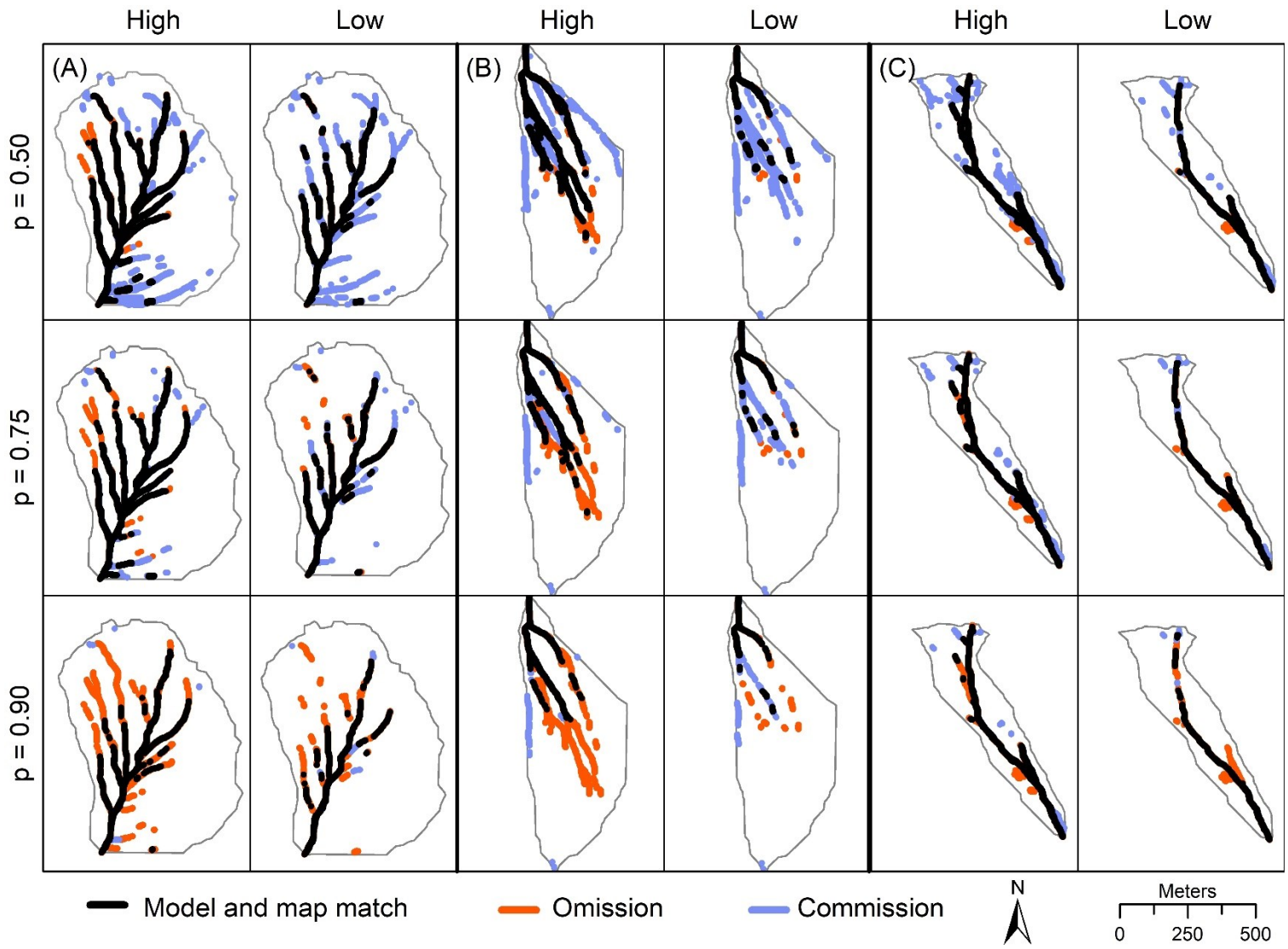

Figure 3. Omission and commission errors at NE42 (A), NE25 (B), and NE13 (C) at the highest and lowest mapped flows for probability thresholds of 0.50, 0.75, and 0.90. See Figure 2 for high and low runoff values.

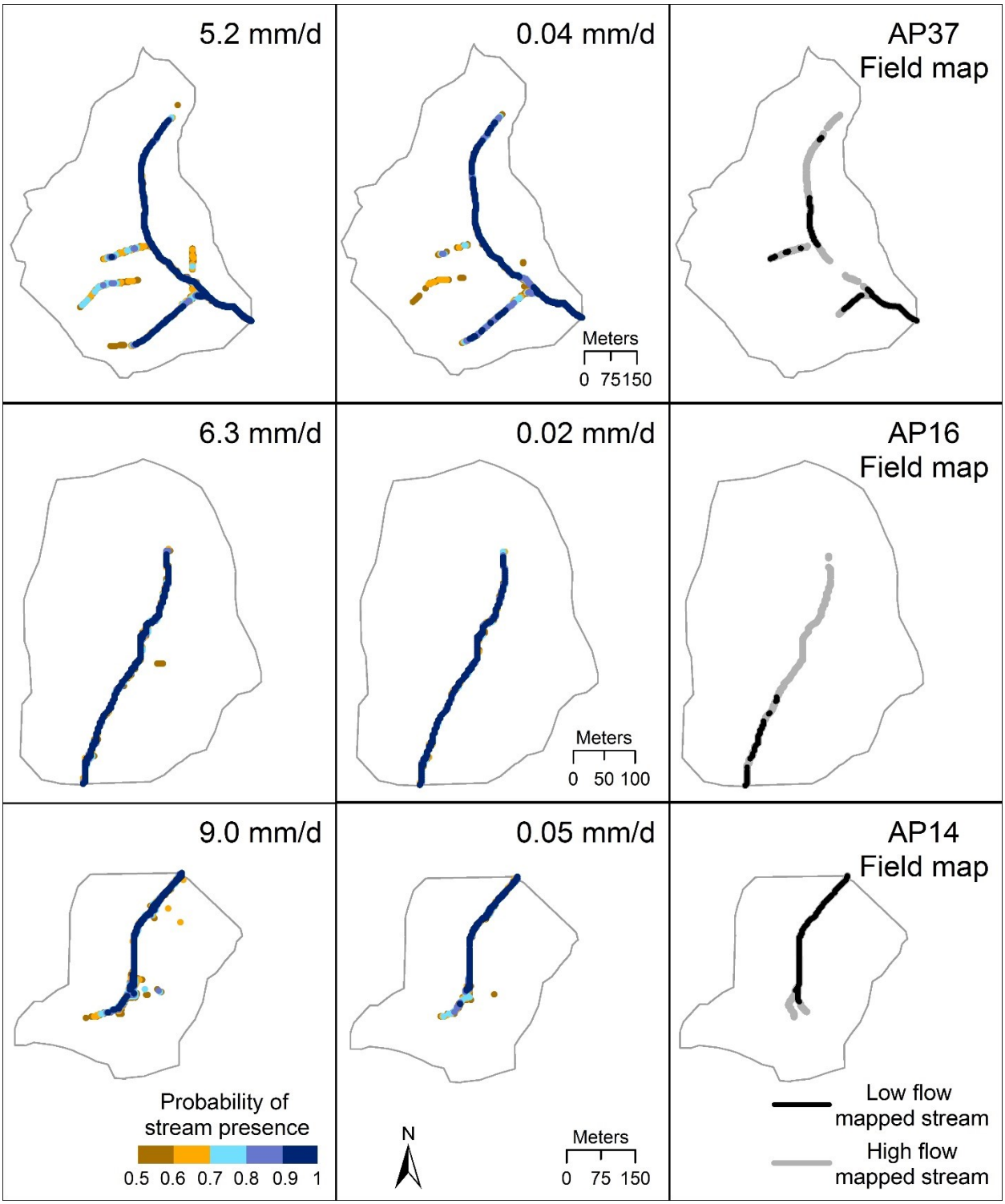

Figure 4. Modeled stream networks for high (left) and low (center) flows in AP. Right columns shows field-surveyed streams for the modeled flows. Only probability values > 0.50 are shown.

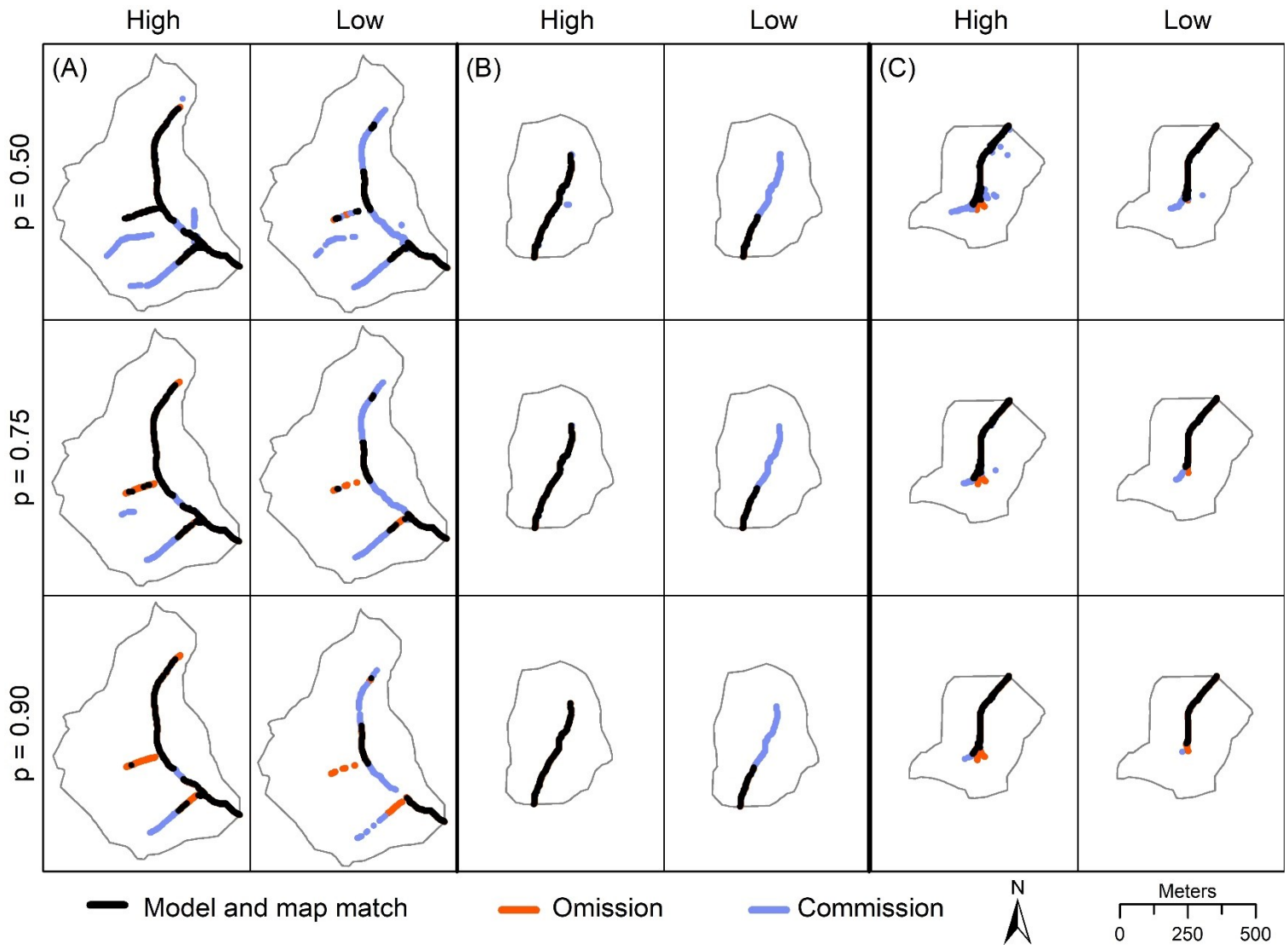

Figure 5. Omission and commission errors at AP37 (A), AP16 (B), and AP14 (C) at the highest and lowest mapped flows for probability thresholds of 0.50, 0.75, and 0.90. See Figure 4 for high and low runoff values.

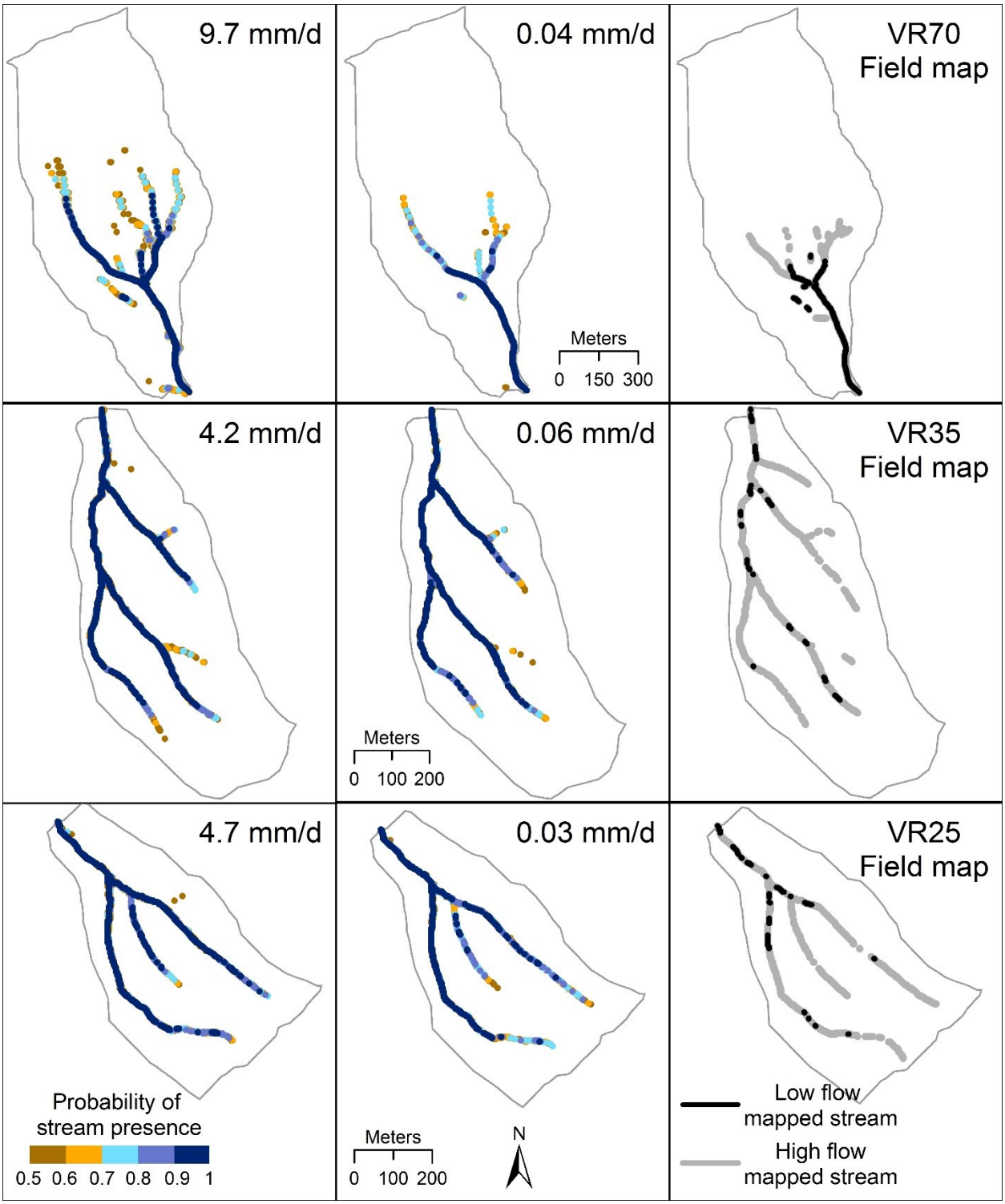

Figure 6. Modeled stream networks for high (left) and low (center) flows in VR. Right columns shows field-surveyed streams for the modeled flows. Only probability values > 0.50 are shown.

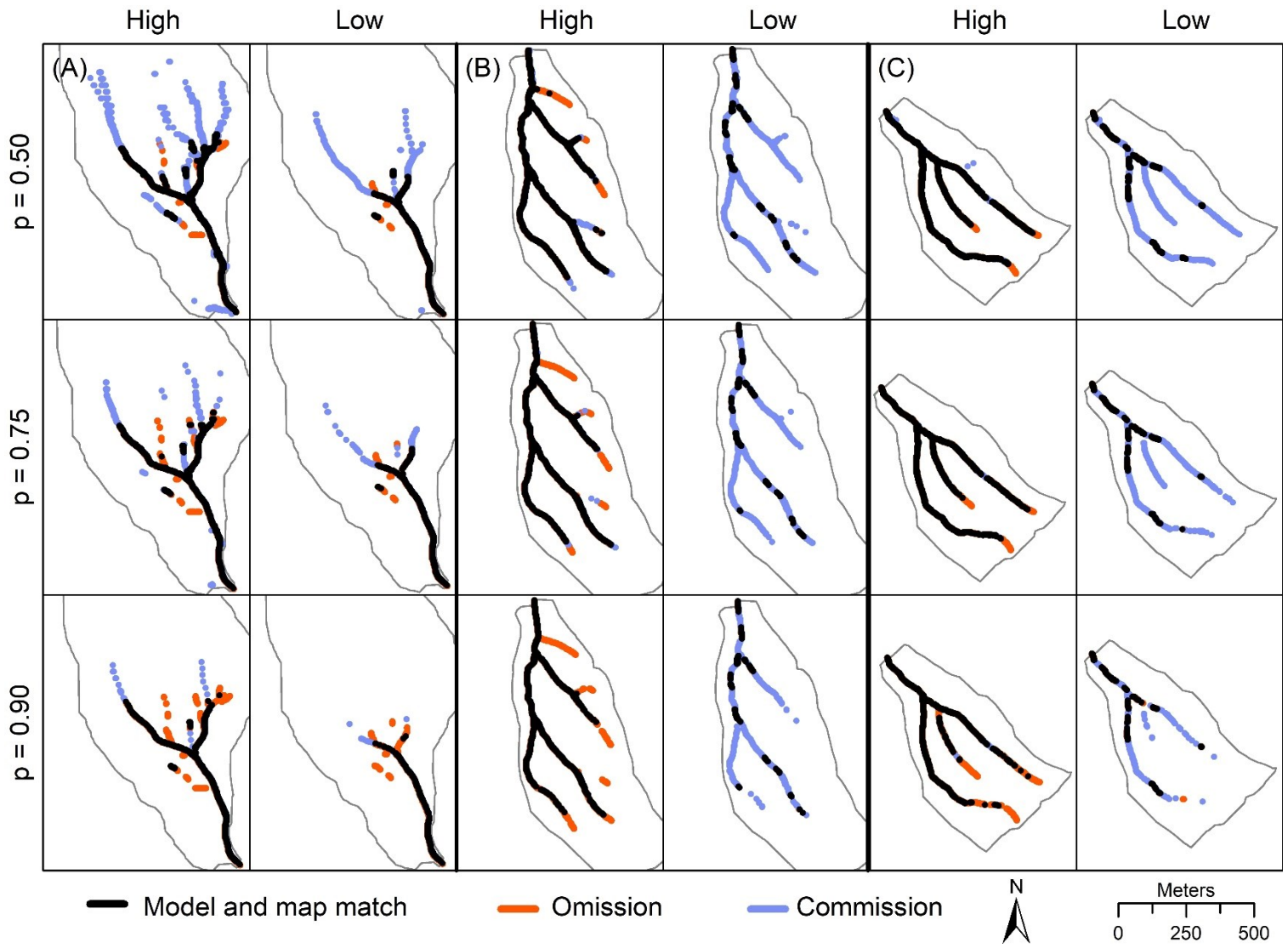

Figure 7. Omission and commission errors at VR70 (A), VR35 (B), and VR25 (C) at the highest and lowest mapped flows for probability thresholds of 0.50, 0.75, and 0.90. See Figure 6 for high and low runoff values.

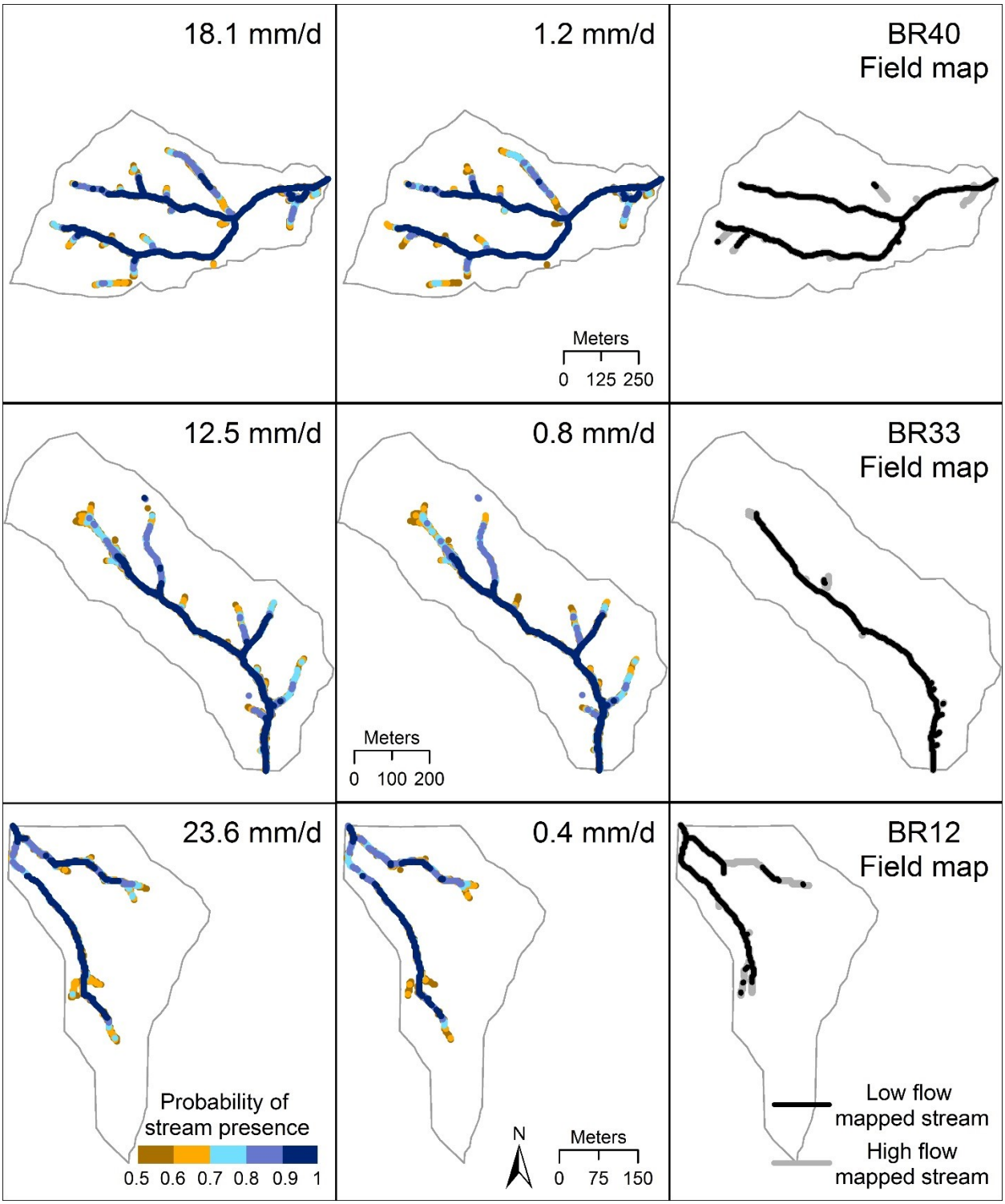

Figure 8. Modeled stream networks for high (left) and low (center) flows in BR. Right columns shows field-surveyed streams for the modeled flows. Only probability values > 0.50 are shown.

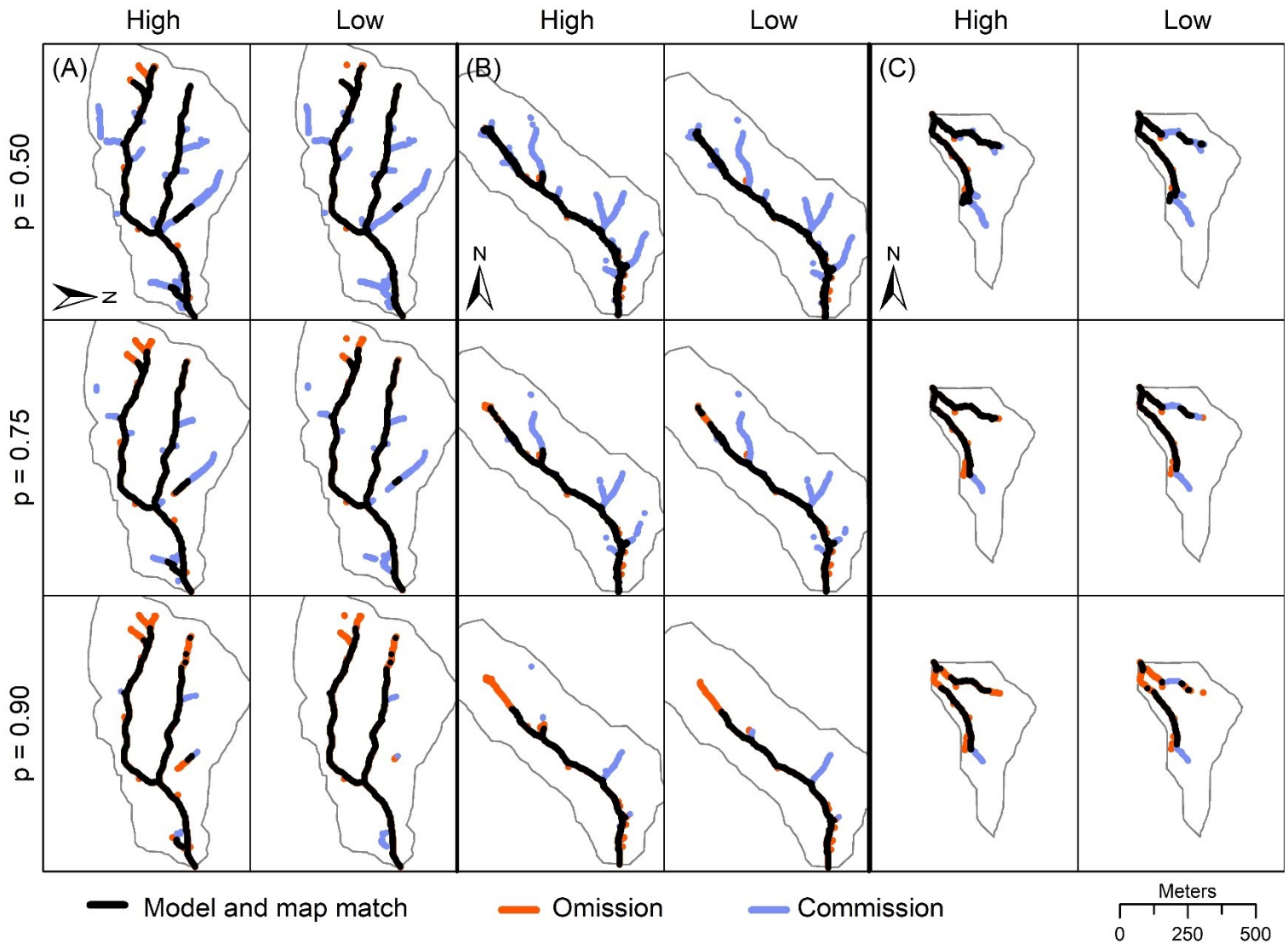

Figure 9. Omission and commission errors at BR12 (A), BR33 (B), and BR40 (C) at the highest and lowest mapped flows for probability thresholds of 0.50, 0.75, and 0.90. See Figure 8 for high and low runoff values. Note north orientation.

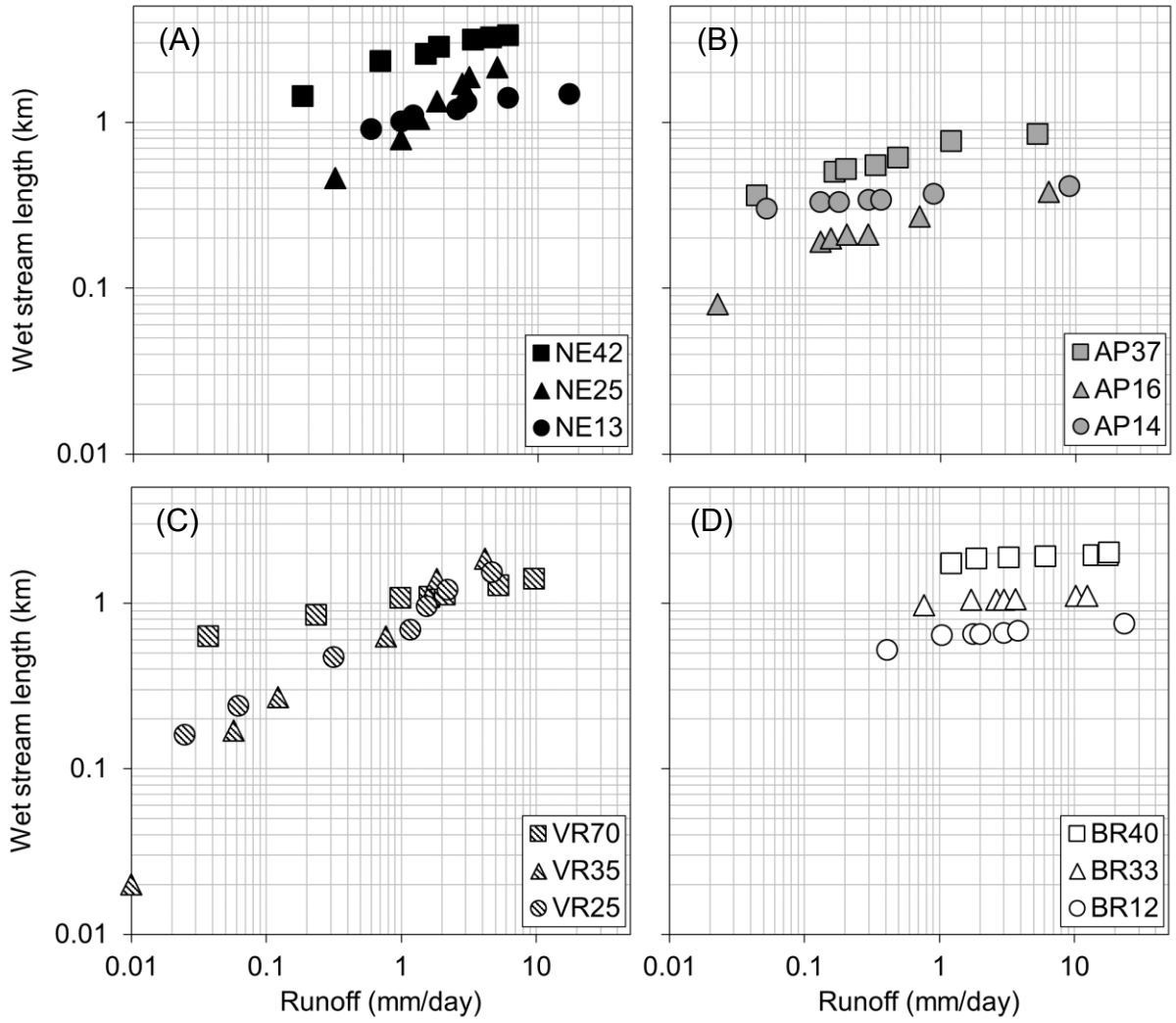

Figure 10. Stream length versus runoff in NE (A), AP (B), VR (C), and BR (D). Modified from Jensen et al. (2017).

References

Adams R. K., & Spotila J. A. (2005). The form and function of headwater streams based on field and modeling investigations in the Southern Appalachian Mountains. *Earth Surface Processes and Landforms*, *30*, 1521-1546.

Adams H. S., & Stephenson S. L. (1983). A description of the vegetation on the south slopes of Peters Mountain, southwestern Virginia. *Bulletin of the Torrey Botanical Club*, *110*, 18-22.

Alexander R. B., Boyer E. W., Smith R. A., Schwarz G. E., & Moore R. B. (2007). The role of headwater streams in downstream water quality. *Journal of the American Water Resources Association*, *43*, 41-59.

Avcioglu B., Anderson C. J., & Kalin L. (2017). Evaluating the slope- area method to accurately identify stream channel heads in three physiographic regions. *Journal of the American Water Resources Association*, *53*, 562-575.

Barton C. C. (1997). Bedrock geologic map of Hubbard Brook Experimental Forest and maps of fractures and geology in roadcuts along Interstate 93, Grafton County, New Hampshire, Scale 1:2000. U.S. Geological Survey Miscellaneous Investigation Series I-2562.

Benettin P., Bailey S. W., Campbell J. L., Green M. B., Rinaldo A., Likens G. E., … & Botter G. (2015). Linking water age and solute dynamics in streamflow at the Hubbard Brook Experimental Forest, NH, USA. *Water Resources Research*, *51*, 9256-9272.

Beven K. J., & Kirkby M. J. (1979). A physically based, variable contributing area model of basin hydrology. *Hydrological Sciences Journal*, *24*, 43-69.

Boulton A. J., Findlay S., Marmonier P., Stanley E. H., & Valett H. M. (1998). The functional significance of the hyporheic zone in streams and rivers. *Annual Review of Ecology and Systematics*, *29*, 59-81.

Buttle J. M., Boon S., Peters D. L., Spence C., van Meerveld H. J., & Whitfield P. H. (2012). An overview of temporary stream hydrology in Canada. *Canadian Water Resources Journal*, *37*, 279-310.

Calkins D., & Dunne T. (1970). A salt tracing method for measuring channel velocities in small mountain streams. *Journal of Hydrology*, *11*, 379-392.

Cardwell D. H., Erwin R. B., & Woodward H. P. (1968). Geologic map of West Virginia, 2 sheets, Scale 1:250,000. West Virginia Geological and Economic Survey.

Carlston C. W. (1963). Drainage density and streamflow. U.S. Geological Survey Professional Paper 422-C.

Cohen M. J., Creed I. F., Alexander L., Basu N. B., Calhoun A. J., Craft C., ... & Jawitz J. W. (2016). Do geographically isolated wetlands influence landscape functions? *Proceedings of the National Academy of Sciences*, *113*, 1978-1986.

Colson T., Gregory J., Dorney J., & Russell P. (2008). Topographic and soil maps do not accurately depict headwater stream networks. *National Wetlands Newsletter*, *30*, 25-28.

Datry T., Larned S. T., & Tockner K. (2014). Intermittent rivers: a challenge for freshwater ecology. *BioScience*, *64*, 229-235.

Dodds W. K., & Oakes R. M. (2008). Headwater influences on downstream water quality. *Environmental Management*, *41*, 367-377.

Downing J. A., Cole J. J., Duarte C. M., Middelburg J. J., Melack J. M., Prairie Y. T., ... & Tranvik L. J. (2012). Global abundance and size distribution of streams and rivers. *Inland Waters*, *2*, 229-236.

Elmore A. J., Julian J. P., Guinn S. M., & Fitzpatrick M. C. (2013). Potential stream density in Mid-Atlantic U.S. watersheds. *PlOS ONE*, *8*, e74819.

Evans S. (1979). An integrated system of terrain analysis and slope mapping. Final report on grant DA-ERO-591-73-G0040. University of Durham, England.

Feminella J. W. (1996). Comparison of benthic macroinvertebrate assemblages in small streams along a gradient of flow permanence. *Journal of the North American Benthological Society*, *15*, 651-669.

Fritz K. M., Johnson B. R., & Walters D. M. (2008). Physical indicators of hydrologic permanence in forested headwater streams. *Journal of the North American Benthological Society*, *27*, 690-704.

Fritz K. M., Hagenbuch E., D'Amico E., Reif M., Wigington P. J., Leibowitz S. G., … & Nadeau T. L. (2013). Comparing the extent and permanence of headwater streams from two field surveys to values from hydrographic databases and maps. *Journal of the American Water Resources Association*, *49*, 867-882.

Gillin C. P., Bailey S. W., McGuire K. J., & Prisley S. P. (2015a). Evaluation of Lidar-derived DEMs through terrain analysis and field comparison. *Photogrammetric Engineering and Remote Sensing*, *81*, 387-396.

Gillin C. P., Bailey S. W., McGuire K. J., & Gannon J. P. (2015b). Mapping of hydropedologic spatial patterns in a steep headwater catchment. *Soil Science Society of America Journal*, *79*, 440-453.

Godsey S. E., & Kirchner J. W. (2014). Dynamic, discontinuous stream networks: hydrologically driven variations in active drainage density, flowing channels and stream order. *Hydrological Processes*, *28*, 5791-5803.

González- Ferreras A. M., & Barquín J. (2017). Mapping the temporary and perennial character of whole river networks. *Water Resources Research*, *53*, 6709-6724.

Grabs T. J., Jencso K. G., McGlynn B. L., & Seibert J. (2010). Calculating terrain indices along streams: A new method for separating stream sides. *Water Resources Research*, *46*.

Guisan A., Weiss S. B., & Weiss A. D. (1999). GLM versus CCA spatial modeling of plant species distribution. *Plant Ecology*, *143*, 107-122.

Hansen W. F. (2001). Identifying stream types and management implications. *Forest Ecology and Management*, *143*, 39-46.

Hatcher Jr. R. D. (1988). Bedrock geology and regional geologic setting of Coweeta Hydrologic Laboratory in the eastern Blue Ridge. In W. T. Swank, & D. A. Crossley Jr. (Eds.), *Ecological Studies: Forest Hydrology and Ecology at Coweeta* (pp. 81-92). New York: Springer-Verlag.

Hedman E. R., & Osterkamp W. R. (1982). Streamflow characteristics related to channel geometry of streams in western United States. U.S. Geological Survey Water Supply Paper no. 2193.

Heine R. A., Lant C. L., & Sengupta R. R. (2004). Development and comparison of approaches for automated mapping of stream channel networks. *Annals of the Association of American Geographers*, *94*, 477-490.

Hewlett J. D., & Hibbert A. R. (1967). Factors affecting the response of small watersheds to precipitation in humid areas. *Forest Hydrology*, *1*, 275-290.

Hewlett J. D. (1982). *Principles of Forest Hydrology*. University of Georgia Press.

Hjerdt K. N., McDonnell J. J., Seibert J., & Rodhe A. (2004). A new topographic index to quantify downslope controls on local drainage. *Water Resources Research*, *40*.

Hooshyar M., Kim S., Wang D., & Medeiros S. C. (2015). Wet channel network extraction by integrating LiDAR intensity and elevation data. *Water Resources Research*, *51*, 10029-10046.

Hughes R. M., Kaufmann P. R., & Weber M. H. (2011). National and regional comparisons between Strahler order and stream size. *Journal of the North American Benthological Society*, *30*, 103-121.

James L. A., & Hunt K. J. (2010). The LiDAR-side of headwater streams: mapping channel networks with high-resolution topographic data. *Southeastern Geographer*, *50*, 523-539.

Jenness J. (2013). DEM Surface Tools for ArcGIS (surface_area.exe). Jenness Enterprises. Available at http://www.jennessent.com/arcgis/surface_area.htm.

Jensen C. K., McGuire K. J., & Prince P. S. (2017). Headwater stream length dynamics across four physiographic provinces of the Appalachian Highlands. *Hydrological Processes*, *31*, 3350-3363. 59

Johnson B. R., Fritz K. M., Blocksom K. A., & Walters D. M. (2009). Larval salamanders and channel geomorphology are indicators of hydrologic permanence in forested headwater streams. *Ecological Indicators*, *9*, 150-159.

Julian J. P., Elmore A. J., & Guinn S. M. (2012). Channel head locations in forested watersheds across the mid-Atlantic United States: a physiographic analysis. *Geomorphology*, *177*, 194-203.

Kuhn M. (2008). Caret package. *Journal of Statistical Software*, *28*, 1-26.

Larned S. T., Datry T., & Robinson C. T. (2007). Invertebrate and microbial responses to inundation in an ephemeral river reach in New Zealand: effects of preceding dry periods. *Aquatic Sciences*, *69*, 554-567.

Larned S. T., Datry T., Arscott D. B., & Tockner K. (2010). Emerging concepts in temporary-river ecology. *Freshwater Biology*, *55*, 717-738.

Larned S. T., Schmidt J., Datry T., Konrad C. P., Dumas J. K., & Diettrich J. C. (2011). Longitudinal river ecohydrology: flow variation down the lengths of alluvial rivers. *Ecohydrology*, *4*, 532-548.

Leibowitz S. G., Wigington Jr. P. J., Rains M. C., & Downing D. M. (2008). Non-navigable streams and adjacent wetlands: addressing science needs following the Supreme Court's Rapanos decision. *Frontiers in Ecology and the Environment*, *6*, 364-371.

Li J., & Wong D. W. (2010). Effects of DEM sources on hydrologic applications. *Computers, Environment and Urban Systems*, *34*, 251-261.

Likens G. E. (2013). *Biogeochemistry of a Forested Ecosystem*. New York: Springer Science & Business Media.

Losche C. K., & Beverage W. W. (1967). Soil survey of Tucker County and part of Northern Randolph County, West Virginia. Soil Survey Reports. U.S. Department of Agriculture.

Mac Nally R. (2000). Regression and model-building in conservation biology, biogeography and ecology: the distinction between—and reconciliation of—'predictive' and 'explanatory' models. *Biodiversity & Conservation*, *9*, 655-671.

Moore I. D., Grayson R. B., & Ladson A. R. (1991). Digital terrain modelling: a review of hydrological, geomorphological, and biological applications. *Hydrological Processes*, *5*, 3-30.

Morisawa M. E. (1962). Quantitative geomorphology of some watersheds in the Appalachian Plateau. *Geological Society of America Bulletin*, *73*, 1025-1046.

Nadeau T. L., & Rains M. C. (2007). Hydrological connectivity between headwater streams and downstream waters: how science can inform policy. *Journal of the American Water Resources Association*, *43*, 118-133.

Paybins K. S. (2003). Flow origin, drainage area, and hydrologic characteristics for headwater streams in the mountaintop coal-mining region of southern West Virginia, 2000-01. U.S. Department of the Interior, U.S. Geological Survey.

Płaczkowska E., Górnik M., Mocior E., Peek B., Potoniec P., Rzonca B., & Siwek J. (2015). Spatial distribution of channel heads in the Polish Flysch Carpathians. *Catena*, *127*, 240-249.

R Core Team. (2017). R: A language and environment for statistical computing. R Foundation for Statistical Computing, Vienna, Austria. http://www.R-project.org/.

Russell P. P., Gale S. M., Muñoz B., Dorney J. R., & Rubino M. J. (2015). A spatially explicit model for mapping headwater streams. *Journal of the American Water Resources Association*, *51*, 226-239.

Sainani K. L. (2014). Explanatory versus predictive modeling. *PM&R*, *6*, 841-844.

Schultz A. P., Stanley C. B., Gathright II T. M., Rader E. K., Bartholomew M. J., Lewis S. E., & Evans N. H. (1986). Geologic map of Giles County, Virginia, Scale 1:50,000. Virginia Division of Mineral Resources.

Seibert J., & McGlynn B. L. (2007). A new triangular multiple flow direction algorithm for computing upslope areas from gridded digital elevation models. *Water Resources Research*, *43*.

Skoulikidis N. T., Sabater S., Datry T., Morais M. M., Buffagni A., Dörflinger G., ... & Tockner K. (2017). Non-perennial Mediterranean rivers in Europe: status, pressures, and challenges for research and management. *Science of The Total Environment*, *577*, 1-18.

Spence C., & Mengistu S. (2016). Deployment of an unmanned aerial system to assist in mapping an intermittent stream. *Hydrological Processes*, *30*, 493-500.

Stanley E. H., Fisher S. G., & Grimm N. B. (1997). Ecosystem expansion and contraction in streams. *Bioscience*, *47*, 427-435.

Sun X., Thompson C. J., & Croke B. (2011). Using a logistic regression model to delineate channel network in southeast Australia. 19th International Congress on Modelling and Simulation (MODSIM 2011), Modelling and Simulation Society of Australia and New Zealand Inc., Perth, Australia, 1916-1922.

Svec J. R., Kolka R. K., & Stringer J. W. (2005). Defining perennial, intermittent, and ephemeral channels in eastern Kentucky: application to forestry best management practices. *Forest Ecology and Management*, *214*, 170-182.

Tarolli P., & Dalla Fontana G. (2009). Hillslope-to-valley transition morphology: new opportunities from high resolution DTMs. *Geomorphology*, *113*, 47-56.

Travis M. R., Elsner G. H., & Iverson W. D. (1975). VIEWIT: computation of seen areas, slope and aspect for land-use planning. U.S. Forest Service General Technical Report PSW-11. U.S. Department of Agriculture.

Velbel M. A. (1988). Weathering and soil-forming processes. In W. T. Swank, & D. A. Crossley Jr. (Eds.), *Ecological Studies: Forest Hydrology and Ecology at Coweeta* (pp. 93-102). New York: Springer-Verlag.

Virginia Division of Mineral Resources. (1993). Geologic Map of Virginia, Scale 1:500,000. Virginia Division of Mineral Resources.

Wang L., & Liu H. (2006). An efficient method for identifying and filling surface depressions in digital elevation models for hydrologic analysis and modelling. *International Journal of Geographical Information Science*, *20*, 193-213.

Whiting J. A., & Godsey S. E. (2016). Discontinuous headwater stream networks with stable flowheads, Salmon River basin, Idaho. *Hydrological Processes*, *30*, 2305-2316.

Williamson T. N., Agouridis C. T., Barton C. D., Villines J. A., & Lant J. G. (2015). Classification of ephemeral, intermittent, and perennial stream reaches using a TOPMODEL-based approach. *Journal of the American Water Resources Association*, *51*, 1739-1759.

Wilson J. P., & Gallant J. C. (Eds). (2000). *Terrain Analysis: Principles and Applications*. John Wiley and Sons.

Winter T. C. (2007). The role of ground water in generating streamflow in headwater areas and in maintaining base flow. *Journal of the American Water Resources Association*, *43*, 15-25.

Wohl E. (2017). The significance of small streams. *Frontiers of Earth Science*, *11*, 447-456.

Wood J. (1996). The geomorphological characterisation of digital elevation models. Doctoral dissertation, University of Leicester.

Zevenbergen L. W., & Thorne C. R. (1987). Quantitative analysis of land surface topography. *Earth Surface Processes and Landforms*, *12*, 47-56.

Chapter 4: Flow intermittency sensors characterize temporary stream length dynamics during storms in a Valley and Ridge headwater catchment

Authors

Carrie K. Jensen

Kevin J. McGuire

Daniel L. McLaughlin

Durelle T. Scott

Abstract

Scientists and policymakers increasingly recognize that headwaters contain numerous temporary streams that expand and contract in length, but accurately mapping and modeling stream network dynamics remain a challenge. We installed 51 flow intermittency sensors in a 33 ha Valley and Ridge catchment at an average spacing of 40 m to characterize variability in wet stream length at a high temporal resolution. The sensors recorded the presence or absence of water every 15 minutes for 10 months. Calculations of wet network connectivity from the sensor data aligned with those from field measurements in the catchment, confirming the efficacy of flow intermittency sensors. The fine temporal scale of the sensor data showed changes in stream length over the course of storm events, which are difficult to capture by field mapping. Wet stream length was higher on the rising limb of events than on the falling limb for dry antecedent conditions, which sometimes caused a delay of several hours between maximum network length and peak runoff at the catchment outlet. Less stream length hysteresis was evident for larger storms with more event and antecedent precipitation resulting in peak runoffs >15 mm/day. The topographic metrics we examined did not fully explain spatial variation in flow duration along the channel network. However, entrenched valleys had longer periods of flow on the rising limbs of events than unconfined reaches. In addition, large upslope contributing areas corresponded to higher flow duration on the falling limbs. Future studies that further explore the magnitude and drivers of stream length hysteresis may provide insights into concentration-discharge (C-Q) relationships of solutes as well as runoff generation processes in headwater regions.

4.0 Introduction

Temporary streams that do not carry perennial flow account for almost half of first- and second-order headwater channels (Nadeau & Rains, 2007; Buttle et al., 2012; Datry et al., 2014), which themselves comprise up to 80% of total river network length (Downing et al., 2012). Incidentally, the proportion of temporary streams is likely to increase in coming decades as a result of urbanization, surface and ground water withdrawals, and a projected decrease in river flows due to climate change (Stanley et al., 1997; Larned et al., 2010; Jaeger et al., 2014). Despite the global abundance of temporary headwaters, society often underestimates the ecological significance of low-order streams and considers these upstream extremities as inconsequential and unworthy of conservation or legal protections (Acuña et al., 2014; Wohl, 2017; Stubbington et al., 2017). Inaccurate maps (Bishop et al., 2008; Fritz et al., 2013; Skoulikidis et al., 2017), difficult access, and intermittent flow regimes continue to hinder public awareness as well as scientific understanding of headwater regions.

Stream length in temporary headwaters expands and contracts in response to flow variation at seasonal to storm-event scales. The wet or active drainage density can easily change by more than an order of magnitude within a single catchment (Gregory & Walling, 1968; Goulsbra et al., 2014; Jensen et al., 2017). The frequency, duration, and spatial extent of network expansion and contraction vary with lithology and other local geologic characteristics (Jaeger et al., 2007; Day, 1980; Whiting & Godsey, 2016; Jensen et al., 2017). As a result, catchments in the same physiographic province (Jensen et al., 2017) or smaller study area (Roberts & Klingeman, 1972; Godsey & Kirchner, 2014) may demonstrate quite different ranges of wet stream length, suggesting distinct ecosystem functions across diverse headwater settings.

Temporary headwater streams contribute a variety of ecosystem services driven by spatial variation in flow duration. Discontinuous reaches may form as temporary streams wet up and dry down (Godsey & Kirchner, 2014), increasing the diversity of microsites for stream habitat, nutrient processing, and material storage and transport (Stanley et al., 1997; Larned et al., 2010; Stubbington et al., 2017). Dry channel reaches without surface flow serve as storage sites for sediment, organic matter, and the eggs and seeds of aquatic species and provide aerobic conditions for mineralization and photodegradation (Steward et al., 2012). Subsurface flow can

occur along both wet and dry channel beds through the hyporheic zone to create habitat refugia, moderate water temperatures, and facilitate biogeochemical transformations such as denitrification (Boulton et al., 1998; Welter & Fisher, 2016). Activation and connection of the stream network with surface flow rapidly transmits water and accumulated channel material to downstream waterways. Because the presence or absence of surface water determines various ecological processes, understanding the spatial and temporal variability of stream length can help to describe the suite of temporary headwater ecosystem functions that are relevant for watershed management and policy.

Early studies of headwater stream length involved repeat field mappings at different flow conditions to characterize seasonal changes in the wet network (Gregory & Walling, 1968; Morgan, 1972; Roberts & Klingeman, 1972; Blyth & Rodda, 1973; Day, 1978; Day, 1980). Mapping even a small (< 50 ha) catchment requires hours or days, so field maps can only describe stream length at relatively stable flow conditions rather than short-term dynamics during storms when discharge changes rapidly. Field surveys currently remain the most accurate method of headwater delineation (Płaczkowska et al., 2015), with recent studies relying on multiple stream mappings with high resolution Global Positioning System (GPS) units to measure network expansion and contraction (Godsey & Kirchner, 2014; Shaw, 2016; Whiting & Godsey, 2016; Jensen et al., 2017; Zimmer & McGlynn, 2017). High resolution aerial photographs (Wigington et al., 2005; Spence & Mengistu, 2016) and LiDAR data (Hooshyar et al., 2015; Roelens et al., 2018) now permit extraction of the wet stream network in areas with sparse tree canopy cover, but the temporal resolution of most remote sensing data is far too coarse to study storm events.

Storm-event stream length dynamics are challenging to capture in headwaters owing to the quick stream flow response to rainfall and highly variable spatial pattern of precipitation, especially in mountainous regions. However, we risk greatly underestimating the maximum wet stream length and connectivity by simply field mapping between storms or using available remote sensing data, as the network may extend into normally dry ephemeral channels that only flow for a few minutes or hours during events. Flow intermittency sensors, also known as electrical resistance sensors, permit the simultaneous collection of stream length data across a catchment at a high

temporal resolution and are, thus, increasingly common for monitoring the wetting and drying of streams (Jaeger & Olden, 2012; Chapin et al., 2014; Goulsbra et al., 2014; Peirce & Lindsay, 2015). Dense instrumentation is only financially feasible in small catchments but can provide detailed data on temporary stream activation and network connectivity over varying time scales, including during individual storm events. Owing to the relatively recent development of flow intermittency sensors, most studies focus on the creation or modification of the sensor design (Goulsbra et al., 2009; Bhamjee & Lindsay, 2011; Chapin et al., 2014; Bhamjee et al., 2016; Peirce & Lindsay, 2015) or analyze the spatial pattern of flow onset in channels (Goulsbra et al., 2014; Peirce & Lindsay, 2015). Myriad research opportunities remain that utilize the high sampling frequency of the sensors to further our knowledge of temporary stream hydrology.

Existing studies of temporary stream length during storms calculate the flow duration of ephemeral channels (Jaeger & Olden, 2012), determine the maximum drainage density of the wet network (Goulsbra et al., 2014), or delineate network contraction on the recession limbs of events (Shaw, 2016). However, few studies seek to compare stream length over the course of individual storms on the rising and falling limbs, with the exception of some field mapping attempts during rainfall events (Morgan, 1972; Day, 1978) that are likely somewhat inaccurate due to the "virtual impossibility of continuous monitoring and the physical difficulty of highly frequent observations of stream length" (Day, 1978). Hysteresis is a common observation in hydrological processes in regards to the concentration-discharge (C-Q) relationships of solutes (Evans & Davies, 1998), sediment transport (Arnborg et al., 1967), soil moisture (Nieber & Walter, 1981), catchment storage-discharge relationships (McGlynn et al., 2004), and infiltration (Batlle-Aguilar & Cook, 2012). We hypothesize that wet stream length may also demonstrate hysteresis during storm events owing primarily to elevated infiltration of precipitation into initially dry channel reaches along temporary streams (Blasch et al., 2006; Niswonger et al., 2008). Transient infiltration rates at the onset of stream flow can be two to three orders of magnitude greater than when the channel reaches steady-state conditions, depending on antecedent moisture (Blasch et al., 2006). Thus, a hysteresis exists for seepage losses, with more infiltration on the rising limb than on the falling limb of events (Batlle-Aguilar & Cook, 2012). Evidence of stream length hysteresis would inform our understanding of controls on runoff

generation in headwater catchments and may also help explain aspects of C-Q relationships and sediment transport.

The purpose of this study is to use flow intermittency sensors to characterize changes in wet stream length in a Valley and Ridge headwater catchment over 10 months of data collection. Research questions include: (1) Does wet stream length display hysteresis on the rising and falling limbs of storms? (2) Does maximum network length occur at the same time as peak discharge? (3) Can we describe the frequency, or exceedance probability, of storm events resulting in different stream lengths of varying flow duration? (4) Do spatial patterns of flow duration correlate with topographic metrics?

4.1 Methods

4.1.1 Study site

The 33 ha study catchment is a tributary to Poverty Creek on the north slope of Brush Mountain in the Jefferson National Forest of Montgomery County, Virginia (Figure 1). Jensen et al. (2017) previously observed extreme expansion and contraction of the stream network at the site compared to other Appalachian streams, making the catchment an ideal setting for instrumentation to further examine the wetting and drying of temporary streams. The site lies in the central Valley and Ridge physiographic province at 660-830 m elevation, and underlying bedrock consists of Devonian shales, siltstones, and sandstones of the Brallier and Chemung Formations (Virginia Division of Mineral Resources, 1993). Soils are of the Berks and Weikert series and are shallow, acidic, nutrient-poor, highly permeable, and well-drained (Creggar et al., 1985). Based on data from the nearby Blacksburg (elevation 641 m), Staffordsville (elevation 594 m), and Mountain Lake (elevation 1180 m) climate stations, mean temperatures vary from -4 to 1°C in January and from 19°C to 22°C in July, depending on the elevation (SERCC, 2012). Yearly precipitation averages 98 to 103 cm for the low-elevation stations and 126 cm at Mountain Lake, with snowfall accounting for less than 10% of the total (SERCC, 2012). Precipitation is generally highest in the summer, but peak stream flows typically occur in the winter and early spring. Widespread logging occurred along Brush Mountain through the early 20th century. Forests have since been subject to wildfire, selective logging, and the extirpation of American chestnut (*Castanea dentata*), but are relatively mature (> 60 years old) in the study

catchment. Oaks (*Quercus coccinea*, *Quercus prinus*, *Quercus velutina*) dominate the forest, although red maple (*Acer rubrum*), pitch pine (*Pinus rigida*), and table mountain pine (*Pinus pungens*) are also common (Adams & Stephenson, 1983; Williams & Johnson, 1990).

4.1.2 Flow intermittency sensors

Flow intermittency sensors are modified temperature loggers that detect the presence of water as a large increase in electrical conductivity (Blasch et al., 2002; Chapin et al., 2014). Earlier studies simply used temperature loggers to determine the onset and cessation of flow in channels (Constantz et al., 2001) but required subjective interpretation of the data to discriminate between wet and dry periods (Blasch et al., 2002). Flow intermittency sensors clearly indicate the presence or absence of water, have a user-defined sampling interval, and are one of the least expensive ways to record the duration of stream flow at $75-100 each (Blasch et al., 2002; Goulsbra et al., 2009; Chapin et al., 2014).

We modified 51 Onset HOBO Pendant Temperature/Light 64K data loggers (UA-002-64) following the methodology of Chapin et al. (2014) to create the flow intermittency sensors. Alteration of the loggers involves removal of the light sensor and the addition of two electrodes, which permit the detection of high electrical conductivity when water is present to connect the electrodes in a continuous circuit. The resulting sensor shows the presence or absence of water as quite high (~400-2000 µS/cm) or low (~0 µS/cm) conductivity readings, respectively. We drilled two holes in the logger caps and inserted 100 mm 24-gauge male-male jumper wires with machine pin heads (Digikey #438-1074-ND) that we cut in half to form the electrodes. We applied marine contact adhesive and sealant around the electrodes to seal the holes. We de-soldered the light sensor on the front of the logger electrical board and attached the cut ends of the two electrodes from the cap to the light sensor contact pads. We reassembled the sensors and tested each unit to ensure proper function before deployment using 15-minute data collection intervals.

4.1.3 Field instrumentation and data collection

We created sensor housings from 2 inch PVC male and cleanout adapters with threaded caps. The housing bottoms were open, and we drilled holes around the sides of the adapters to allow

water to flow in and out. We covered the bottoms and sides of the adapters with screen material secured with zip ties to help prevent the accumulation of sediment around the sensors. We drilled two holes in the threaded caps to tied fishing line to the sensors so that we did not lose them if the housings moved during a storm event. The threaded caps permitted the easy retrieval of sensors for downloading data in the field.

We drove 50 cm sections of steel fence U-posts into the channel bed with a sledgehammer so that less than 15 cm of the posts remained above ground. We attached the housings with zip ties through the holes along the post at the channel bed surface. The sensors lay sideways in the base of the adapters with the electrode pins just above the channel bed so as to detect even low water depths. There were 51 sensors to span nearly 2 km of the stream network that Jensen et al. (2017) mapped in the field during high flow conditions, yielding an average sensor spacing of 40 m. However, we did not always install the sensors at even intervals. The channel bed was too rocky to drive in the posts at some locations, and we slightly modified the spacing interval in some reaches to ensure that there were sensors in both confined and wide, unconfined valley floor settings. Our spacing of 40 m was finer than other studies that placed flow intermittency sensors at average intervals of 60 m (Goulsbra et al., 2014) to 2 km (Jaeger & Olden, 2012). We marked the locations with a Bad Elf GNSS Surveyor GPS unit with 1 m reported accuracy. In addition, we measured valley width at each sensor as the distance between the valley walls at a height of 1 m above the channel thalweg. The sensors collected data every 15 minutes from May 2017 through February 2018. A pressure transducer installed at the catchment outlet recorded stream stage at 15-minute intervals for the duration of the study. We used salt dilution gauging (Calkins & Dunne, 1970) to determine stream discharge multiple times and created a stage-discharge curve to estimate runoff over the course of storm events.

4.1.4 Field data analysis

We examined the conductivity readings for each sensor and selected individual thresholds to convert the values into binary data showing the presence or absence of water. We decided to manually choose the thresholds rather than developing an automated approach owing to fluctuations in sensor readings through time and some confounding intermediate conductivity values higher than the dry signal (> 50) but lower than the wet signal (< 200-400). In the cases of

intermediate values, we checked for recent precipitation or a rise in stream stage at the watershed outlet and compared the change in conductivity to the background dry signal to determine whether the reading corresponded to wet or dry conditions. We calculated flow duration for each sensor as the percentage of time with water present during the 10-month study period as well as individual storm events. We also determined the wet proportion of the channel network as the percentage of sensors with flow at each 15-minute interval as a proxy for wet stream length.

Sub-hourly precipitation data were from a nearby weather station (Weather Underground KVABLACK18) near Laurel Ridge on Brush Mountain (37° 15' 39" N, 80° 26' 56"). The station is on the south slope of Brush Mountain at an elevation of 646 m and a distance of 3 km from the center of the study catchment. We did not install a precipitation gauge at the site owing to tree cover and a high risk of vandalism from heavy recreational use in the area. We calculated precipitation totals for storm events causing an increase in the stream hydrograph during the 10-month deployment period. We defined events as periods of continuous or intermittent precipitation separated by at least 24 hours without measurable rainfall. Once we determined the beginning and end of each event, we calculated the 7-day, 14-day, and 30-day total antecedent precipitation (AP) as well as the antecedent precipitation index (API) according to Mosley (1982).

To summarize the wet proportion, flow duration, and frequency of stream network expansion during storm events, we organized the sensor data in the style of intensity-duration-frequency (IDF) curves. We divided the dataset according to events, with all data points after the storm until the next hydrograph rise pertaining to the previous event. For every storm, we counted the frequency of observations for each wet proportion value and created cumulative counts to determine the amount of time the network was at or above a given wet proportion per event. We then sorted the cumulative counts for each wet proportion value to calculate the exceedance probability according to the Weibull plotting position of storms producing various flow durations of given wet proportions.

4.1.5 Terrain analysis

We imported the GPS points of the sensor locations into ArcGIS (ArcMap version 10.5, ESRI 2016, Redlands, CA). Average GPS accuracy at the site was 5 to 8 m, so we verified that the points intersected the field-mapped channel network that Jensen et al. (2017) delineated. We used a 3 m Digital Elevation Model (DEM) derived from LiDAR data collected in 2011 for the Virginia Geographic Information Network for the calculation of terrain metrics. We re-sampled the LiDAR bare earth DEM to 1 m, coarsened the DEM to 3 m by mean cell aggregation, and applied a low-pass (3 x 3) filter and sink-filling algorithm (Wang & Liu, 2006), as is customary for hydrological correction. We calculated the upslope accumulated area (UAA) according to the multiple triangular flow direction algorithm (Seibert & McGlynn, 2007); maximum slope (Travis et al., 1975); topographic wetness index (TWI), using the multiple triangular flow direction and maximum slope algorithms (Beven & Kirkby, 1979); and topographic position index (TPI) (Guisan et al., 1999), which compares the elevation of a pixel to the mean elevation in a 100 m radius around the cell. These metrics are often among the most significant variables in stream network models (Elmore et al., 2013; Russell et al., 2015; González-Ferreras & Barquín, 2017; Jensen et al., 2018). We derived additional "mean" raster grids for the slope, topographic wetness index, and topographic position index metrics by determining the mean of all cell values in the upslope area contributing to each pixel. We then extracted values from the raster grids at the sensor locations for performing Pearson correlations between the terrain metrics, valley width we measured in the field, and flow duration.

4.2 Results

4.2.1 Efficacy of flow intermittency sensors

The sensors recorded data for a total of 10 months between May 2017 and February 2018. We had to replace several sensors over the course of the study due to missing or malfunctioning sensors. However, the maximum number of missing or non-functioning sensors at any time was 3 out of the 51, so data gaps were not a major issue. Overall, the field instrumentation and sensor deployment were quite successful in a channel with a flashy flow regime (Jensen et al., 2017) that we have observed to move substantial bedload.

We compared the wet channel proportion recorded by the sensors, which is the percentage of sensors with flow, to the wet network connectivity that Jensen et al. (2017) measured in the field along the same channel network (Figure 2). Jensen et al. (2017) mapped wet stream length in the study catchment with a GPS unit 7 times at different runoffs. We divided the wet stream length at each mapping by the maximum stream length delineated at the highest runoff, which included both wet and intervening dry reaches, to calculate wet network connectivity. There was excellent agreement between the sensor and field-mapped data, although the sensors slightly underestimated the actual wet network connectivity at lower runoffs. As point measurements, the sensors were more likely to miss isolated pools that formed along the network during low flows.

4.2.2 Flow duration and wet network proportion

The temporal distribution of precipitation during the study period was highly uneven (Figure 3), although the total precipitation was only slightly below the 30-year normals (1981–2010) (Table 1). May, October, and February were wetter than the normals for these months owing to several large storms, but the remaining 7 months were all drier than usual. The winter months in particular were quite dry, with December receiving almost 6 cm less than the December normals. Stream flows in the region are generally higher in the winter than in the summer and fall, so conditions during the study were somewhat atypical. Most of the sensors had a flow duration of less than 30% during the 10-month monitoring period, and more than half had a flow duration of less than 10% (Figure 4). The wet channel proportion was also strongly skewed with a wet proportion of less than 20% for nearly 80% of the time. However, the wet proportion did remain above 80% for several days in total during the study period. Flow duration and wet proportion values were undoubtedly lower overall due to the extended dry period from November through January.

We analyzed 24 storm events (Table 2; Figures 5 & 6) that resulted in a response among the sensors and a rise in the stream hydrograph above background variation that created a defined peak with rising and falling limbs. The maximum wet proportion ranged from 4 to 100% across the 24 events. The relationship between stream flow and the wet proportion varied between events. A peak runoff of less than 0.25 mm/day on 07/05/17 and 08/05/17 produced wet proportions of 10-15%, whereas the event on 12/24/17 with a maximum runoff above 0.30

mm/day reached a wet proportion of only 4% (Figure 6). Similarly, the event on 06/16/17 had a peak runoff of less than 1.2 mm/day and a maximum wet proportion of nearly 60% (Figure 5). However, the events on 01/13/18 and 01/28/18 with greater peak runoffs of more than 1.4 mm/day and larger event precipitation totals (Table 2) resulted in lower wet proportions of 30-50%. In both cases, the events with higher runoffs but lower wet proportions had drier antecedent conditions with lower 14- and 30-day AP and API values.

The wet proportion demonstrated varying degrees of hysteresis across storm events (Figures 5 & 6). The largest events with peak runoffs above 15 mm/day had similar wet proportions on the rising and falling limbs, although the event on 10/23/17 briefly showed a higher wet proportion on the falling limb between runoffs of 3 and 7 mm/day (Figure 5). For the remaining events, the wet proportion was almost always higher on the rising limb (Figures 5 & 6). The difference between the wet proportion on the rising and falling limbs was usually greatest at low to moderate runoffs relative to each event and tended to decrease near peak runoff, as was most evident for storms on 06/05/17, 06/16/17, 08/13/17, 01/28/18, and 02/04/18. Aside from the largest events that had nearly identical wet proportions on the rising and falling limbs, the amount of hysteresis did not correspond to maximum runoff or the wet proportion. For example, the event on 05/06/17 displayed only a slight decrease in the wet proportion on the falling limb, but events with both higher (01/28/18 and 02/04/18) and lower (06/16/17, 08/13/17, and 01/13/18) runoff and/or connectivity showed clear hysteretic loops (Figure 5). Of these events with similar runoffs, the 05/06/17 storm had the highest event precipitation total and, with the exception of the storm on 08/13/17, the greatest 14- and 30-day API values (Table 2).

For 13 of the 24 events, the maximum wet proportion during each storm either coincided with peak discharge at the catchment outlet or occurred both before and after peak flow (Table 2). Of the remaining storms, only the events on 08/13/17 and 06/16/17 produced the maximum wet proportion following the hydrograph peak by 15 minutes. For the other 9 events, the maximum wet proportion preceded peak runoff, in some cases by several hours. Accordingly, the events with the greatest lag between maximum stream length and peak flow (07/19/17, 07/05/17, and 01/13/18) were also those that demonstrated considerable hysteresis (Figures 5 & 6).

We did not have precipitation gauges at the site to measure the amount, intensity, and spatial distribution of rainfall across the catchment, which would be necessary to model the expansion and contraction of the wet network during a particular storm. In order to visualize general relationships among the storm events between the maximum wet proportion, time lag between the maximum wet proportion and peak runoff, and the precipitation metrics derived from rainfall data at the Laurel Ridge weather station (Table 2), we performed a principal components analysis to examine correlation with a biplot (Figure 7). The first dimension explained 59% of the variance and primarily distinguished events according to antecedent moisture. Storms with high AP and API appear on the left half of the biplot at low values of the first principal component. The second dimension accounted for an additional 14% of the variance and mostly corresponded to event precipitation totals, with larger storms in the bottom half of the biplot. The second principal component additionally differentiated many storms by leaf-on and -off conditions, so events during the summer months are predominantly in the top half of the biplot. The event on 05/24/17 was one exception that appears near the bottom of the biplot, but this storm had the highest event precipitation total as well as API values (Table 2). The maximum wet proportion closely aligned with event precipitation but also correlated with the 7-day AP and API (Figure 7). The time to maximum stream length variable did not load highly on either of the first two principal components but correlated with the 7-day AP and 14-day API along the first dimension. Thus, events with low antecedent moisture in the right half of the biplot tended to reach the maximum wet proportion before peak runoff (corresponding to negative values of the time lag variable).

Like IDF curves, the wet proportion-flow duration-frequency curves indicate the exceedance probability over 10 months of wet proportions at varying flow durations in response to storm events (Figure 8). Like the histogram of overall flow duration (Figure 4), the curves show that wet proportions are frequently below 20%, while wet proportions above 80% are uncommon and correspond to high exceedance probabilities (Figure 8). However, the curves illustrate changes in the exceedance probability with flow duration for intermediate wet proportions, which we cannot determine from histograms. For example, wet proportions of 50% or more are relatively common with an exceedance probability of ~40% for low flow durations of less than 1 hour, but the exceedance probability decreases to ~10% for flow durations greater than 100 hours.

4.2.3 Spatial patterns of flow duration

Expansion and contraction of the wet network mainly occurred by the growth and disconnection of discontinuous reaches (Figure 9). Although the stream did not show a strictly bottom-up or top-down wetting and drying progression over the course of storm events, we did observe that sensors at the top of the catchment near the tributary heads tended to activate with flow first on the rising limb (Figure 9 A & B) but were also the first to cease flow on the falling limb (Figure 9 C & D). Flow duration at the sensors over the full 10-month period correlated significantly with UAA, mean TPI, and TWI (Table 3). We separated the sensor data pertaining to the rising and falling limbs of all storm events during the study period and repeated the correlation analysis. UAA was positively correlated to flow duration and had the highest Pearson's r value on the falling limbs and for the entire 10-month dataset. Mean TPI had a negative correlation, since negative TPI values correspond to valleys and positive values indicate ridges, and resulted in the highest r value on the rising limbs. However, all r values were less than 0.50. We also calculated correlation coefficients on the rising and falling limbs of each of the 24 storm events, as opposed to pooling all events, but the r values did not notably improve on a per-storm basis.

4.3 Discussion

4.3.1 Storm stream length dynamics

The maximum wet proportion of the sensors increases with event precipitation (Figure 7) and stream runoff (Figure 2) but also greatly depends on antecedent wetness. Some events in our dataset with low antecedent wetness resulted in lower wet proportions than storms with smaller peak runoffs and similar or less event precipitation (Table 2; Figures 5 & 6). As an example, events two weeks apart on 10/08/17 and 10/23/17 had maximum wet proportions of 26 and 94% respectively, for nearly identical rainfall amounts of ~5 cm (Table 2). The AP and API values for the storm on 10/08/17 are all quite low, but this event increased catchment wetness and associated antecedent moisture metrics to permit greater network expansion for the 10/23/17 event. Day (1978) likewise notes different stream lengths for comparable precipitation totals and qualitatively attributes this variation to antecedent moisture.

The timing of network activation also varies with storm event magnitude and antecedent moisture conditions. The largest storms with high event precipitation totals and AP or API values

create maximum wet proportions above 80% (Figure 5), which occur at the same time as peak runoff at the catchment outlet (Table 2). Goulsbra et al. (2014) similarly found that maximum stream length in a peatland catchment coincides with peak flow. The wet proportion during these large events does not display major hysteresis, with comparable values on the rising and falling limbs. In contrast, the wet proportion is often greater on the rising limb than on the falling limb for storms with lower peak runoffs (< 15 mm/day) (Figures 5 & 6). As a result, the maximum wet proportion can occur before peak runoff during these smaller events. Unlike Goulsbra et al. (2014), Day (1978) observed that the highest stream length in Australia precedes peak flow, but only by several minutes. Conversely, the time lags in our catchment are several hours for some storms (Table 2). Events with greater hysteresis, corresponding to a large decrease in the wet proportion from the rising to the falling limb, or a delay between the maximum wet proportion and peak runoff tend to have low antecedent moisture (Table 2) and primarily appear in the right half of the biplot (Figure 7).

Minor seasonality is evident in our data between the summer months and the remainder of the study period despite the below-average winter precipitation (Table 1). Event precipitation totals are generally smaller during the summer (Table 2) due to the prevalence of isolated thunderstorms rather than widespread frontal systems. Therefore, the maximum wet proportion also tends to be lower for summer storms, which mostly appear in the top half of the biplot (Figure 7). Between June and mid-October, the stream network reaches a maximum wet proportion of only 60% for just one storm (Table 2). In addition, two of the largest delays between the maximum wet proportion and peak runoff are in July. Besides the lower and less spatially extensive rainfall during the summer, this seasonal variation likely reflects higher evapotranspiration rates that further reduce antecedent wetness.

4.3.2 Possible mechanisms of stream length hysteresis

Because the stream network in our study catchment has a low overall flow duration (Figure 4), we initially postulated that stream length would be lower on the rising limb of events due to increased infiltration along dry channel reaches (Blasch et al., 2006; Niswonger et al., 2008). Weill et al. (2013) also modeled a lower connected saturated area on the rising limb of storm events for a headwater catchment in Italy, which the authors attribute to rainfall during the rising

limb that increases stream flow. However, the sensor data show that the wet proportion is actually higher on the rising limb for events with dry antecedent conditions, when transient infiltration should be highest. Network expansion and contraction in the catchment primarily occur by the coalescence and disintegration of disconnected reaches (Bhamjee & Lindsay, 2011; Peirce & Lindsay, 2015). Thus, surface water that appears in channels and flows to the outlet is continuously infiltrating into the channel bed of dry reaches, slowing flow velocity (Niswonger et al., 2008). By the time the water arrives at the gauge, the channels upstream may already be dry, especially if the precipitation is short in duration or an isolated thunderstorm. However, surface flow from the tributaries often never reaches the outlet. Disconnected pools and flowing reaches expand and contract during small events without always connecting downstream (Goulsbra et al., 2014). For several of the storm events with low runoff during the study period, sensors along the main channel stem just upstream of the outlet never activated with flow to create a continuous wet network with reaches higher in the catchment. Therefore, stream length hysteresis and the delay between maximum stream length and peak flow are also likely due to the time necessary for rain to infiltrate in the uplands and form zones of saturation within the soil to contribute to lateral interflow or raise the water table and increase discharge downstream.

Studies of catchment storage-discharge relationships describe clockwise hysteretic loops, with changes in subsurface storage lagging stream flow response for dry antecedent conditions (McGlynn et al., 2004; Penna et al., 2011; Camporese et al., 2014). As a result, ground water levels on hillslopes can be higher on the falling limb of an event than on the rising limb for a given stream discharge value (Haught & Meerveld, 2011; Camporese et al., 2014). Our findings suggest the additional consideration of changes in the spatial extent of surface water for storage-discharge relationships, which may differ from subsurface storage dynamics. While hillslope ground water levels can lag behind discharge for storms with low antecedent moisture, the stream network lengthens to increase surface storage before the stream flow response at the catchment outlet (Figures 5 & 6). Subsurface storage is higher after peak runoff for these small events (Camporese et al., 2014), but settings with deep water tables may not have a sufficient increase in ground water levels to supply stream channels with surface flow on the falling limb. In this manner, storage in our study catchment shifts from the surface along the channel network to the subsurface over the course of low-runoff events during dry periods. Relative contributions

of surface versus subsurface storage and the resulting degree of stream length hysteresis would likely additionally vary with geology, topography, catchment size, and channel pattern.

The delay between subsurface storage and stream flow disappears for events with high antecedent moisture and subsequent runoff (Myrabø, 1997; Weill et al., 2013). The lack of hysteresis in storage-discharge relationships for storm events above some threshold runoff or antecedent wetness agrees with our results that indicate a similar wet stream length on the rising and falling limbs of high-runoff events (> 15 mm/day). Ward et al. (2018) also discuss distinct hydrologic states with increasing discharge as the controls on wet stream length shift from the event magnitude to geology and network topology. A greater proportion of subsurface flow on the rising limb of large events in combination with reduced transient infiltration into channel reaches with high antecedent moisture may increase subsurface as well as surface hydrological connectivity of the catchment (Jencso et al., 2009) to synchronize peak flow and the maximum wet proportion during these storms.

4.3.3 Topographic controls on flow duration

The stream network in our study catchment displays a discontinuous spatial pattern of wetting and drying, which other studies of stream length dynamics also describe in a variety of headwater settings (Day, 1978; Godsey & Kirchner, 2014; Goulsbra et al., 2014; Peirce & Lindsay, 2015; Shaw, 2016; Jensen et al., 2017). However, some degree of top-down activation (Peirce & Lindsay, 2015) is also evident (Figure 9). Mean TPI has the highest correlation with flow duration at the sensors on the rising limbs of events (Table 3), suggesting flow onset occurs first in more entrenched valleys. Interestingly, mean TPI is one of the primary variables in a logistic regression model explaining the location of wet headwater streams in the Valley and Ridge (Jensen et al., 2018). Goulsbra et al. (2014) did not examine TPI but found that the closely related gully depth was a significant predictor of water table depth and flow duration at the sensor locations. UAA is also significant on the rising limbs, albeit with a much lower correlation, which supports our observation of top-down wetting in addition to the coalescence of disconnected wet reaches. Top-down wetting is associated with a low infiltration capacity of the substrate or high-intensity rainfall that inhibits infiltration (Peirce & Lindsay, 2015). Clearly, the

spatial distribution and intensity of precipitation would also impact the timing of sensor activation across the network.

UAA has the best correlation with flow duration on the falling limbs of events and for the entire 10-month period (Table 3), since falling limbs comprise most of the dataset. The calculation of TWI incorporates UAA and local slope (Beven & Kirkby, 1979), so lower correlations for TWI indicate UAA forms the primary contribution. Accordingly, locations with large contributing areas retain flow for longer periods of time after a storm, which Camporese et al. (2014) explain as the redistribution of subsurface soil moisture storage on the falling limb of events. UAA or TWI appears in numerous channel network models (Elmore et al., 2013; Russell et al., 2015; Schneider et al., 2017; Jensen et al., 2018). Catchment area was also the most important predictor of water table depth and flow duration along the stream network for Goulsbra et al. (2014).

Correlations between flow duration and the topographic metrics we examined are significant but do not fully explain fine spatial patterns of wetting and drying (Table 3). We expected the field measurements of valley width to have much higher and negative correlations with flow duration, since we noticed in the field that confined reaches with steep valley side slopes contain water more frequently than those with a wide valley floor, which is a common observation elsewhere (Stanley et al., 1997). The amount of valley fill, rather than the width, may be the actual determinant of flow duration at these locations. In addition, TPI accounts for valley confinement at a larger scale that may be more relevant for network expansion and contraction than the field measurement. Slope has a negative but insignificant correlation with flow duration, since steep channel reaches efficiently transport water and tend to be dry (Goulsbra et al., 2014). Additional variables describing the geology, sediment depth, and spatial variability in precipitation are necessary to better characterize channel wetting, drying, and flow persistence.

4.3.4 Value of flow intermittency sensors and sources of uncertainty

The sensor data describing the wet network proportion match the field measurements of network connectivity (Figure 2), affirming the accuracy of flow intermittency sensors. A major advantage of using sensors is the ability to record network dynamics during storm events and over longer time scales. Sensors produce continuous datasets appropriate for the creation of wet proportion-

flow duration-frequency curves (Figure 8) that could be valuable for watershed management and planning to determine the return period of various stream lengths. Multiple years of data would be preferable for this analysis, so our example provides a template for future studies.

We acknowledge several issues with the flow intermittency sensors in our study. Interpretation of the sensor data to indicate the presence or absence of water is usually simple, as the electrical conductivity rapidly increases from low (< 50) to high (400-2000) values. However, the sensors do not always show a clear break in conductivity during channel wetting and drying. Chapin et al. (2014) note intermediate values slightly higher than the dry signal can result from sediment burial of the sensor electrodes, but the adapter caps and screen material of our housing design prevent the accumulation of sediment. We positioned the sensors sideways in the adapters rather than vertically to minimize the amount of water necessary to connect the circuit between the electrodes and, thus, show a wet signal. Otherwise, several centimeters of flow depth are necessary to reach the electrodes. The proximity of the electrodes to the ground permit contact with the dry or wet channel bed, which may contribute to the intermediate signals. Overall, these intermediate readings are rare, and data interpretation is relatively straightforward.

The flow intermittency sensors provide only point measurements of the presence or absence of water, which can result in an underestimation of stream length, particularly during low flows (Figure 2). We installed the sensors in the channel thalweg where the flow duration should ideally be highest, but the channel may have contained water at another location in the cross-section or just upstream or downstream of the sensor location. In addition, leaves, sediment, and woody debris can move during storm events to reroute flow around, rather than toward, the sensors. As a result, the flow duration and wet proportion results from sensor studies are most certainly a low estimate of the actual time and length of stream flow.

4.4 Conclusion

The wet network proportion and time lag between the maximum wet proportion and peak runoff vary with event precipitation and antecedent wetness. Network expansion is greater for storms with high event and antecedent precipitation totals, and the maximum wet proportion coincides with peak stream flow. Events with drier antecedent conditions can demonstrate considerable

hysteresis, with higher wet proportions on the rising limb than on the falling limb. For some of these events during dry periods, the maximum wet proportion precedes peak flow by up to several hours. Channel reaches in confined valleys are the first to activate with flow on the rising limbs of storms, while locations with high upslope contributing areas are the last to dry after storms. Analysis of other topographic metrics and geologic characteristics is necessary to better explain spatial patterns of flow duration along the channel network.

Flow intermittency sensors are an effective method for recording stream length dynamics during storm events and permit the development of wet proportion-flow duration-frequency curves to aid watershed management. However, because sensors provide point measurements of the presence of water, stream length estimates using this technique are always a lower bound approximation of the actual wet network extent and connectivity. Future research should incorporate an examination of stream length hysteresis alongside solute transport from headwaters and associated C-Q relationships. Studies may also seek to understand shifts from surface- to subsurface-dominated storage during events and quantify the relative contributions of downstream surface water movement, rises in the water table, and increases in lateral flow that result in delays between maximum stream length and peak runoff during dry periods.

Figures and Tables

Table 1. 30-year precipitation normals and measured precipitation during the monitoring period at the National Weather Service Forecast Office in Blacksburg, Virginia.

Month	Precipitation normals 1981-2010 (cm)	Measured precipitation 2017-2018 (cm)
May	11.0	16.0
June	10.2	7.4
July	10.8	8.4
August	9.1	6.4
September	7.9	3.7
October	7.1	19.6
November	7.3	3.1
December	7.5	1.6
January	7.8	4.1
February	7.1	11.8
Total	85.8	82.1

Table 2. Storm event characteristics.

		AP (cm)			API (Mosley, 1982)			Maximum wet proportion (%)	Time from peak runoff to maximum wet proportion (minutes)[a]
Event date	Event precipitation (cm)	30 day	14 day	7 day	30 day	14 day	7 day		
05/06/17	2.72	7.87	6.50	0.91	0.81	0.74	0.23	65	-180
05/13/17	2.41	11.53	4.95	4.04	1.87	1.52	1.44	98	0
05/21/17	1.93	12.95	4.14	0.33	0.86	0.46	0.05	26	-45
05/24/17	7.34	13.13	5.66	1.93	2.14	1.82	1.50	100	0
06/05/17	1.65	13.94	8.99	0.36	0.99	0.78	0.07	17	0
06/09/17	0.69	15.19	3.07	1.65	1.34	0.67	0.55	12	-15
06/16/17	0.86	12.14	2.34	0.03	0.66	0.24	0.00	60	15
07/05/17[b]	3.07	4.37	0.61	0.00	0.23	0.06	0.00	12	-480
07/19/17	1.22	5.69	4.63	0.58	0.47	0.43	0.12	4	-570
07/24/17	2.44	6.38	1.80	1.22	0.55	0.30	0.24	29	-30
07/28/17	3.15	8.28	4.24	2.44	1.16	0.97	0.80	12	0
08/05/17	1.85	11.68	6.86	3.66	1.17	0.97	0.66	15	0
08/08/17	2.95	10.52	8.51	3.12	1.37	1.27	0.80	17	-15
08/13/17	2.54	13.97	6.60	3.45	1.84	1.44	1.10	50	15
10/08/17[b]	5.16	0.97	0.00	0.00	0.05	0.00	0.00	26	-30
10/23/17	5.26	6.68	5.59	0.03	0.49	0.42	0.01	94	0
10/29/17	4.04	11.94	5.31	5.26	1.41	1.06	1.05	98	0
12/24/17	0.97	1.04	0.46	0.03	0.08	0.04	0.01	4	0
01/13/18	1.57	1.91	0.61	0.61	0.31	0.24	0.24	33	-390
01/23/18	0.74	2.97	1.88	0.10	0.23	0.19	0.03	8	0
01/28/18	1.35	2.59	0.81	0.71	0.25	0.15	0.14	48	0
02/04/18	1.98	4.50	2.62	1.91	0.67	0.58	0.52	77	0
02/07/18	2.90	6.50	4.50	2.57	1.43	1.35	1.15	98	0
02/10/18	4.11	8.92	6.93	5.03	1.56	1.48	1.31	98	0

[a] Negative sign indicates that the maximum wet proportion precedes peak flow.

[b] Events with two peaks separated by a recession > 24 hours, although precipitation was intermittent. We limited analysis to the first peak.

Table 3. Pearson's r correlations between topographic metrics and flow duration at each sensor over the entire 10-month study period and for all rising limbs and falling limbs of events. Values in bold indicate significance at $p < 0.05$.

	Pearson's r correlation coefficients		
Topographic metric	All data	All rising limbs	All falling limbs
Valley width	0.03	-0.01	0.06
Slope	-0.13	-0.10	-0.14
Mean slope	0.12	0.22	0.07
TWI	**0.33**	**0.28**	**0.35**
Mean TWI	0.05	0.06	0.04
TPI	-0.05	-0.15	-0.02
Mean TPI	**-0.35**	**-0.41**	**-0.33**
UAA	**0.38**	**0.30**	**0.42**

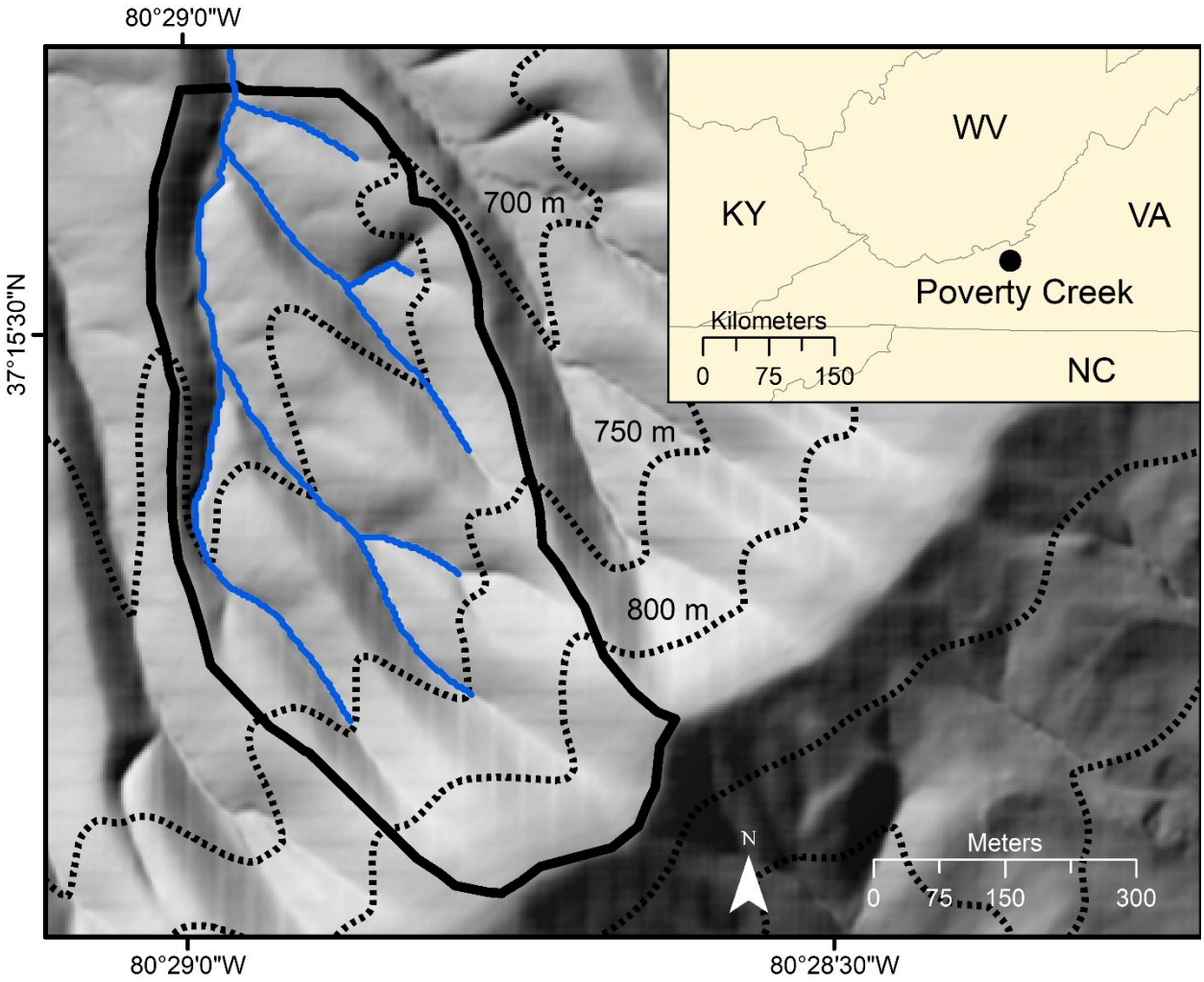

Figure 1. Hillshade of the Poverty Creek study catchment. Contour intervals are 50 m. Blue line represents the perennial and intermittent channel network as mapped in the field by Jensen et al. (2017) in 2015 and 2016.

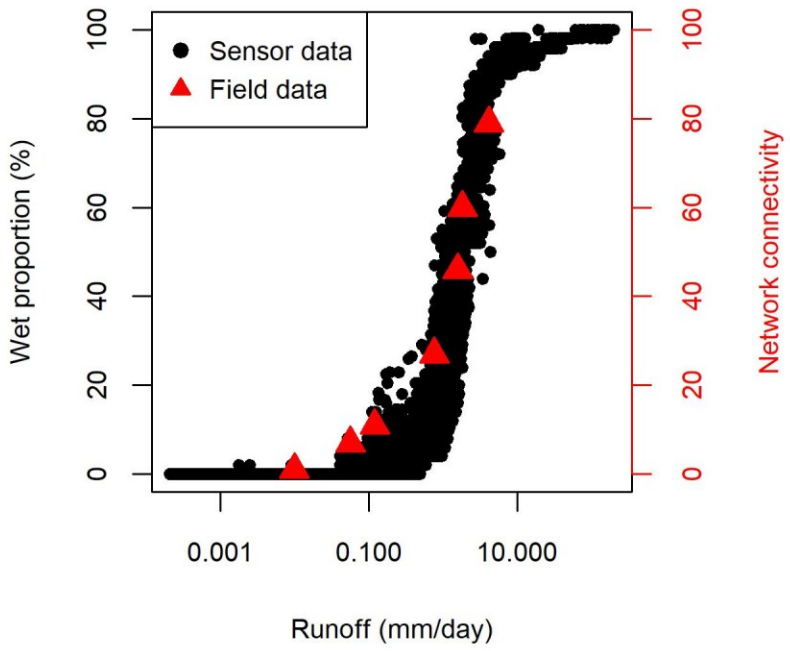

Figure 2. Runoff versus the wet proportion of the stream network for the 10-month monitoring period as calculated from the flow intermittency sensors and the network connectivity from Jensen et al. (2017) as calculated from field mapping.

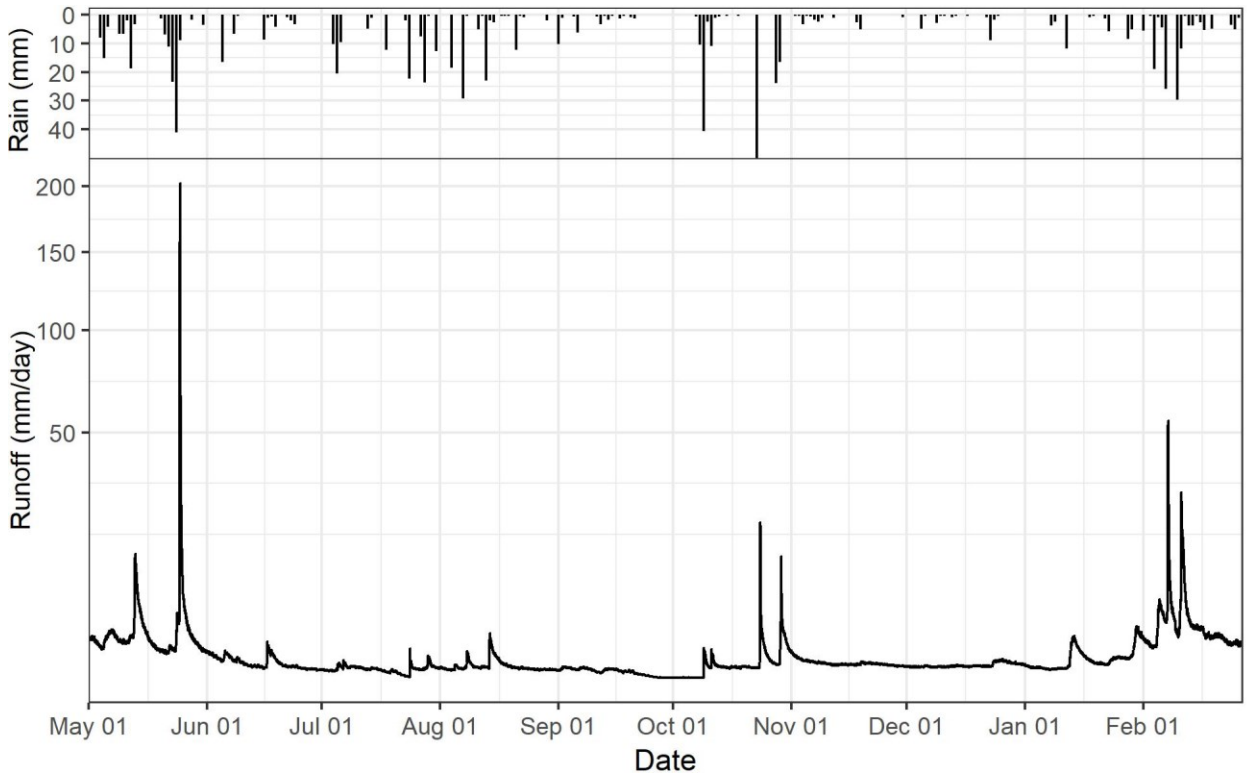

Figure 3. Rainfall and runoff data over the 10-month study period. The y-axis for runoff has a square root transformation to aid visualization.

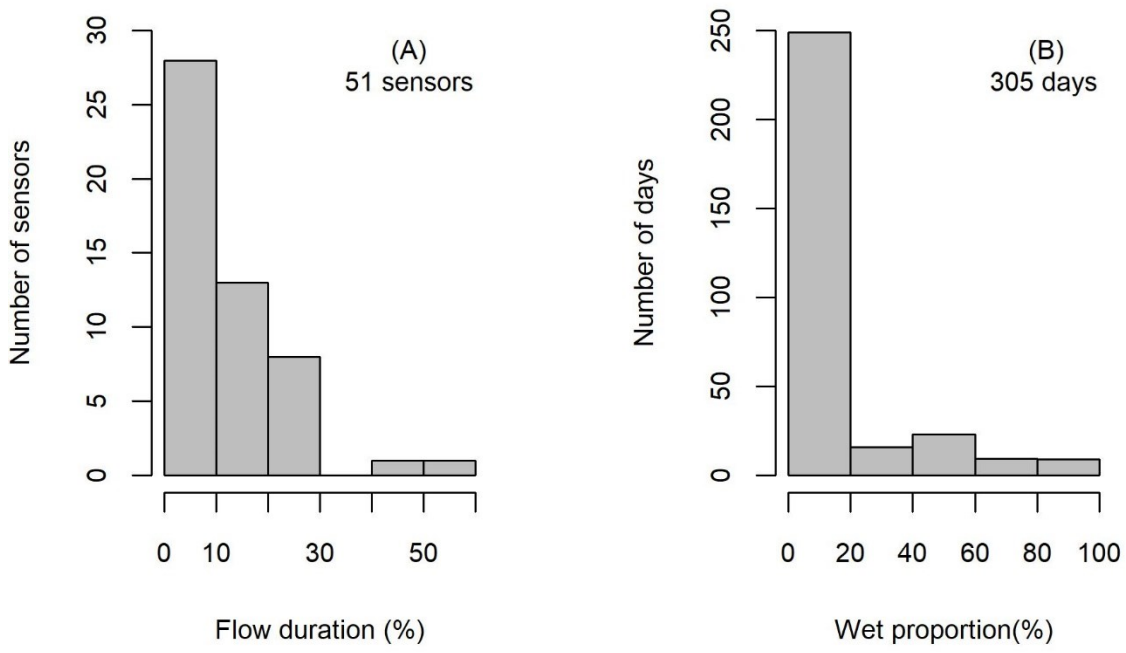

Figure 4. Histograms of flow duration among sensors (A) and the wet proportion of the stream network (B) over the 10-month monitoring period.

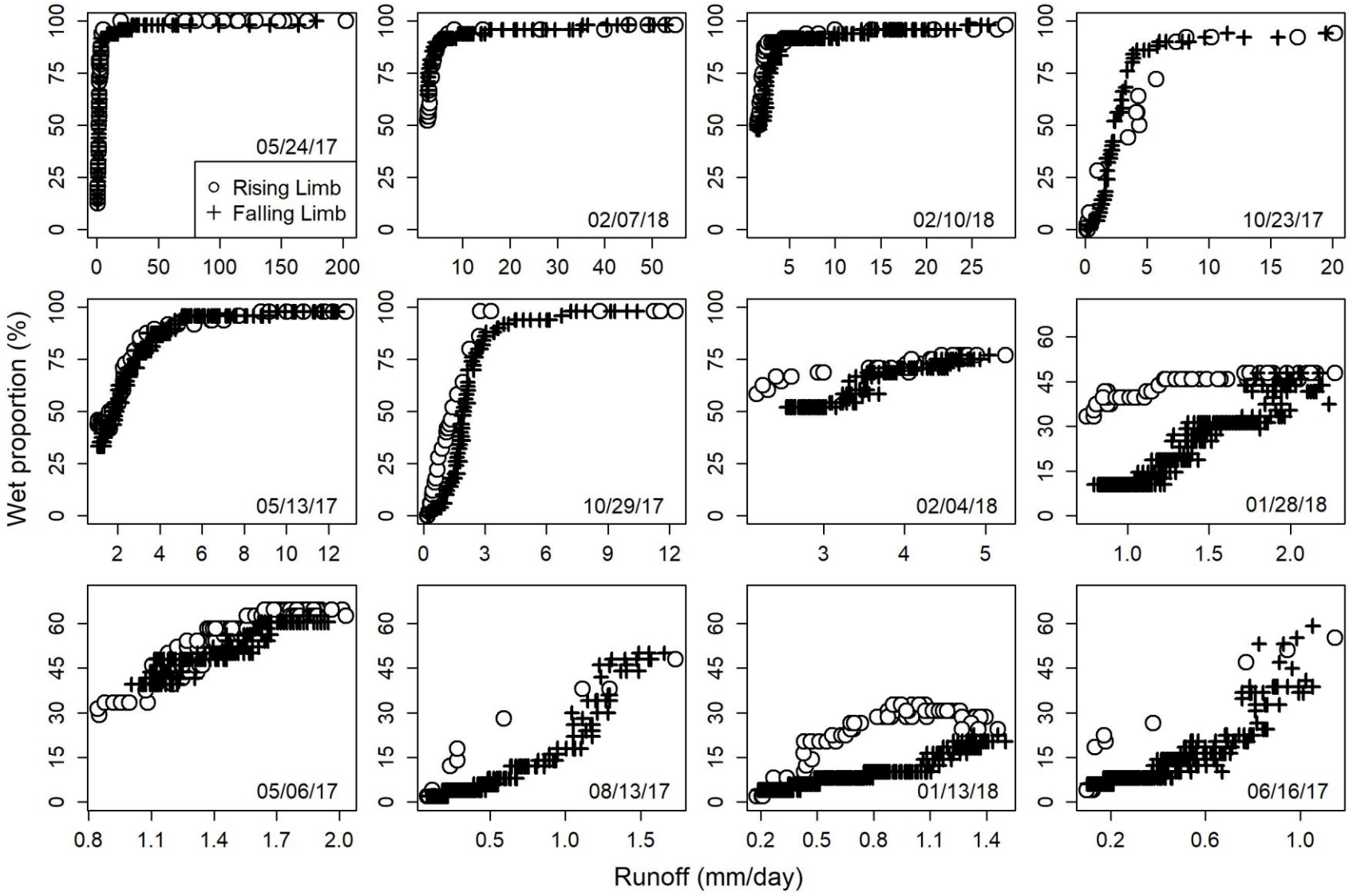

Figure 5. Runoff versus the wet proportion of the stream network during storm events with a maximum runoff > 1 mm/day.

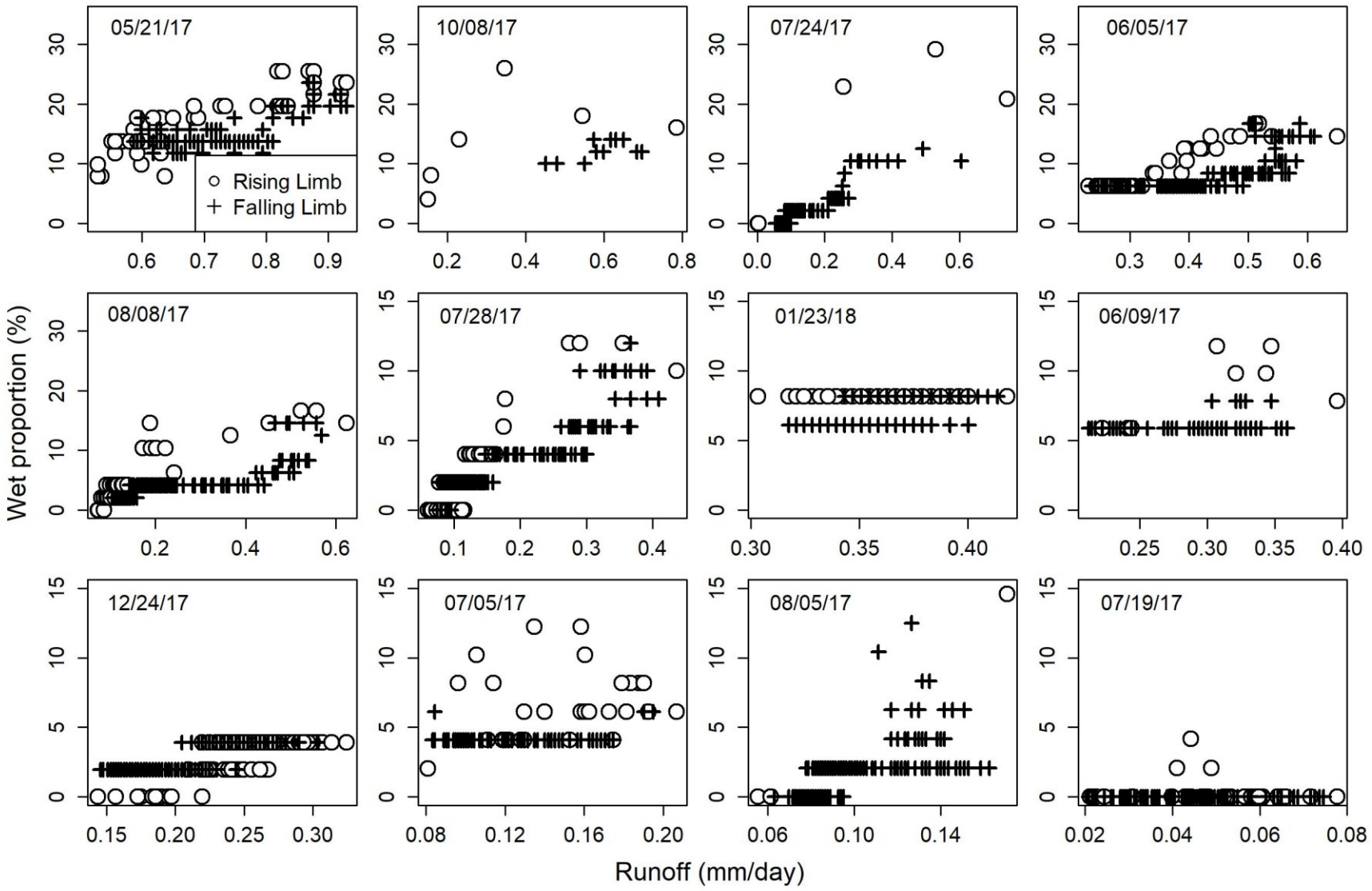

Figure 6. Runoff versus the wet proportion of the stream network during storm events with a maximum runoff < 1 mm/day.

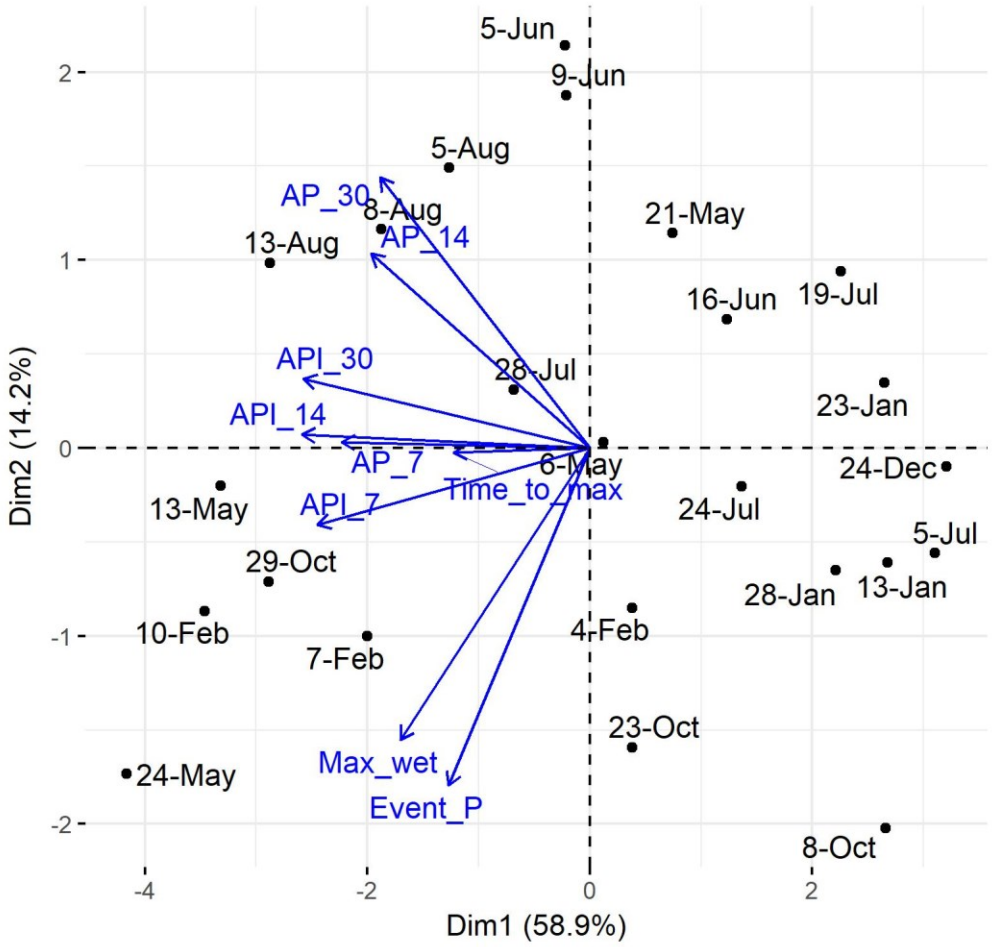

Figure 7. Principal components analysis biplot of the precipitation metrics in Table 2, the maximum wet proportion (Max_wet), and time lag between maximum stream length and peak runoff (Time_to_max).

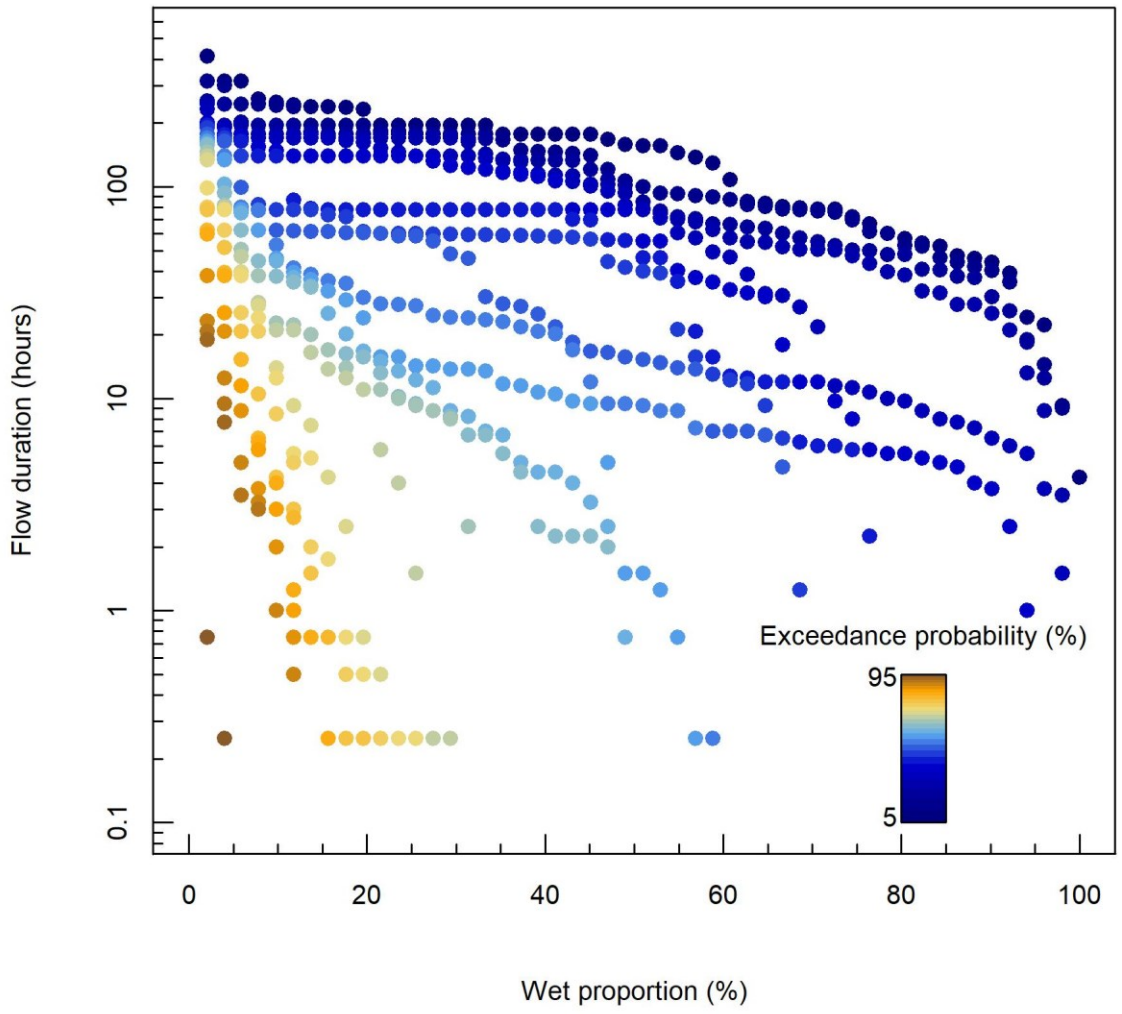

Figure 8. Wet proportion-flow duration-frequency curves for the 10-month monitoring period.

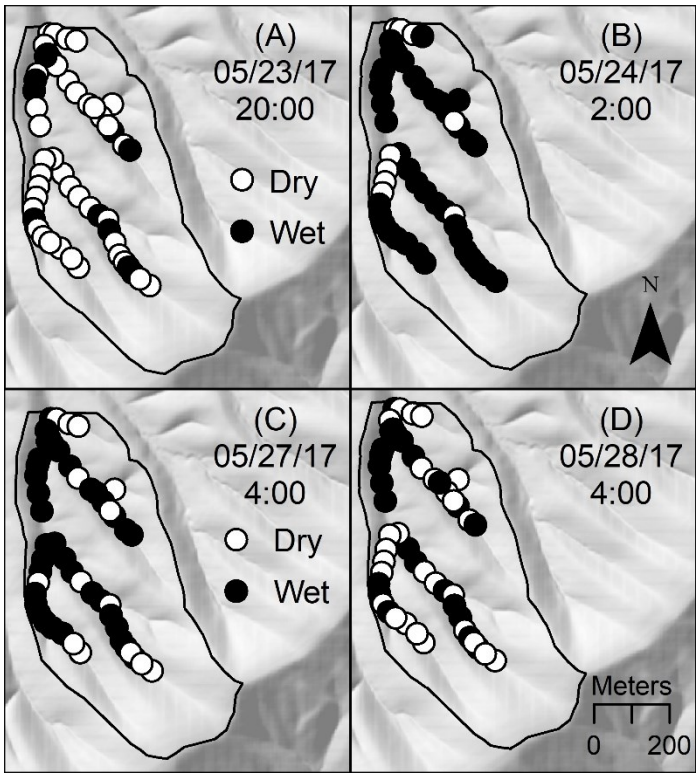

Figure 9. Sensor activation with flow on the rising (A & B) and falling (C & D) limbs of the 05/24/17 storm event.

References

Acuña, V., Datry, T., Marshall, J., Barceló, D., Dahm, C. N., Ginebreda, A., ... & Palmer, M. A. (2014). Why should we care about temporary waterways?. *Science*, *343*, 1080-1081.

Adams, H. S., & Stephenson, S. L. (1983). A description of the vegetation on the south slopes of Peters Mountain, southwestern Virginia. *Bulletin of the Torrey Botanical Club*, *110*, 18-22.

Alexander, R. B., Boyer, E. W., Smith, R. A., Schwarz, G. E., & Moore, R. B. (2007). The role of headwater streams in downstream water quality. *Journal of the American Water Resources Association*, *43*, 41-59.

Arnborg, L., Walker, H. J., & Peippo, J. (1967). Suspended load in the Colville river, Alaska, 1962. *Geografiska Annaler: Series A, Physical Geography*, *49*, 131-144.

Batlle-Aguilar, J., & Cook, P. G. (2012). Transient infiltration from ephemeral streams: A field experiment at the reach scale. *Water Resources Research*, *48*.

Beven K. J., & Kirkby M. J. (1979). A physically based, variable contributing area model of basin hydrology. *Hydrological Sciences Journal*, *24*, 43-69.

Bhamjee, R., & Lindsay, J. B. (2011). Ephemeral stream sensor design using state loggers. *Hydrology and Earth System Sciences*, *15*, 1009-1021.

Bishop, K., Buffam, I., Erlandsson, M., Fölster, J., Laudon, H., Seibert, J., & Temnerud, J. (2008). Aqua Incognita: the unknown headwaters. *Hydrological Processes*, *22*, 1239-1242.

Blasch, K. W., Ferré, T., Christensen, A. H., & Hoffmann, J. P. (2002). New field method to determine streamflow timing using electrical resistance sensors. *Vadose Zone Journal*, *1*, 289-299.

Blasch, K. W., Ferré, T., Hoffmann, J. P., & Fleming, J. B. (2006). Relative contributions of transient and steady state infiltration during ephemeral streamflow. *Water Resources Research*, *42*.

Blyth, K., & Rodda, J. C. (1973). A stream length study. *Water Resources Research*, *9*, 1454-1461.

Boulton, A. J., Findlay, S., Marmonier, P., Stanley, E. H., & Valett, H. M. (1998). The functional significance of the hyporheic zone in streams and rivers. *Annual Review of Ecology and Systematics*, *29*, 59-81.

Buttle, J. M., Boon, S., Peters, D. L., Spence, C., van Meerveld, H. J., & Whitfield, P. H. (2012). An overview of temporary stream hydrology in Canada. *Canadian Water Resources Journal*, *37*, 279-310.

Calkins, D., & Dunne, T. (1970). A salt tracing method for measuring channel velocities in small mountain streams. *Journal of Hydrology*, *11*, 379-392.

Camporese, M., Penna, D., Borga, M., & Paniconi, C. (2014). A field and modeling study of nonlinear storage- discharge dynamics for an Alpine headwater catchment. *Water Resources Research*, *50*, 806-822.

Chapin, T. P., Todd, A. S., & Zeigler, M. P. (2014). Robust, low-cost data loggers for stream temperature, flow intermittency, and relative conductivity monitoring. *Water Resources Research*, *50*, 6542-6548.

Constantz, J., Stonestorm, D., Stewart, A. E., Niswonger, R., & Smith, T. R. (2001). Analysis of streambed temperatures in ephemeral channels to determine streamflow frequency and duration. *Water Resources Research*, *37*, 317-328.

Creggar, W. H., Hudson, H. C., & Porter, H. C. (1985). Soil survey of Montgomery County, Virginia. U.S. Department of Agriculture Soil Conservation Service: Washington D.C. 158 pp.

Datry, T., Larned, S. T., & Tockner, K. (2014). Intermittent rivers: a challenge for freshwater ecology. *BioScience*, *64*, 229-235.

Day, D. G. (1978). Drainage density changes during rainfall. *Earth Surface Processes and Landforms*, *3*, 319-326.

Day, D. G. (1980). Lithologic controls of drainage density: A study of six small rural catchments in New England, NSW. *Catena*, *7*, 339-351.

Downing, J. A., Cole, J. J., Duarte, C. M., Middelburg, J. J., Melack, J. M., Prairie, Y. T., ... & Tranvik, L. J. (2012). Global abundance and size distribution of streams and rivers. *Inland Waters*, *2*, 229-236.

Elmore, A. J., Julian, J. P., Guinn, S. M., & Fitzpatrick, M. C. (2013). Potential stream density in Mid-Atlantic US watersheds. *PLoS One*, *8*, e74819.

Evans, C., & Davies, T. D. (1998). Causes of concentration/discharge hysteresis and its potential as a tool for analysis of episode hydrochemistry. *Water Resources Research*, *34*, 129-137.

Fritz, K. M., Hagenbuch, E., D'Amico, E., Reif, M., Wigington, P. J., Leibowitz, S. G., ... & Nadeau, T. L. (2013). Comparing the extent and permanence of headwater streams from two field surveys to values from hydrographic databases and maps. *Journal of the American Water Resources Association*, *49*, 867-882.

Godsey, S. E., & Kirchner, J. W. (2014). Dynamic, discontinuous stream networks: hydrologically driven variations in active drainage density, flowing channels and stream order. *Hydrological Processes*, *28*, 5791-5803.

González- Ferreras A. M., & Barquín J. (2017). Mapping the temporary and perennial character of whole river networks. *Water Resources Research*, *53*, 6709-6724.

Goulsbra, C. S., Lindsay, J. B., & Evans, M. G. (2009). A new approach to the application of electrical resistance sensors to measuring the onset of ephemeral streamflow in wetland environments. *Water Resources Research*, *45*.

Goulsbra, C., Evans, M., & Lindsay, J. (2014). Temporary streams in a peatland catchment: pattern, timing, and controls on stream network expansion and contraction. *Earth Surface Processes and Landforms*, *39*, 790-803.

Gregory, K. J., & Walling, D. E. (1968). The variation of drainage density within a catchment. *Hydrological Sciences Journal*, *13*, 61-68.

Guisan A., Weiss S. B., & Weiss A. D. (1999). GLM versus CCA spatial modeling of plant species distribution. *Plant Ecology*, *143*, 107-122.

Haught, D. R. W., & Meerveld, H. J. (2011). Spatial variation in transient water table responses: differences between an upper and lower hillslope zone. *Hydrological Processes*, *25*, 3866-3877.

Hooshyar, M., Kim, S., Wang, D., & Medeiros, S. C. (2015). Wet channel network extraction by integrating LiDAR intensity and elevation data. *Water Resources Research*, *51*, 10029-10046.

Jaeger, K. L., Montgomery, D. R., & Bolton, S. M. (2007). Channel and perennial flow initiation in headwater streams: management implications of variability in source-area size. *Environmental Management*, *40*, 775.

Jaeger, K. L., & Olden, J. D. (2012). Electrical resistance sensor arrays as a means to quantify longitudinal connectivity of rivers. *River Research and Applications*, *28*, 1843-1852.

Jaeger, K. L., Olden, J. D., & Pelland, N. A. (2014). Climate change poised to threaten hydrologic connectivity and endemic fishes in dryland streams. *Proceedings of the National Academy of Sciences*, *111*, 13894-13899.

Jencso, K. G., McGlynn, B. L., Gooseff, M. N., Wondzell, S. M., Bencala, K. E., & Marshall, L. A. (2009). Hydrologic connectivity between landscapes and streams: Transferring reach- and plot- scale understanding to the catchment scale. *Water Resources Research*, *45*.

Jensen, C. K., McGuire, K. J., & Prince, P. S. (2017). Headwater stream length dynamics across four physiographic provinces of the Appalachian Highlands. *Hydrological Processes*, *31*, 3350-3363.

Jensen, C. K., McGuire, K. J., Shao, Y., & Dolloff, C.A. (2018). Modeling headwater stream networks across multiple flow conditions in the Appalachian Highlands. In revision to *Earth Surface Processes and Landforms.*

Larned, S. T., Datry, T., Arscott, D. B., & Tockner, K. (2010). Emerging concepts in temporary-
river ecology. *Freshwater Biology*, *55*, 717-738.

McGlynn, B. L., McDonnell, J. J., Seibert, J., & Kendall, C. (2004). Scale effects on headwater catchment runoff timing, flow sources, and groundwater- streamflow relations. *Water Resources Research*, *40*.

Morgan, R. P. C. (1972). Observations on factors affecting the behaviour of a first-order stream. *Transactions of the Institute of British Geographers*, 171-185.

Mosley, M. P. (1982). Subsurface flow velocities through selected forest soils, South Island, New Zealand. *Journal of Hydrology*, *55*, 65-92.

Myrabø, S. (1997). Temporal and spatial scale of response area and groundwater variation in till. *Hydrological Processes*, *11*, 1861-1880.

Nadeau, T. L., & Rains, M. C. (2007). Hydrological connectivity between headwater streams and downstream waters: how science can inform policy. *Journal of the American Water Resources Association*, *43*, 118-133.

Nieber, J. L., & Walter, M. F. (1981). Two- dimensional soil moisture flow in a sloping rectangular region: Experimental and numerical studies. *Water Resources Research*, *17*, 1722-1730.

Niswonger, R. G., Prudic, D. E., Fogg, G. E., Stonestrom, D. A., & Buckland, E. M. (2008). Method for estimating spatially variable seepage loss and hydraulic conductivity in intermittent and ephemeral streams. *Water Resources Research*, *44*.

Peirce, S. E., & Lindsay, J. B. (2015). Characterizing ephemeral streams in a southern Ontario watershed using electrical resistance sensors. *Hydrological Processes*, *29*, 103-111.

Penna, D., Tromp-van Meerveld, H. J., Gobbi, A., Borga, M., & Dalla Fontana, G. (2011). The influence of soil moisture on threshold runoff generation processes in an alpine headwater catchment. *Hydrology and Earth System Sciences*, *15*, 689.

Płaczkowska, E., Górnik, M., Mocior, E., Peek, B., Potoniec, P., Rzonca, B., & Siwek, J. (2015). Spatial distribution of channel heads in the Polish Flysch Carpathians. *Catena*, *127*, 240-249.

Roberts, M. C., & Klingeman, P. C. (1972). The relationship of drainage net fluctuation and discharge. Proceedings of the 22nd International Geographical Congress, Canada, 181-91.

Roelens, J., Rosier, I., Dondeyne, S., Van Orshoven, J., & Diels, J. (2018). Extracting drainage networks and their connectivity using Lidar data. *Hydrological Processes*.

Russell, P. P., Gale, S. M., Muñoz, B., Dorney, J. R., & Rubino, M. J. (2015). A spatially explicit model for mapping headwater streams. *Journal of the American Water Resources Association*, *51*, 226-239.

Schneider, A., Jost, A., Coulon, C., Silvestre, M., Théry, S., & Ducharne, A. (2017). Global-scale river network extraction based on high- resolution topography and constrained by lithology, climate, slope, and observed drainage density. *Geophysical Research Letters*, *44*, 2773-2781.

Shaw, S. B. (2016). Investigating the linkage between streamflow recession rates and channel network contraction in a mesoscale catchment in New York state. *Hydrological Processes*, *30*, 479-492.

Skoulikidis, N. T., Sabater, S., Datry, T., Morais, M. M., Buffagni, A., Dörflinger, G., ... & Rosado, J. (2017). Non-perennial Mediterranean rivers in Europe: status, pressures, and challenges for research and management. *Science of The Total Environment*, *577*, 1-18.

Seibert J., & McGlynn B. L. (2007). A new triangular multiple flow direction algorithm for computing upslope areas from gridded digital elevation models. *Water Resources Research*, *43*.

Spence, C., & Mengistu, S. (2016). Deployment of an unmanned aerial system to assist in mapping an intermittent stream. *Hydrological Processes*, *30*, 493-500.

Stanley, E. H., Fisher, S. G., & Grimm, N. B. (1997). Ecosystem expansion and contraction in streams. *BioScience*, *47*, 427-435.

Steward, A. L., von Schiller, D., Tockner, K., Marshall, J. C., & Bunn, S. E. (2012). When the river runs dry: human and ecological values of dry riverbeds. *Frontiers in Ecology and the Environment*, *10*, 202-209.

Stubbington, R., England, J., Wood, P. J., & Sefton, C. E. (2017). Temporary streams in temperate zones: recognizing, monitoring and restoring transitional aquatic- terrestrial ecosystems. *Wiley Interdisciplinary Reviews: Water*, *4*, e1223.

Travis M. R., Elsner G. H., & Iverson W. D. (1975). VIEWIT: computation of seen areas, slope and aspect for land-use planning. U.S. Forest Service General Technical Report PSW-11. U.S. Department of Agriculture.

The Southeast Regional Climate Center (SERCC). (2012). Historical Climate Summaries for Virginia. http://www.sercc.com/climateinfo/historical/historical_va.html.

Virginia Division of Mineral Resources. (1993). Geologic Map of Virginia, Scale 1:500,000. Virginia Division of Mineral Resources.

Wang L., & Liu H. (2006). An efficient method for identifying and filling surface depressions in digital elevation models for hydrologic analysis and modelling. *International Journal of Geographical Information Science*, *20*, 193-213.

Ward, A. S., Schmadel, N. M., & Wondzell, S. M. (2018). Simulation of dynamic expansion, contraction, and connectivity in a mountain stream network. *Advances in Water Resources*, *114*, 64-82.

Weill, S., Altissimo, M., Cassiani, G., Deiana, R., Marani, M., & Putti, M. (2013). Saturated area dynamics and streamflow generation from coupled surface–subsurface simulations and field observations. *Advances in Water Resources*, *59*, 196-208.

Welter, J. R., & Fisher, S. G. (2016). The influence of storm characteristics on hydrological connectivity in intermittent channel networks: implications for nitrogen transport and denitrification. *Freshwater Biology*, *61*, 1214-1227.

Whiting, J. A., & Godsey, S. E. (2016). Discontinuous headwater stream networks with stable flowheads, Salmon River basin, Idaho. *Hydrological Processes*, *30*, 2305-2316.

Wigington, P. J., Moser, T. J., & Lindeman, D. R. (2005). Stream network expansion: a riparian water quality factor. *Hydrological Processes*, *19*, 1715-1721.

Williams, C. E., & Johnson, W. C. (1990). Age structure and the maintenance of Pinus pungens in pine-oak forests of southwestern Virginia. *American Midland Naturalist*, 130-141.

Wohl, E. (2017). The significance of small streams. *Frontiers of Earth Science*, *11*, 447-456.

Zimmer, M. A., & McGlynn, B. L. (2017). Ephemeral and intermittent runoff generation processes in a low relief, highly weathered catchment. *Water Resources Research*, *53*, 7055-7077.

Chapter 5: Conclusions

Headwaters account for a majority of global river length (Downing et al., 2012) and greatly impact downstream water quality (Alexander et al., 2007; Dodds & Oakes, 2008). The significance of headwaters is gaining recognition among the scientific community, and low-order streams are becoming a greater priority in water conservation (Wohl, 2017). The ability to locate waterways is a basic and foremost consideration for conservation efforts as well as watershed management, water policy, and catchment science. Despite the simplicity of the question, "where are the streams?", headwaters are difficult to map, leading to a severe underestimation of stream length. To compound this difficulty, many headwater streams regularly expand and contract in length (Buttle et al., 2012). Temporary stream length dynamics re-entered the scientific literature in recent years (Godsey & Kirchner, 2014), but many studies focus on arid environments where flow intermittency is a more obvious feature. The innumerable implications of headwater stream length necessitate a better understanding of network dynamics to facilitate progress in the aquatic ecology, biogeochemistry, and hydrology of temporary streams.

The scale of study is always a challenge in headwaters. The small, disconnected, and often ephemeral nature of headwater streams requires detailed spatial coverage in field studies as well as repeated measurements through time. However, the vast expanse of headwaters encompasses a broad range of geology, climate, vegetation, land use, and level of anthropogenic disturbance. Beyond simply mapping changes in wet stream length at individual catchments, we must strive to understand network dynamics across scales and environmental gradients to categorize and, therefore, better predict the location and length of headwater streams in different landscapes.

This dissertation sought to describe and explain temporary stream length dynamics along a physiographic gradient in the Appalachian Highlands at multiple spatial and temporal scales. Extensive field data collected across the Appalachians in Chapter 2 informed modeling of headwater networks in Chapter 3 and field instrumentation of a single catchment at a high spatial and temporal resolution in Chapter 4.

In Chapter 2, we mapped wet stream length in four Appalachian physiographic provinces at different flow conditions. Even though all sites were within the Appalachian Highlands, network dynamics differed markedly as a function of regional and local geologic characteristics. Stream length was quite stable in the Blue Ridge (CWT) but varied over orders of magnitude at shale catchments on a scarp slope in the Valley and Ridge (PVY). Flow origins were generally farther downslope at larger contributing areas in sedimentary rock than in provinces with crystalline substrate. The degree of network expansion correlated with several metrics including the base flow index (BFI), bankfull channel width, length of the geomorphic network, and surface connectivity of the stream.

In Chapter 3, we built logistic regression models to predict the probability of the presence or absence of a wet stream at each catchment pixel using the field maps as training data. Explanatory variables included topographic metrics and runoff measured at the catchment outlet. Although precise configurations of the network for a given runoff value were not possible, the models were able to reproduce the length and connectivity of streams at high and low flows in each province with high accuracy by varying the probability threshold. The topographic wetness index (TWI) and topographic position index (TPI) were the most significant model variables.

Finally, in Chapter 4, we instrumented one catchment in the Valley and Ridge with flow intermittency sensors that detect the presence or absence of water. The sensors collected data for 10 months at 15-minute intervals to record channel wetting and drying during storm events. For storms with dry antecedent conditions, stream length tended to be higher on the rising limb than on the falling limb of the event hydrograph. For these storms, maximum stream length often occurred before peak runoff. Little to no hysteresis was evident for wetter events, and maximum network extension coincided with peak flow. In general, more incised valley segments experienced flow first on the rising limbs, and locations with high upslope accumulated areas dried last on the falling limbs.

The findings of this dissertation support the analysis of wet stream length dynamics and associated drivers across multiple scales. As such, there are numerous opportunities for future research. Our results emphasize the importance of site geology for stream length variability. For

example, flow origins in the sedimentary Valley and Ridge catchments all occurred at similar mean upslope areas, but the magnitude of network expansion and contraction differed considerably between sandstone and shale catchments on dip and scarp slopes, respectively. Therefore, studies may compare wet stream length within a single physiographic province across gradients of lithology and geologic structure. All of our catchments had second-growth forests, so similar projects that examine headwater length across forest stand ages, land cover types, and disturbance histories are essential, especially given the rapid pace of land use conversion and global environmental change. Data from these studies may suggest additional metrics to improve the accuracy of wet stream models and permit application of these models over diverse landscapes. Finally, the installation of flow intermittency sensors in other study areas may help identify site controls on stream length hysteresis.

Further research on stream length dynamics will continue to improve the accuracy of headwater stream maps and estimates of network length. In addition, the coordination of temporary stream length studies and research questions concerning the availability of aquatic habitat, nutrient cycling, C-Q relationships, and sediment transport has the potential to produce novel insights and promote communication and progress across disciplines.

References

Alexander, R. B., Boyer, E. W., Smith, R. A., Schwarz, G. E., & Moore, R. B. (2007). The role of headwater streams in downstream water quality. *Journal of the American Water Resources Association*, *43*, 41-59.

Buttle, J. M., Boon, S., Peters, D. L., Spence, C., van Meerveld, H. J., & Whitfield, P. H. (2012). An overview of temporary stream hydrology in Canada. *Canadian Water Resources Journal*, *37*, 279-310.

Dodds, W. K., & Oakes, R. M. (2008). Headwater influences on downstream water quality. *Environmental Management*, *41*, 367-377.

Downing J. A., Cole J. J., Duarte C. M., Middelburg J. J., Melack J. M., Prairie Y. T., ... & Tranvik L. J. (2012). Global abundance and size distribution of streams and rivers. *Inland Waters*, *2*, 229-236.

Godsey, S. E., & Kirchner, J. W. (2014). Dynamic, discontinuous stream networks: Hydrologically driven variations in active drainage density, flowing channels and stream order. *Hydrological Processes*, *28*, 5791-5803.

Wohl, E. (2017). The significance of small streams. *Frontiers of Earth Science*, *11*, 447-456.

Appendix A: Field stream length measurements

Table A1. Field data for HB/NE13

Date		6/23/2015	6/10/2015	6/3/2015	6/25/2015	6/27/2015	7/6/2015	7/10/2015
Runoff (mm/day)		17.1	5.99	2.95	2.52	1.19	0.97	0.58
Active water width (m)	Transect1	1.29	1.15	1.15	1.11	0.80	0.76	0.65
	Transect2	1.04	1.00	0.92	0.91	0.83	0.77	0.69
	Transect3	0.64	0.50	0.49	0.49	0.37	0	0
	Transect4	0.66	0.49	0.46	0.46	0	0	0
	Transect5	1.32	1.27	1.14	1.13	1.12	0.70	0.67
	Transect6	0.90	0.89	0.78	0.75	0.75	0.73	0.50
Active water depth (m)	Transect1	0.24	0.23	0.21	0.19	0.17	0.15	0.14
	Transect2	0.14	0.14	0.12	0.11	0.11	0.10	0.10
	Transect3	0.11	0.09	0.07	0.07	0.04	0	0
	Transect4	0.09	0.09	0.07	0.06	0	0	0
	Transect5	0.12	0.12	0.10	0.10	0.07	0.07	0.06
	Transect6	0.31	0.23	0.22	0.21	0.16	0.14	0.13
Origin slope (%)	Trib1	21	21	21	21	21	21	21
	Trib2	28	27	27	27	27	27	27
	Trib3	35	35	35	35	35	35	35
	Trib4	23.5	23.5	23.5	23.5	23.5	23.5	23.5
	Trib5	16.5	15	15	23	23	23	NA
	Trib6	12.5	12.5	12.5	12.5	12.5	14	NA
	Trib7	0	0	0	0	0	0	0
	Trib8	34	34	34	34	34	34	34
	Trib9	22	22	22	22	22	22	22
	Trib10	22	22	22	22	22	22	22
	Trib11	19	NA	NA	NA	NA	NA	NA
	Trib12	23.5	NA	NA	NA	NA	NA	NA
Total wet length (km)		1.48	1.40	1.32	1.19	1.10	1.01	0.91
Total network length (km)		1.74	1.59	1.59	1.56	1.55	1.53	1.33

Table A2. Field data for HB/NE25

Date		6/24/2015	6/22/2015	6/19/2015	7/4/2015	6/27/2015	7/7/2015	7/14/2015
Runoff (mm/day)		4.99	3.10	2.75	1.79	1.31	0.96	0.31
Active water width (m)	Transect1	1.63	1.52	1.51	1.48	1.45	1.43	1.13
	Transect2	1.59	1.09	0.96	0.93	0.91	0.89	0.79
	Transect3	0.75	0.59	0.58	0	0	0	0
	Transect4	0.76	0.76	0.76	0	0	0	0
Active water depth (m)	Transect1	0.21	0.16	0.16	0.15	0.14	0.14	0.11
	Transect2	0.14	0.09	0.08	0.07	0.07	0.07	0.07
	Transect3	0.11	0.08	0.08	0	0	0	0
	Transect4	0.15	0.12	0.10	0	0	0	0
Origin slope (%)	Trib1	21	21	21	21	21	21	21
	Trib2	23	18	18	18	18	18	18
	Trib3	40	40	40	40	40	40	40
	Trib4	23	23	23	23	23	23	21
	Trib5	32	32	32	32	27	21	NA
	Trib6	26	26	26	26	26	26	NA
	Trib7	17	17	17	17	24	24	24
	Trib8	25	19	18	18	18	15	NA
	Trib9	21	34.5	34.5	34.5	34.5	34.5	34.5
	Trib10	28	28	28	21	15	15	14
	Trib11	29	29	29	29	NA	NA	NA
	Trib12	15	15	15	15	15	15	15
Total wet length (km)		2.15	1.87	1.71	1.34	1.05	0.79	0.46
Total network length (km)		2.89	2.77	2.76	2.68	2.61	2.59	1.91

Table A3. Field data for HB/NE42

Date		6/2/2015	6/29/2015	6/16/2015	6/18/2015	7/5/2015	6/7/2015	7/13/2015
Runoff (mm/day)		6.02	4.51	3.31	1.86	1.47	0.68	0.18
Active water width (m)	Transect1	1.90	1.74	1.67	1.64	1.62	1.53	0.97
	Transect2	0.90	0.88	0.84	0.83	0.78	0.54	0
	Transect3	1.15	1.14	1.13	1.11	1.09	1.05	0
	Transect4	0.87	0.85	0.85	0.80	0.79	0.77	0.76
	Transect5	0.62	0.54	0.52	0.50	0.50	0.48	0.25
	Transect6	0.75	0.68	0.66	0.65	0.65	0.65	0
	Transect7	0.87	0.65	0.62	0.61	0.58	0.41	0
Active water depth (m)	Transect1	0.27	0.25	0.23	0.21	0.19	0.18	0.13
	Transect2	0.09	0.08	0.07	0.07	0.06	0.03	0
	Transect3	0.12	0.11	0.11	0.11	0.11	0.08	0
	Transect4	0.10	0.10	0.10	0.08	0.07	0.07	0.07
	Transect5	0.07	0.07	0.07	0.06	0.06	0.06	0.05
	Transect6	0.06	0.05	0.05	0.05	0.05	0.04	0
	Transect7	0.13	0.12	0.12	0.10	0.08	0.07	0
Origin slope (%)	Trib1	36	36	34	34	34	34	17
	Trib2	25	25	35	35	35	35	25
	Trib3	25	25	25	25	24	24	NA
	Trib4	26	26	26	26	26	24	23.5
	Trib5	8.5	8.5	8.5	8.5	15	15	15
	Trib6	32.5	32.5	32.5	32.5	32.5	24	24
	Trib7	28	28	25	25	25	25	16
	Trib8	34	34	26	26	26	26	20
	Trib9	25	25	25	25	25	25	25
	Trib10	26	26	26	26	7	7	7
	Trib11	16	16	16	16	16	16	NA
	Trib12	14	14	14	16	14	14	17
	Trib13	24	24	24	24	24	24	15
	Trib14	17	17	17	17	21	21	16

	Trib15	27.5	27.5	32.5	32.5	32.5	32.5	NA
	Trib16	28	28	28	28	28	28	NA
	Trib17	24	24	24	24	25	25	NA
	Trib18	23	23	23	23	23	22	NA
	Trib19	29	29	29	29	29	29	29
Total wet length (km)		3.33	3.24	3.14	2.85	2.58	2.34	1.43
Total network length (km)		4.21	4.21	4.14	4.13	4.02	3.91	2.93

Table A4. Field data for FNW/AP14

Date		12/7/2016	6/6/2016	6/1/2016	6/11/2016	6/13/2016	6/14/2016	8/27/2016
Runoff (mm/day)	Stage	8.99	0.89	0.36	0.29	0.18	0.13	0.05
Active water width (m)	Transect1	-	1.71	1.49	1.43	1.43	1.39	1.36
	Transect2	-	1.48	1.48	1.48	1.41	1.41	1.35
	Transect3	-	2.30	2.12	2.12	2.12	2.12	2.08
	Transect4	-	1.23	1.03	1.01	0.95	0.95	0.91
Active water depth (m)	Transect1	-	0.05	0.04	0.03	0.03	0.02	0.02
	Transect2	-	0.08	0.05	0.03	0.02	0.02	0.01
	Transect3	-	0.04	0.01	0.01	0.01	0.01	0.01
	Transect4	-	0.02	0.02	0.01	0.01	0.01	0.01
Origin slope (%)	Trib1	29	29	29	29	29	29	23
	Trib2	13	16	16	16	14	14	9
Total wet length (km)		0.41	0.37	0.34	0.34	0.33	0.33	0.30
Total network length (km)		0.43	0.40	0.36	0.36	0.36	0.36	0.33

Table A5. Field data for FNW/AP16

Date		12/7/2016	6/6/2016	5/31/2016	6/11/2016	6/13/2016	6/14/2016	8/27/2016
Runoff (mm/day)		6.30	0.70	0.29	0.20	0.15	0.13	0.02
Active water width (m)	Transect1	-	1.09	1.09	1.09	1.06	1.06	0.98
	Transect2	-	1.39	1.13	1.13	1.11	1.08	0
	Transect3	-	0.76	0.50	0.46	0.39	0.36	0
Active water depth (m)	Transect1	-	0.08	0.06	0.06	0.05	0.04	0.02
	Transect2	-	0.07	0.05	0.04	0.04	0.03	0
	Transect3	-	0.06	0.05	0.05	0.05	0.05	0
Origin slope (%)	Trib1	3	17	16	16	17	17	4
Total wet length (km)		0.38	0.27	0.21	0.21	0.20	0.19	0.08
Total network length (km)		0.43	0.35	0.33	0.33	0.32	0.32	0.16

Table A6. Field data for FWN/AP37

Date		12/7/2016	6/6/2016	5/31/2016	6/11/2016	6/13/2016	6/14/2016	8/27/2016
Runoff (mm/day)		5.24	1.20	0.48	0.33	0.20	0.16	0.04
Active water width (m)	Transect1	-	1.76	1.76	1.76	1.74	1.74	1.56
	Transect2	-	1.10	1.10	1.01	1.01	1.01	0.92
	Transect3	-	1.46	1.46	1.46	1.46	1.46	1.20
Active water depth (m)	Transect1	-	0.11	0.10	0.10	0.10	0.10	0.04
	Transect2	-	0.04	0.03	0.03	0.02	0.02	0.01
	Transect3	-	0.07	0.06	0.06	0.06	0.06	0.04
Origin slope (%)	Trib1	34	34	34	34	34	34	15
	Trib2	13	13	13	13	13	13	13
	Trib3	2	2	2	2	2	2	9
Total wet length (km)		0.85	0.77	0.61	0.55	0.52	0.50	0.36
Total network length (km)		1.07	1.07	1.07	1.07	1.07	1.07	0.97

Table A7. Field data for PVY/VR25

Date		11/20/2015	11/21/2015	12/5/2015	1/15/2016	11/4/2015	10/23/2015	9/7/2015
Runoff (mm/day)		4.69	2.21	1.55	1.17	0.32	0.06	0.03
Active water width (m)	Transect1	1.49	1.48	1.34	1.25	1.02	0.97	0.91
	Transect2	0.44	0.42	0.41	0.41	0.37	0.34	0.16
	Transect3	0.53	0.51	0	0	0	0	0
	Transect4	1.08	0.85	0.71	0.64	0.55	0.48	0
	Transect5	0.36	0.36	0.27	0	0	0	0
Active water depth (m)	Transect1	0.14	0.12	0.12	0.10	0.07	0.07	0.06
	Transect2	0.05	0.04	0.04	0.03	0.03	0.02	0.01
	Transect3	0.05	0.05	0	0	0	0	0
	Transect4	0.11	0.08	0.07	0.07	0.07	0.06	0
	Transect5	0.07	0.06	0.05	0	0	0	0
Origin slope (%)	Trib1	26.5	23	24	13	19	20	17
	Trib2	17	17	24	24	9	NA	NA
	Trib3	3	3	6	6	17	17	17
	Trib4	NA	NA	NA	NA	NA	NA	NA
Total wet length (km)		1.53	1.20	0.96	0.69	0.47	0.24	0.16
Total network length (km)		1.79	1.78	1.78	1.74	1.37	1.19	1.10

Table A8. Field data for PVY/VR35

Date		12/3/2015	12/4/2015	11/11/2015	11/13/2015	11/6/2015	10/21/2015	9/7/2015
Runoff (mm/day)		4.17	1.84	1.59	0.77	0.12	0.06	0.01
Active water width (m)	Transect1	1.75	1.75	1.72	1.70	1.64	0.72	0
	Transect2	0.66	0.59	0.53	0.52	0.46	0.43	0.38
	Transect3	0.52	0.47	0.31	0	0	0	0
	Transect4	0.62	0.60	0	0	0	0	0
	Transect5	0.45	0.42	0.14	0	0	0	0
Active water depth (m)	Transect1	0.08	0.08	0.08	0.065	0.05	0.03	0
	Transect2	0.09	0.08	0.08	0.07	0.05	0.02	0.01
	Transect3	0.05	0.04	0.03	0	0	0	0
	Transect4	0.05	0.04	0	0	0	0	0
	Transect5	0.03	0.02	0.01	0	0	0	0
Origin slope (%)	Trib1	31	31	35	3	15	15	15
	Trib2	17.5	17	NA	NA	NA	NA	NA
	Trib3	22	22	24	16	16	16	19
	Trib4	20	20	20	14	22	22	NA
	Trib5	22	22	NA	NA	NA	NA	NA
	Trib6	19	NA	NA	NA	NA	NA	NA
Total wet length (km)		1.85	1.40	1.09	0.63	0.27	0.17	0.02
Total network length (km)		2.35	2.21	1.93	1.44	1.30	1.30	1.00

Table A9. Field data for SFP/VR70

Date		2/4/2016	2/5/2016	12/6/2015	1/14/2016	3/31/2016	10/26/2015	8/26/2015
Runoff (mm/day)		9.72	5.28	2.11	1.62	0.99	0.23	0.04
Active water width (m)	Transect1	2.63	2.63	2.60	2.45	2.45	1.75	1.36
	Transect2	2.52	2.52	2.39	2.35	2.32	2.30	0.99
	Transect3	1.92	1.90	1.44	1.41	1.35	1.35	0.45
	Transect4	1.38	1.35	1.14	1.14	0.60	0	0
	Transect5	1.42	1.39	1.22	1.13	1.05	0.89	0
Active water depth (m)	Transect1	0.22	0.20	0.15	0.13	0.09	0.08	0.07
	Transect2	0.19	0.16	0.09	0.08	0.07	0.04	0.01
	Transect3	0.20	0.17	0.12	0.08	0.08	0.04	0.01
	Transect4	0.13	0.10	0.07	0.07	0.04	0	0
	Transect5	0.22	0.13	0.07	0.07	0.06	0.02	0
Origin slope (%)	Trib1	35	35	22	22	22	23	NA
	Trib2	15	11	11	11	11	15	15
	Trib3	5	25	28	28	19	14	13
	Trib4	6	13	30	16	NA	NA	NA
	Trib5	26	26	10	10	10	NA	NA
	Trib6	27	27	34	34	34	NA	NA
	Trib7	4	4	4	4	4	NA	NA
	Trib8	15	15	15	15	15	NA	NA
	Trib9	13	NA	NA	NA	NA	NA	NA
	Trib10	4	4	NA	NA	NA	NA	NA
	Trib11	20	20	20	20	20	NA	NA
	Trib12	30	30	NA	NA	NA	NA	NA
Total wet length (km)		1.40	1.28	1.12	1.09	1.07	0.85	0.63
Total network length (km)		2.10	2.03	1.74	1.64	1.54	1.35	1.07

Table A10. Field data for CWT/BR12

Date		12/26/2015	12/22/2015	11/24/2015	5/10/2016	5/16/2016	7/21/2016	12/23/2016
Runoff (mm/day)		23.58	3.85	3.01	2.01	1.79	1.05	0.41
Active water width (m)	Transect1	2.13	2.05	1.82	1.75	1.75	1.75	-
	Transect2	1.40	1.38	1.36	1.32	1.32	1.32	-
	Transect3	2.00	1.95	1.73	1.73	1.73	1.73	-
	Transect4	1.92	1.91	1.91	1.87	1.87	1.87	-
Active water depth (m)	Transect1	0.13	0.07	0.07	0.03	0.03	0.03	-
	Transect2	0.12	0.03	0.03	0.03	0.03	0.02	-
	Transect3	0.11	0.07	0.06	0.03	0.03	0.03	-
	Transect4	0.07	0.03	0.03	0.03	0.03	0.01	-
Origin slope (%)	Trib1	57	61	61	61	61	61	61
	Trib2	35	35	35	35	35	35	35
	Trib3	23.5	23.5	23.5	23.5	23.5	23.5	23
	Trib4	14	14	14	14	14	14	14
	Trib5	55	55	55	55	55	55	55
	Trib6	34	34	34	34	34	34	NA
Total wet length (km)		0.75	0.68	0.66	0.65	0.65	0.64	0.52
Total network length (km)		0.78	0.77	0.77	0.77	0.77	0.77	0.73

Table A11. Field data for CWT/BR33

Date		1/4/2016	1/7/2016	11/25/2015	5/8/2016	5/16/2016	7/21/2016	12/23/2016
Runoff (mm/day)		12.45	10.2	3.66	3.02	2.64	1.72	0.77
Active water width (m)	Transect1	1.70	1.70	1.68	1.64	1.57	1.57	-
	Transect2	1.75	1.55	1.50	1.50	1.50	1.45	-
	Transect3	0.91	0.89	0.83	0.81	0.81	0.80	-
Active water depth (m)	Transect1	0.24	0.22	0.10	0.10	0.09	0.09	-
	Transect2	0.16	0.15	0.08	0.08	0.07	0.07	-
	Transect3	0.12	0.07	0.04	0.03	0.03	0.02	-
Origin slope (%)	Trib1	60	60	60	60	60	60	60
	Trib2	38	38	38	38	38	38	NA
	Trib3	39	39	39	39	39	39	NA
	Trib4	10	10	10	10	10	10	NA
	Trib5	36	36	36	36	36	36	36
	Trib6	36	36	36	36	36	36	NA
	Trib7	40	40	40	40	40	40	40
	Trib8	56	56	56	56	56	56	56
	Trib9	57	57	57	57	57	57	57
	Trib10	44	44	44	44	44	44	44
	Trib11	49	49	49	49	49	49	49
	Trib12	53	53	53	53	53	53	53
	Trib13	75	75	75	75	75	75	75
Total wet length (km)		1.11	1.11	1.06	1.05	1.05	1.05	0.97
Total network length (km)		1.19	1.19	1.18	1.18	1.18	1.18	1.09

Table A12. Field data for CWT/BR40

Date		12/27/2015	1/2/2016	1/6/2016	3/8/2016	5/9/2016	7/20/2016	12/22/2016
Runoff (mm/day)		18.05	17.85	13.88	6.10	3.26	1.89	1.22
Active water width (m)	Transect1	2.30	2.20	2.20	2.20	2.20	2.15	-
	Transect2	2.00	2.00	2.00	1.90	1.70	1.60	-
	Transect3	1.50	1.44	1.43	1.40	1.40	1.20	-
Active water depth (m)	Transect1	0.19	0.18	0.16	0.11	0.10	0.08	-
	Transect2	0.20	0.18	0.18	0.12	0.11	0.09	-
	Transect3	0.15	0.11	0.09	0.09	0.06	0.06	-
Origin slope (%)	Trib1	19	NA	NA	NA	NA	NA	NA
	Trib2	26	26	26	26	26	26	26
	Trib3	17.5	17.5	17.5	17.5	17.5	17.5	NA
	Trib4	53	53	53	53	53	53	53
	Trib5	48	48	48	48	42	49	49
	Trib6	38	38	38	38	38	38	38
	Trib7	41	41	41	41	41	41	41
	Trib8	40	40	40	40	40	40	40
	Trib9	28	28	28	28	28	28	28
	Trib10	27	27	27	27	27	27	27
	Trib11	4	4	4	4	4	4	NA
	Trib12	57	57	57	57	57	57	58
	Trib13	54	54	54	54	54	54	NA
Total wet length (km)		2.02	1.94	1.94	1.92	1.88	1.85	1.73
Total network length (km)		2.20	2.12	2.12	2.12	2.12	2.09	2.05